

University of Montana

ScholarWorks at University of Montana

Graduate Student Theses, Dissertations, &
Professional Papers

Graduate School

1984

Harvest age-structure as an indicator of grizzly bear population status

Richard B. Harris
The University of Montana

Follow this and additional works at: <https://scholarworks.umt.edu/etd>

Let us know how access to this document benefits you.

Recommended Citation

Harris, Richard B., "Harvest age-structure as an indicator of grizzly bear population status" (1984).
Graduate Student Theses, Dissertations, & Professional Papers. 7379.
<https://scholarworks.umt.edu/etd/7379>

This Thesis is brought to you for free and open access by the Graduate School at ScholarWorks at University of Montana. It has been accepted for inclusion in Graduate Student Theses, Dissertations, & Professional Papers by an authorized administrator of ScholarWorks at University of Montana. For more information, please contact scholarworks@mso.umt.edu.

COPYRIGHT ACT OF 1976

THIS IS AN UNPUBLISHED MANUSCRIPT IN WHICH COPYRIGHT SUBSISTS. ANY FURTHER REPRINTING OF ITS CONTENTS MUST BE APPROVED BY THE AUTHOR.

MANSFIELD LIBRARY
UNIVERSITY OF MONTANA
DATE: 1984

HARVEST AGE-STRUCTURE
AS AN INDICATOR OF
GRIZZLY BEAR POPULATION STATUS

by

Richard B. Harris

B.A., Bennington College, 1974

Presented in partial fulfillment of the requirement
for the degree of Master of Science

University of Montana

1984

Approved By:


Chairman, Board of Examiners


Dean, Graduate School

12-4-84
Date

UMI Number: EP38180

All rights reserved

INFORMATION TO ALL USERS

The quality of this reproduction is dependent upon the quality of the copy submitted.

In the unlikely event that the author did not send a complete manuscript and there are missing pages, these will be noted. Also, if material had to be removed, a note will indicate the deletion.



UMI EP38180

Published by ProQuest LLC (2013). Copyright in the Dissertation held by the Author.

Microform Edition © ProQuest LLC.

All rights reserved. This work is protected against unauthorized copying under Title 17, United States Code



ProQuest LLC.
789 East Eisenhower Parkway
P.O. Box 1346
Ann Arbor, MI 48106 - 1346

Harvest Age-structure as an Indicator of Grizzly Bear Population Status (204 pp.)

Director: Lee H. Metzgar



Managers of harvested grizzly bear (Ursus arctos) populations face the problem of setting harvest regulations for a species with extremely low reproductive rates in the absence of reliable data on population abundance. Although harvest age-structure data are often cited as a means of determining the status of such populations, consensus is lacking regarding the best treatment of these data and sample sizes necessary for valid conclusions. This study examined simulated grizzly bear harvests, interpreted age-structures of populations relative to the sustained yield curve, developed an index to declining trajectory, and evaluated the sensitivity of the index.

Age-structures were generated by stochastic, discrete-time, age-structured projection models that followed the history of individual bears. Four models simulated slightly different mechanisms of population regulation via density-dependence. All satisfactorily simulated longevity of individuals, non-stationary age-structures, and synchrony of breeding.

Age-structures of harvested populations displayed 3 patterns with increasing harvest pressure: (i) sex ratios favored females, (ii) male age declined, and (iii) female age increased slightly. Although clearly evident in unexploited populations that were subsequently overharvested to extinction, differences in age-structures between populations above and below the sustained yield curve were virtually undetectable. Harvest age-structures exhibited high yearly variability and a substantial lag-time in their response to changing harvest rates.

Differences in harvest age-structures of declining and stable populations were summarized and quantified by 2-group discriminant function analysis. The power of the resulting discriminant index was estimated by setting the probability of erroneously classifying a declining population at 10%, and noting the percentage of stable populations correctly classified. Under circumstances typically confronting a manager, power of the index was low: with large sample sizes, just over 50%; with small sample sizes, about 20%.

Harvesting grizzly bears merely to obtain age-structure data for inferring population status was concluded to be a questionable practice. Decisions about harvesting small populations of grizzlies must be viewed conservatively, because harvests data contain inherent uncertainty. Managers must work in the context of risk rather than irrefutable quantitative evidence.

ACKNOWLEDGEMENTS

This study was funded by the U.S. Fish and Wildlife Service, through the office of the Grizzly Bear Recovery Coordinator. Administrative support came from the Montana Cooperative Wildlife Research Unit.

The study was originated by Dr. Lee Metzgar, who also participated in the development of the model, made invaluable suggestions, shared his expertise, and improved the manuscript, while providing warmth and humor throughout. Thanks go also to Drs. Les Marcum and Christopher Servheen, members of my committee, for having the patience necessary to review such a lengthy document. The computer model was written by Collin Bevins of Systems for Environmental Management, without whose insight and abilities the project simply would not have been possible.

I also benefited from stimulating conversations with biologists Rick Mace, Bob Klaver and Bruce McClellan, all of whom added to my knowledge of bear biology. Bob Klaver also participated in the analysis of the Montana data appearing at the end of the thesis, and allowed me access to his own unpublished analyses. Sterling Miller, Alaska Department of Fish and Game, Anchorage, also consulted on the nature of grizzly bear harvests. Frank Tompa, British Columbia Fish and Wildlife Branch, Victoria, graciously provided harvest data from B.C., and shared his analyses with me.

Finally, I am grateful to Barbara Burke, who married a frenzied graduate student, confident that, before too long, he would once again turn into a real human being.

TABLE OF CONTENTS

Abstract	ii
Acknowledgments	iii
Table of Contents	iv
List of Tables	vi
List of Figures	ix
INTRODUCTION	1
Overview	1
Properties of Harvested Populations	3
Sustained Yield Curve	3
Other Curves	5
Shape of the Sustained Yield Curve	7
Dynamics of the Sustained Yield Curve	9
Age-Structure Analyses	13
OBJECTIVES	17
SIMULATION MODEL	18
General Structure	18
Overview	18
Density-Dependence	19
Environmental Stochasticity	23
Sequence of Events	25
Specific Models	29
Life History Rates Used in Simulations	32
Survival	34
Natality	35
Relative Vulnerability to Hunting	35
Environmental Variability	36
Review of Assumptions	36
METHODS	39
Definition of Terms	39
Behavior of the Model	41
Sustained Yield Curves	44
Description of Age-Structures	50
Discrimination of Declining and Stable Age-Structures...	53
RESULTS	58
Behavior of the Model	58
Natality and Mortality Rates at Equilibrium	58
Population Variability and Equilibrium	63
Growth from of unexploited populations	78
Sustained Yield Curves	83
Factors Influencing Trajectories of Individual Populations	85

Factors Influencing Average Sustainable Harvests....	91
Description of Grizzly Bear Age-Structures	102
Harvested Populations Initially at K	102
Standing Population Age-Structures	102
Age-Structures of Hunted Samples	110
Harvested Populations Initially at 2 Cross-sections of the SYC.....	115
Standing Population Age-Structures	115
Age-Structures of Hunted Samples	119
Harvested Populations Growing in Response to Increased K	125
Differences Among the 4 Specific Models	125
Discrimination of Declining and Stable Populations	134
Discriminant Function Analysis	134
Interpretation of the Discriminant Function	135
Power of the Discriminant Function	140
Discrimination Using Single Variables	148
Using the Discriminant Function as an Index to Decline ..	148
Confirmation Tests	151
 APPLICATION TO FIELD DATA	 158
British Columbia Data	158
Montana Data	161
 DISCUSSION	 167
The Simulation Model	167
Sustainable Yield	170
Harvest Age-Structures	173
The Discriminant Index	177
Assumptions and research	183
 MANAGEMENT SUMMARY	 185
 APPENDICES	
1. Life-history rates used in the simulation model	190
2. Relative vulnerabilities to hunting used in the simulation model	194
3. Discriminant function equations from year-groups 2 and 3 ..	195
.....	
 REFERENCES	 197

LIST OF TABLES

Table 1.	The 10 trial harvest levels applied to each cross-section population.	48
Table 2.	Ten descriptive statistics computed for each data sample.	52
Table 3.	Litter sizes in this simulation and other published figures. .	60
Table 4.	Breeding intervals in this simulation and other published figures.	60
Table 5.	Ages at first reproduction in this simulation and other published figures.	62
Table 6.	Variability of population equilibrium as a function of environmental stochasticity and population size at K.	69
Table 7.	Mean equilibrium values of 6 simulations with expected K=100, 3 with 13% coefficient of variation for K, 3 with no environmental stochasticity.	77
Table 8.	Stability of sustained harvests, as calculated over a 10-year period.	86
Table 9.	Stability of sustained harvests, as calculated over a 30-year period.	87
Table 10.	Stability of sustained harvests, as calculated over a 10-year period.	88
Table 11.	Stability of sustained harvests, as calculated over a 30-year period.	89
Table 12.	Mean sustainable yield, comparing calculations over 10 years and 30 years.	96
Table 13.	Mean sustainable yield, comparing populations with theoretical K=200 and K=600.	100
Table 14.	Summary of the relationships between 10 descriptive statistics of standing age-structure and population size as equilibrium populations are overharvested to extinction.	111
Table 15.	Summary of the relationships between 10 descriptive statistics of harvest age-structure and population size as equilibrium populations are overharvested to extinction.	114
Table 16.	Summary of the relationships between 10 descriptive statistics of standing age-structure and population size as	

	populations that were initially at K=600.	156
Table 33.	Power of the discriminant function for harvest samples from populations that were initially at K=600, where discrimination is made for an entire simulation run.	156
Table 34.	The power of the discriminant function as applied to growing populations.	157
Table 35.	Discriminant index scores for 3 populations in British Columbia, 1976-1982.	160
Table 36.	Discriminant index score for each population by years 1976-1978, 1979-1981 and 1982-1983.	160
Table 37.	Discriminant index score for the Southern Rockies area for each year from 1976 through 1982.	163
Table 38.	Discriminant index score for Montana grizzly bear harvests. ...	163

LIST OF FIGURES

Fig. 1.	A generalized sustained yield curve.	4
Fig. 2.	Two curves often confused with the sustained yield curve.	6
Fig. 3.	A generalized sustained yield curve, showing trajectories of populations.	10
Fig. 4.	The dynamics of sustained yield, adapted from May (1977).	12
Fig. 5.	Life-history events of grizzly bears, as simulated in the model.	20
Fig. 6.	A generalized Michaelis-Menton function, as used in the simulation model.	22
Fig. 7.	A generalized distribution of K values, showing the log-normal distribution used in the simulation.	24
Fig. 8.	A generalized sustained yield curve, showing the stable and declining region.	42
Fig. 9.	A schematic diagram of the process by which sustained yields were located.	46
Fig. 10.	A generalized distribution of discriminant scores along the canonical axis, showing the procedure used to calculate Type I and Type II errors.	56
Fig. 11.	Mean survival rates of males and females in the simulated population at unharvested equilibrium (K).	64
Fig. 12.	The mean age-structure of the simulated population at K.	65
Fig. 13.	Age-structures from 2 consecutive years, selected randomly.	66
Fig. 14.	A typical 50-year simulation run at K=600 with environmental variability.	67
Fig. 15.	A typical 50-year simulation run at K=600 with environmental variability removed.	70
Fig. 16.	A typical 50-year simulation run at K=200 with environmental variability removed.	71
Fig. 17.	A typical 50-year simulation run at K=200 with	

	environmental variability.	72
Fig. 18.	A typical 50-year simulation run at $K=200$ with environmental variability, showing the number of cubs each year.	73
Fig. 19.	A typical 50-year simulation run at $K=200$ with environmental variability removed, showing the number of cubs each year.	74
Fig. 20.	Correlation coefficients (r) of the number of cubs in year 0 with the number of cubs a specified time interval later, plotted against the time interval.	76
Fig. 21.	Relative equilibrium values attained by simulated populations plotted against expected carrying capacities. ...	79
Fig. 22.	A typical simulation run with $K=600$, starting from an arbitrary population of 50 animals.	80
Fig. 23.	The simulation run in Fig. 22 plotted with number of animals on a logarithmic scale.	81
Fig. 24.	A typical increment curve, as generated by a growing population.	82
Fig. 25.	A generalized sustained yield curve, showing the probability band of sustained yields.	84
Fig. 26.	A typical frequency distribution of sustainable yield, as seen schematically in the inset of Fig. 25.	85a
Fig. 27.	The frequency distribution of sustained yield for the 0.7K cross-section of Model DMADM populations with a theoretical $K=200$, as calculated over 30 years.	93
Fig. 28.	Trajectories of harvested populations along the sustained yield curve.	94
Fig. 29.	Sustained yield frequency distribution, showing the difference between yields resulting in stability over 10 years and 30 years.	97
Fig. 30.	Sustained yield frequency distributions for Models DM and ADM, showing the difference between the 2.	99
Fig. 31.	The mean age-structure of the standing population when subjected to an initial, stable harvest.	103
Fig. 32.	The mean age-structure of the standing population when subjected to overharvesting from K	104

Fig. 33.	Mean male age in the standing population age-structure, as a population at $K=600$ was overharvested to extinction.	100
Fig. 34.	Mean female age from 2 differing sets of simulations, plotted against time.	107
Fig. 35.	The proportion males among adults in the standing age-structure as a population at $K=600$ was overharvested to extinction.	108
Fig. 36.	Mean age-distribution of males in harvests that led to extinction, during the years 1-3 of the harvest.	112
Fig. 37.	Mean age-distribution of males in harvests that led to extinction, during years 8-10 of the harvest.	113
Fig. 38.	Median male age in the harvest sample as a population initially at $K=600$ was overharvested to extinction.	116
Fig. 39.	Mean female age in the harvest sample as a population initially at $K=600$ was overharvested to extinction.	117
Fig. 40.	Proportion males among adults in the harvest sample as a population initially at $K=600$ was overharvested to extinction.	118
Fig. 41.	Mean age-structure of a population when it arrives at $0.7K$ after being overharvested from K .	120
Fig. 42.	Mean trajectories of populations initially at $0.7K$ from 2 different sets of simulations.	121
Fig. 43.	Mean male harvest age-structures from populations at $0.7K$ subjected to stable harvesting.	122
Fig. 44.	Mean male harvest age-structures from populations at $0.7K$ subjected to an overharvest.	123
Fig. 45.	Mean male age in the harvest as populations at $0.7K$ decline or return to stable equilibria.	127a
Fig. 46.	Mean female age in the harvest as populations at $0.7K$ decline or return to stable equilibria.	127b
Fig. 47.	Median male age in the harvest as populations at $0.7K$ decline or return to stable equilibria.	127c
Fig. 48.	Proportion male among adults in the harvest as populations at $0.7K$ decline or return to stable equilibria.	127d
Fig. 49.	The proportion male among adults in the harvest as	

populations at $0.4K$ decline to extinction or return to stable equilibria.

Fig. 50. Mean male age in the harvest sample from populations allowed to increase despite harvesting by increasing their carrying capacity.128

Fig. 51. Proportion males among adults in the harvest sample from populations allowed to increase despite harvesting by increasing their carrying capacity.129

Fig. 52. Mean male age-distributions, showing the subtle differences between the 4 Specific Models.131

Fig. 53. A schematic diagram of a sustained yield curve, showing the comparisons made between age-structures of populations at different cross-sections subjected to the same harvest level.146

Fig. 54. The discriminant index as applied to Montana grizzly bear harvest data (Greer 1971-1982), compared with the analysis by Klaver (unpubl.) and the total legal harvest each year.164

Fig. 55. The discriminant index as applied to the Montana grizzly bear harvest data, showing contributions made by the individual variables.165

Fig. 56. A generalized sustained yield curve, showing the region of stability implied by the existence of the probability band.172

Fig. 57. The power of the discriminant index as a function of the probability of Type I errors.179

Fig. 58. Harvest rates associated with different values of the discriminant index.181

INTRODUCTION

Overview

The grizzly bear (*Ursus arctos*) has evolved a life-history characterized by low reproductive capacity, long and vigorous protection of young, high survival of adults, and long life-span. Although this 'K'-selected strategy (Pianka 1970) has enabled the grizzly to inhabit diverse ecosystems throughout the Northern Hemisphere, it has become a liability in its interactions with man (Goodman 1981). While aggressive defense of young, along with the capability of killing large animals, has left the bear free of natural enemies, it has frequently made an enemy of man. And while low productivity has been balanced by high survival under natural conditions, it has exposed grizzly populations to a high risk of extirpation where mortality rates are increased by man.

The inability of grizzly populations to absorb significant human-caused mortality has made it an especially difficult animal to manage. Because of the impossibility of censusing bears, (Hebert et al. 1983), grizzly population managers invariably lack reliable population estimates. Even reliably discerning gross population trends is difficult within the relatively short time-frame which management agencies must work (Harris, in press). In many big-game species, the size and composition of hunter-harvests may help managers assess population status. But the complexity of grizzly bear population dynamics and the small size of hunter-harvests presently make

interpretation of kill statistics ambiguous.

Despite the lack of data on specific populations, there is no reason to doubt that grizzly populations behave qualitatively like most large-mammal populations when subjected to harvest. Some are relatively stable and produce a sustainable yield; others are over-harvested and decline. The dichotomy between 2 states - stable, with a sustainable yield, and declining, possibly to extinction - has been shown by theoretical models to be characteristic of harvested populations (Noy-Meir 1975). Theoretical models have also shown that the boundary between these 2 states may be abrupt rather than gradual (May 1977), and that big-game harvest systems may often exist near this boundary (Metzgar 1984). Given the insensitivity of present techniques for monitoring grizzly bear populations, it is likely that a grizzly population could move from a stable to a declining state without detection.

In this thesis, I examine simulated hunter-kill data for grizzlies, with a focus on detecting population declines. Although I depend on basic concepts of harvested population dynamics arising from differential equation models, my perspective is that of a game manager. Thus, I touch upon both the theoretical and the applied domains. My hope is that the reader whose interest is restricted to only 1 of these domains will have patience with the portions of the thesis that explore the other.

Properties of Harvested Populations

The basic dynamics of harvested populations are well known (Clark 1976, Beddington and May 1977). Net growth rates are usually functions of density, so that per capita increases are greater at low densities than at high. In the unharvested state, net growth rate becomes zero at the equilibrium density, K . A constant and sustainable harvest reduces the equilibrium density to some K^* , which is always less than K .

Sustained Yield Curve

The dynamics of a harvested population are summarized by its sustained yield curve (Fig. 1). The curve represents all the equilibrium points in the 2-dimensional space representing sustained yield (Y axis) and population level prior to harvest (X axis). It is analogous to the prey zero-isocline that would be produced by a predator-prey model in which the predators had no functional response (Holling 1965).

Sustained yields are small at low population levels because the absolute number of individuals is small. At population levels near K , the sustained yield is also low, because the regulatory factors that lead to equilibrium in the unharvested state (i.e. declining recruitment, increasing mortality) predominate. This leads to low net growth rates, and few surplus (harvestable) individuals. Sustained yield is greatest at some intermediate population level where the stock

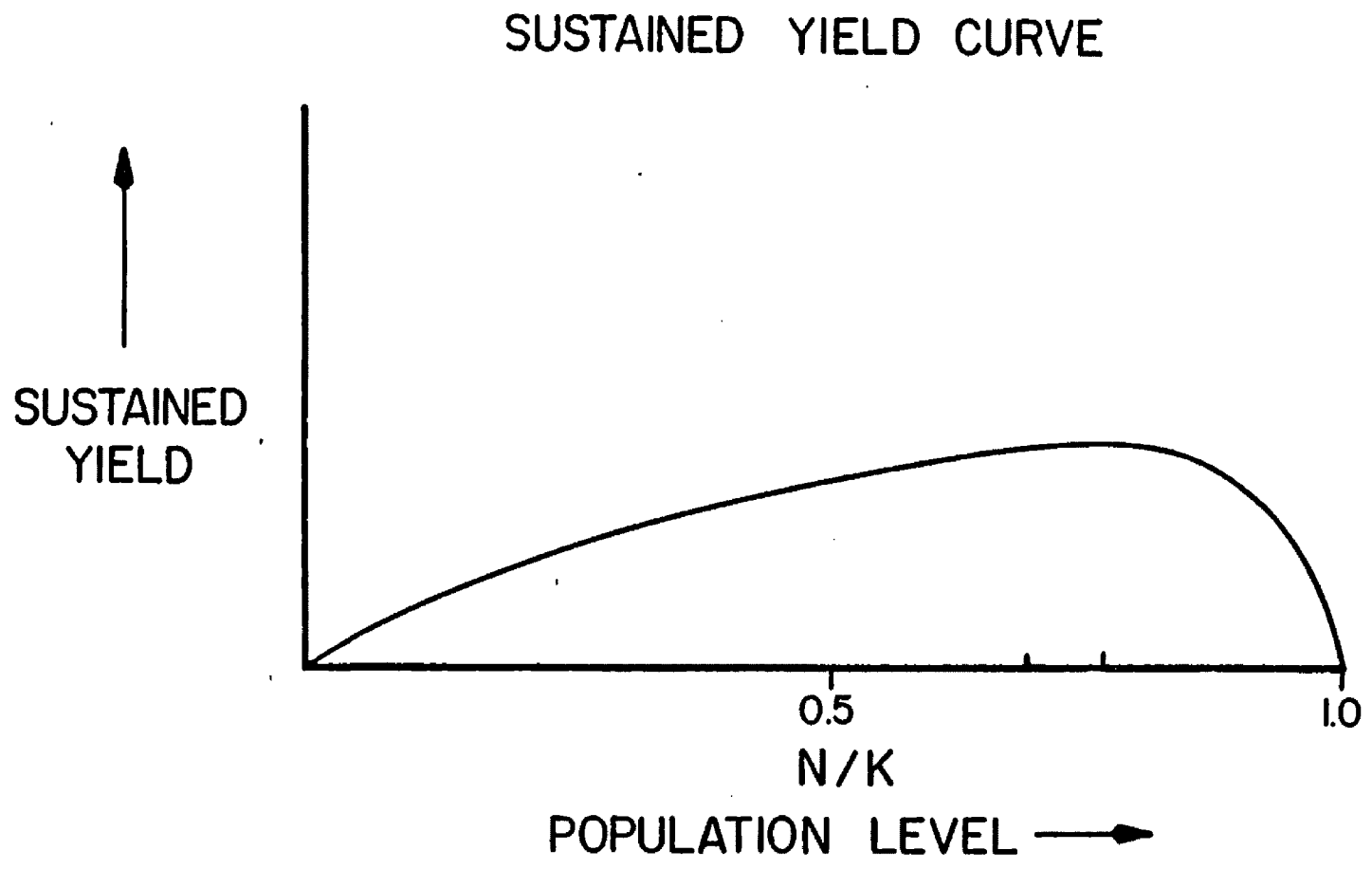


Fig. 1. A generalized sustained yield curve. Population is considered relative to its carrying capacity, K .

is moderately high but the natural regulatory factors relatively weak. These combined dynamics produce a characteristic dome-shaped yield curve (Fig. 1).

Yield curves have been explored primarily in differential equation models (e.g. Brauer and Sanchez 1975), but they also accurately portray the qualitative behavior of real systems (Caughley 1977, Gross 1969, Fowler et al. 1980, Metzgar unpubl. data).

Other curves

The sustained yield curve is sometimes equated (erroneously) with the stock/recruitment curve and with the increment, or net production curve (e.g. Gross 1969,1972; Caughley 1977; Savidge and Ziesenis 1980). The latter 2 curves are similar, but not identical, to the sustained yield curve. Each of the 3 related curves is generated by different data, and their correct interpretation produces slightly different management implications.

The stock/recruitment curve (Fig. 2.a) represents the effect of adult density on the number of recruits. It's shape is usually not a closed dome, because some young are recruited even at very high stock levels (Ricker 1975). It can be generated directly from field data, if available (e.g. McCullough 1979,1981; Stringham 1983). General models for stock/recruitment relationships have been developed primarily in the fisheries literature (Ricker 1975).

The increment, or net production curve represents population growth as a function of population level (Fig. 2.b). It can be generated by data of population growth over time, or by a model of

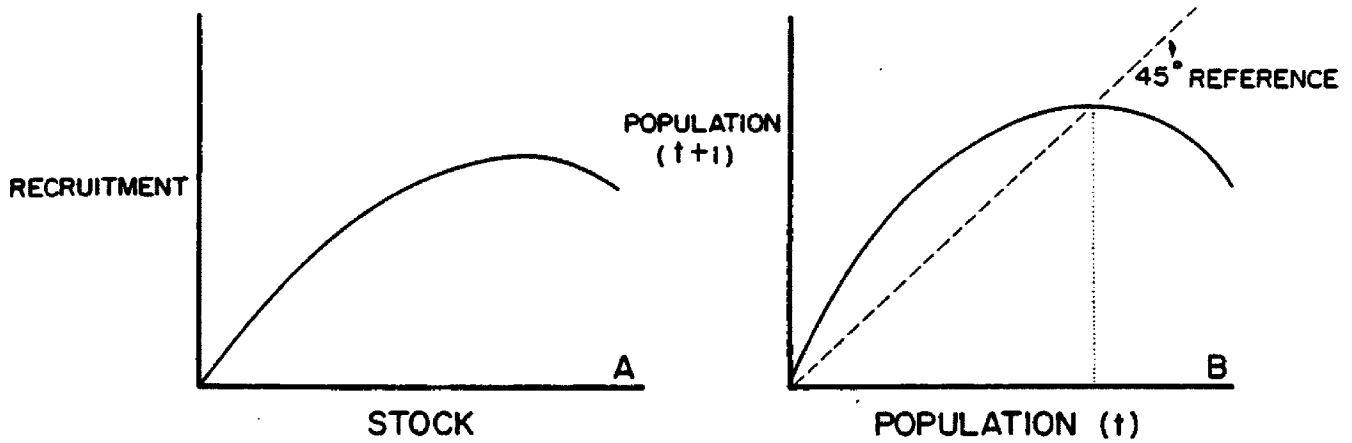


Fig. 2. Two curves often confused with the sustained yield curve. a. Generalized stock/recruitment curve. b. Generalized increment, or net production curve. The dashed line represents equal population sizes at times t and $t+1$.

population growth (e.g. the logistic). Although the increment curve has approximately the same shape as the sustained yield curve (and for the same reasons), it is not capable of accurately quantifying sustainable harvests. Actual sustainable yield will differ from that implied by the increment curve according to the sex and age of the animals harvested (McCullough 1979, Fowler 1981, Harris and Kochel 1981).

The sustained yield curve plots actual sustainable harvest against population level, and is thus the most difficult of the 3 to generate empirically. Rarely can a natural population be manipulated to explore its response to a broad range of harvest levels. The few existing data sets arising from empirical studies come from small experimental populations (e.g. Silliman and Gutsell 1958, Harris and Kochel 1981). Most often, the sustained yield curve must be generated by simulation (e.g. Lett et al. 1981).

The 3 curves coincide exactly only for a population with non-overlapping generations, in which the size of each generation depends on the size of the previous generation. In age-structured wildlife populations, where each age class typically has a unique reproductive value (Fisher 1958, Wilson and Bossert 1967), only the sustained yield curve accurately depicts the population's response to constant harvest.

Shape of the Sustained Yield Curve

The logistic model is the most often used population growth model that incorporates density dependence:

$$dN/dt = rN (1-N/K)$$

In logistic growth, the inflection point occurs at exactly $N = K/2$. This is generally interpreted as the population level giving maximum sustained yield (MSY). The symmetrically domed shape, often seen in text-book illustrations of sustained yield curves, results from population level N_{msy} occurring exactly half way between the origin and K (Caughley 1977).

Despite its intuitive appeal, the logistic model fails, even in the abstract, to adequately describe the growth form of most large-mammal populations (Fowler 1981). Its failings stem from oversimplified assumptions, specifically that the addition of 1 individual decreases the growth rate by a constant amount at all population levels, (i.e. r decreases linearly with density), and that density dependence influences even the very smallest populations, (i.e. there is no density at which growth is exponential).

The idea that density dependence in large-mammal populations occurs primarily at high population levels, near carrying capacity, is supported by both empirical and theoretical evidence (Gross 1969; Fowler et al. 1980, Folwer 1981; Eberhardt and Siniff 1977; Eberhardt 1977b; Gulland 1970; McCullough 1979). Typically, growth rates are nearly exponential over a broad range of low densities and drop off markedly only as resources become relatively scarce, at high population levels. This leads to an asymmetrical curve, skewed to the left (Fig. 1).

Dynamics of the Sustained Yield Curve

Regardless of its exact shape, the sustained yield curve always has the same general properties (Fig. 3). The curve itself is dynamic; that is, minor stochastic perturbations continuously move the population around, prohibiting it from settling on any part of the curve indefinitely.

On the portion of the curve to the right of N_{msy} (solid line, Fig. 3), this is of little consequence. If the population level declines slightly, compensatory increases in natality and survival move the population to the right, back toward the curve. Conversely, if the population grows too large, the effects of high population levels combine with the harvest to push the population back to the left until it again hits the curve. Because of this tendency toward adjustment following disturbance, the descending right-hand portion of the curve is always stable. However, the situation is qualitatively different on that portion of the curve to the left of N_{msy} (dashed line, Fig. 3). Here, the dynamic curve produces a knife-edge, or release point, because populations to the right move toward the stable portion of the curve, but populations to the left move towards extinction. The descending left-hand portion of the curve thus represents unstable equilibria (May 1977, 1979; Beddington 1979).

A population declines chronically if it contains just 1 less individual than is sustainable for a particular harvest. Similarly, it declines chronically if it is continuously harvested by just 1 more individual than is sustainable at a particular population size. The abrupt change from stability to eventual extinction, due to the

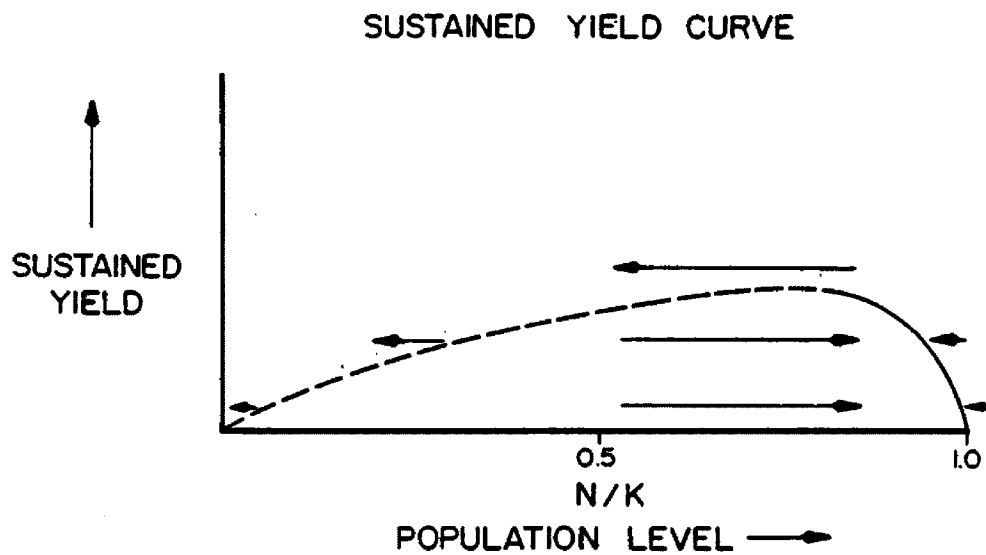


Fig. 3. A generalized sustained yield curve, showing trajectories of populations. The arrows indicate directions populations will follow.

additional harvest of 1 critical individual, is demonstrated by Fig. 4, adapted from May (1977). Here the axes of the previous figures are reversed, and the effect of "dropping off" the surface of stability towards extinction is more clearly seen.

The population decline may not progress fully to extinction if, as population levels decrease, the effort needed to keep yield constant becomes impossibly high. If declining yield per effort results in a reduction in harvest at low population levels, the population may enter an "effort refuge", stabilizing at a lower equilibrium (May 1977, 1979; Beddington 1979; Peterman et al. 1979), and thus avoid extinction. However, whether or not an "effort refuge" exists, the general behavior of the system is the same. In either case, the unstable equilibria are always release points. Whether or not depressing a population below a release point leads to extinction equilibrium depends on the degree to which harvest is reduced at low population levels. Review of this subject is beyond the scope of this paper, but the alternative to extinction, a second stable equilibrium, is likely to be a dangerously low population level. This small population would face the threat of eventual extinction from the effects of stochastic demographic variation (Shaffer 1978), lack of genetic variability (Frankel and Soule 1981), or both. Were harvesting stopped and genetic and random effects benign, the population would slowly recover to an acceptable level. However, a grizzly bear population would take many years to do so.

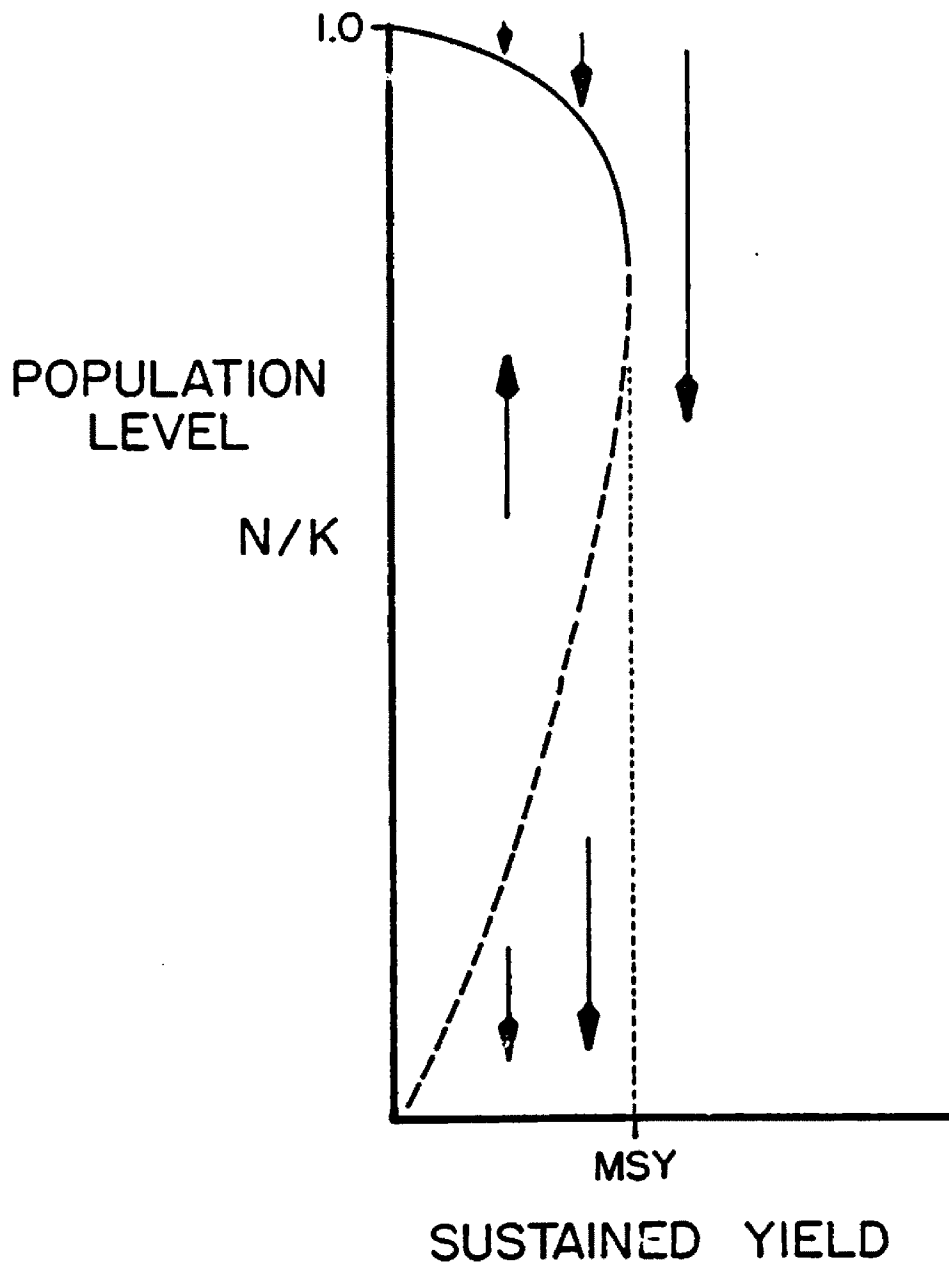


Fig. 4. The dynamics of sustained yield, adapted from May (1977). The arrows indicate population trajectories. The solid line at the top of the curve represents stable equilibria; the dashed line represents release points. As yield increases, population level declines slowly until yield reaches MSY; then drops precipitously to extinction.

Age-Structure Analyses

A population's rate of increase is determined by its natality rate, its survival rate, and its age-structure. In attempting to assess population change, wildlife biologists have often used such age ratios as fawn:doe or young:adult. If the data collected are sufficiently detailed, such indices provide a measure of recruitment, but they cannot, of themselves, indicate the direction of population change (Gill 1953, Caughley 1974, Grier 1979). For example, Caughley (1974) demonstrated that increased or decreased survival over all age classes produced no change in commonly reported age ratios. Further, he noted similar age ratios among those populations that increased due to higher recruitment rates, and those that declined due to lower adult survival rates. He concluded that "...age ratios cannot be interpreted without a knowledge of rate of increase, and if we have an estimate of this rate, we do not need age ratios." Bunnell and Tait (1980) developed this theme by looking not merely at simple ratios, but at the entire age-structure relative to the youngest age class (S_x schedule). They similarly concluded that age-structure alone could not indicate the direction of population change unambiguously.

However, if declining and increasing populations show similar age-structures, they do so for different reasons. A "younger" age structure can result from more young animals or less old animals, but in the former case the total number of animals increases, and in the latter it decreases. If the population is subjected to a hunt in which the

probability of survival differs by sex/age class, then the harvest structure will respond to both the relative numbers in each class (S_x) and to the absolute numbers in each class. Applying a constant harvest with unchanging relative vulnerabilities to a changing population is analagous to taking a fixed slice out of a changing pie. The size of the slice remains constant, but the composition changes with the size of the pie. The harvest may thus contain more information than age ratios alone, and may be capable of indicating population trajectory.

The ratio of males to females in the harvest is known to respond both to the male:female ratio of the pre-harvest population and to the degree of hunting pressure. Heavier harvests display increased percentages of females among older harvested moose (Fraser 1976), reindeer (Reimers 1975), and black bears (Bunnell and Tait 1980, Gilbert et al. 1978). Bunnell and Tait (1980) demonstrated that this correlation necessarily results when harvests are biased towards males. Because few males survive to the older age classes, sex ratios of older harvested animals favor females. In the extreme case, where all animals die from hunting, the overall sex ratio of the harvest equals the sex ratio at birth, but is biased toward males in the young age-classes, and toward females in the old age-classes. Gilbert et al. (1978), followed this same line of reasoning in suggesting guidelines for interpreting harvest statistics from legal hunts of black bears. They concluded that the percent males in the kill, the sex ratio in both young and old ages-classes, and the "average" age of the kill could all provide clues to population status. However, they did not quantify their guidelines, and they warned that chance variability associated with small samples

could easily mislead the investigator.

Following on the work of Fraser (1976), Paloheimo and Fraser (1981) developed a procedure that exploits differential vulnerability by sex in estimating the rate of harvest from hunter-kill data. If the hunter-kill is assumed to be the total harvest, population estimates follow directly from the harvest rates. The method grew out of analyses of fisheries, and, as such, requires some assumptions that are often violated by large-mammal populations. It requires an independent estimate of harvest effort, or alternatively, the assumption of constant effort, but reliable estimates of effort are difficult to obtain for recreational harvests. Additionally, it requires a natural mortality rate that is independent of age, a constant relative vulnerability to hunting within each sex, and a known (or assumed) sex ratio at the first harvestable year. These assumptions may not be met by bear populations, in which a distinct sub-adult class is generally considered to have higher natural and hunting mortality rates than adults, and in which differential mortality of male cubs may skew the sex ratio prior to the first harvestable class. In such a situation, Paloheimo and Fraser (1981) recommended using only the relatively homogenous adult age-classes. However, doing so reduces sample size and severely impairs the method's utility for bears. Fraser et al. (1982) reviewed the applicability of the procedure for black bear populations and made suggestions for minimizing violation of assumptions.

Tait (1983) also developed a procedure for analyzing population status that relies on the different vulnerability to hunting of age/sex classes. The procedure uses harvest data from a series of years, as

well as estimates of life-history parameters to "reconstruct" the most probable population for each year of the data set. The procedure performed well on simulated populations, but has yet to be rigorously tested on field data (Tait, pers. comm.).

OBJECTIVES

The 2 primary objectives of this study were:

(1) To describe the sex and age structures of grizzly bear populations and grizzly bear hunter-kill data from simulated stable and overharvested systems.

(2) To develop an index to discriminate stable from overharvested populations using age-structures from hunter-kill data, and to quantify the sensitivity of the index.

The data for analysis were generated by a simulation model that incorporated the relevant aspects of grizzly bear population biology. The simulation model is described in the next section.

SIMULATION MODEL

General Structure

Overview

The simulator is a stochastic, discrete time, age-structured projection model that follows the history of individual grizzly bears from birth until death. As with Leslie-matrix based models (Leslie 1945), it uses age-specific mortality and natality rates, but unlike Leslie-based models, survival and reproduction of each individual in each year is randomly determined with probabilities equal to the age-specific rates. Mortality and natality may be density-dependent or density-independent. Natality is determined from 3 separate functions: breeding, birth of cubs, and dispersal (weaning) of juveniles. This procedure retains the 3 important determinants of overall natality in bears; age of first reproduction, litter size, and breeding interval (Bunnell and Tait 1981). Environmental variation may be introduced through the variable K , the carrying capacity.

In addition to age-class (0 - 24), the model considers bears as belonging to 1 of 8 life-history categories:

- 1) juvenile of either sex (with mother);
- 2) lone male;
- 3) female without juvenile;
- 4) pregnant female;

- 5) female accompanied by 1 juvenile;
- 6) female accompanied by 2 juveniles;
- 7) female accompanied by 3 juveniles;
- 8) dead.

In this thesis, a juvenile is defined as a bear of any age that is under the care of its mother. A cub is a bear in its first year. A sub-adult is a pre-reproductive bear that no longer travels with its mother. Thus, for example, an 18-month old bear may be either a juvenile or a sub-adult, depending on whether it had been cast-off by its mother the previous spring.

During each iteration, each bear is subjected to 5 events at which it can change from 1 category to another (Fig. 5). Whether it changes or retains its category is determined by comparing its age-specific probability of change to a random (0,1) variate from a uniform distribution. This sequence of Bernoulli events creates demographic stochasticity, the magnitude of which is inversely related to population size (May 1974).

Density-Dependence

Natural survival and the 3 natality components can be modeled as functions of N/K , where N is the total number of animals at the time of calculation. This is a resource per capita approach (Getz 1983), implying that individual animals compete for a finite resource. Alternatively, survival of sub-adult males can be considered a function of N_m/K_m , where N_m is the number of adult males in the population at the

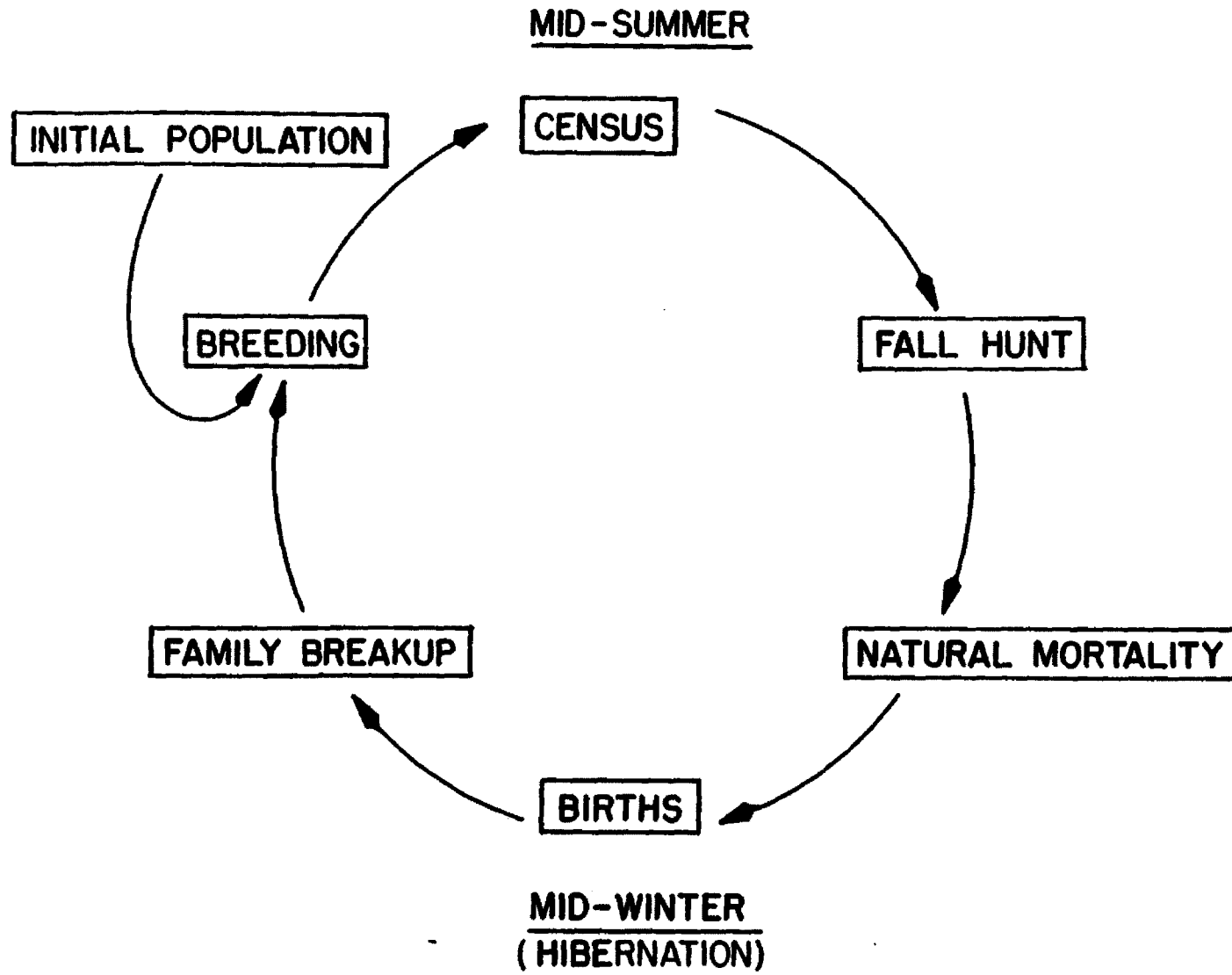


Fig. 5. Life-history events of grizzly bears, as simulated in the model.

time of calculation, and K_m is the saturation number of adult males. This alternative is discussed further in the Specific Models section.

Density dependent functions take the general Michaelis-Menton (MM) form:

$$\text{Rate} = m + s \left[1 - \frac{(N/K)^x}{(0.05 p^x) + (N/K)^x} \right] \quad (2)$$

where:

- m = the minimum value the rate can take, $0 \Rightarrow m > 1$
- s = scaling factor for the rate, $s = (\text{maximum value} - \text{minimum value})$
- N = population size at time of calculation
- K = carrying capacity at time of calculation
- p = value of N/K at which the rate is to take the value 95% of the maximum
- x = exponent, controlling the slope of the function

Despite its imposing appearance, the MM equation facilitates simple fitting of density-dependent functions flexibly while retaining the biological interpretation of each variable. The part of Eq. 2 in brackets can take values from 0 to 1. As some function may have a minimum of greater than 0 and/or a maximum of less than 1, the variables m and s are used to re-scale the function appropriately. The variable p is a saturation level; it gives that population level relative to the carrying capacity at which essentially no further change in the rate is biologically possible. Exponent x controls the shape of the response relative to the change in density, N/K . An algorithm within the simulator solves for x when supplied with 2 points along the N/K axis (Fig. 6). The required points are the value of N/K at which 50% and 95% of the change in rate is to occur. Thus, fitting a density-dependent

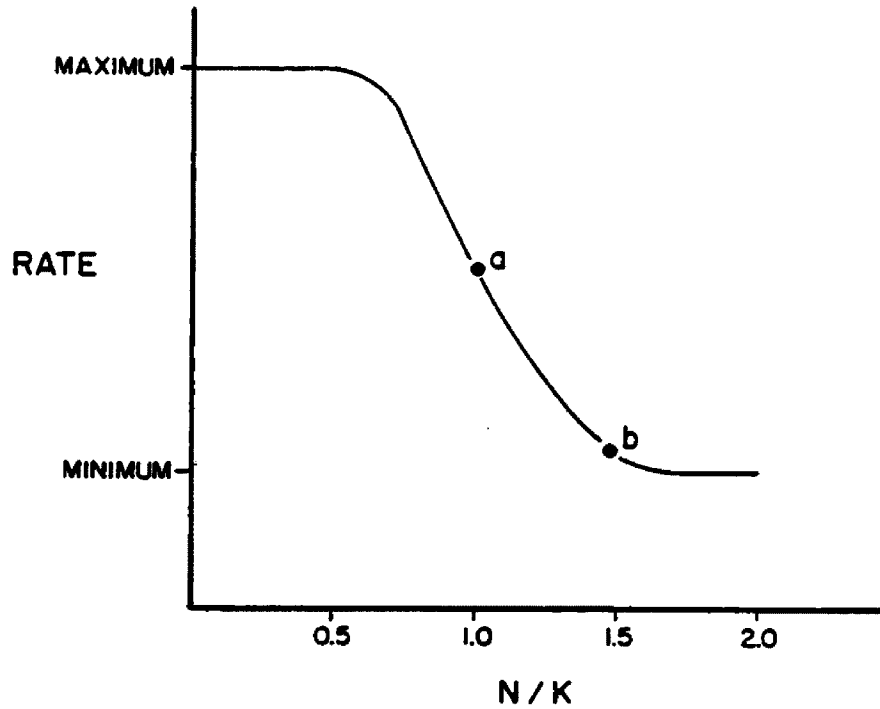


Fig. 6. A generalized Michaelis-Menton function, as used in the simulation model. Point 'a' is chosen by the user at the N/K value at which 50% of the change from maximum rate to minimum rate is to occur; point 'b' is analogous for 95% of the change. Functions used in the simulation typically changed little at low N/K values, but dropped steeply as N/K approached 1.0.

function with a MM equation simplifies to choosing these 2 points, as well as setting the minimum and maximum values the rate may take.

A density-independent (i.e. constant) rate can also be fitted in either of 2 ways. First, by simply designating both minimum and maximum values as the desired constant rate, it can be seen that $s = 0$, so the rate takes the value m (the minimum) for all values of N/K . Alternatively, the value of N in the equation can be set permanently at K , (instead of the actual number in the population). This way, N/K always takes the value 1.0 if K is constant (but see below), resulting in a constant rate.

Environmental Stochasticity

The carrying capacity, K , may be assumed constant throughout the simulation, or may vary independently each year to simulate environmental variation among years. With variable K , density-dependent rates are calculated using the MM equation with N_i/K_i , where K_i as well as N_i is year-specific. Density-independent rates are calculated by substituting the median (expected value) K for N_i in the MM equation. Thus, when K_i equals K , all rates assume values corresponding to a population exactly at carrying capacity.

Variation in K_i is proportional to K , e.g. values of twice and one-half the median are equally probable in any given year. The log-normal is used as the underlying frequency distribution for K_i because it models equal probabilities of proportional deviations from the expected value (Fig. 7). The magnitude of variability in K_i is

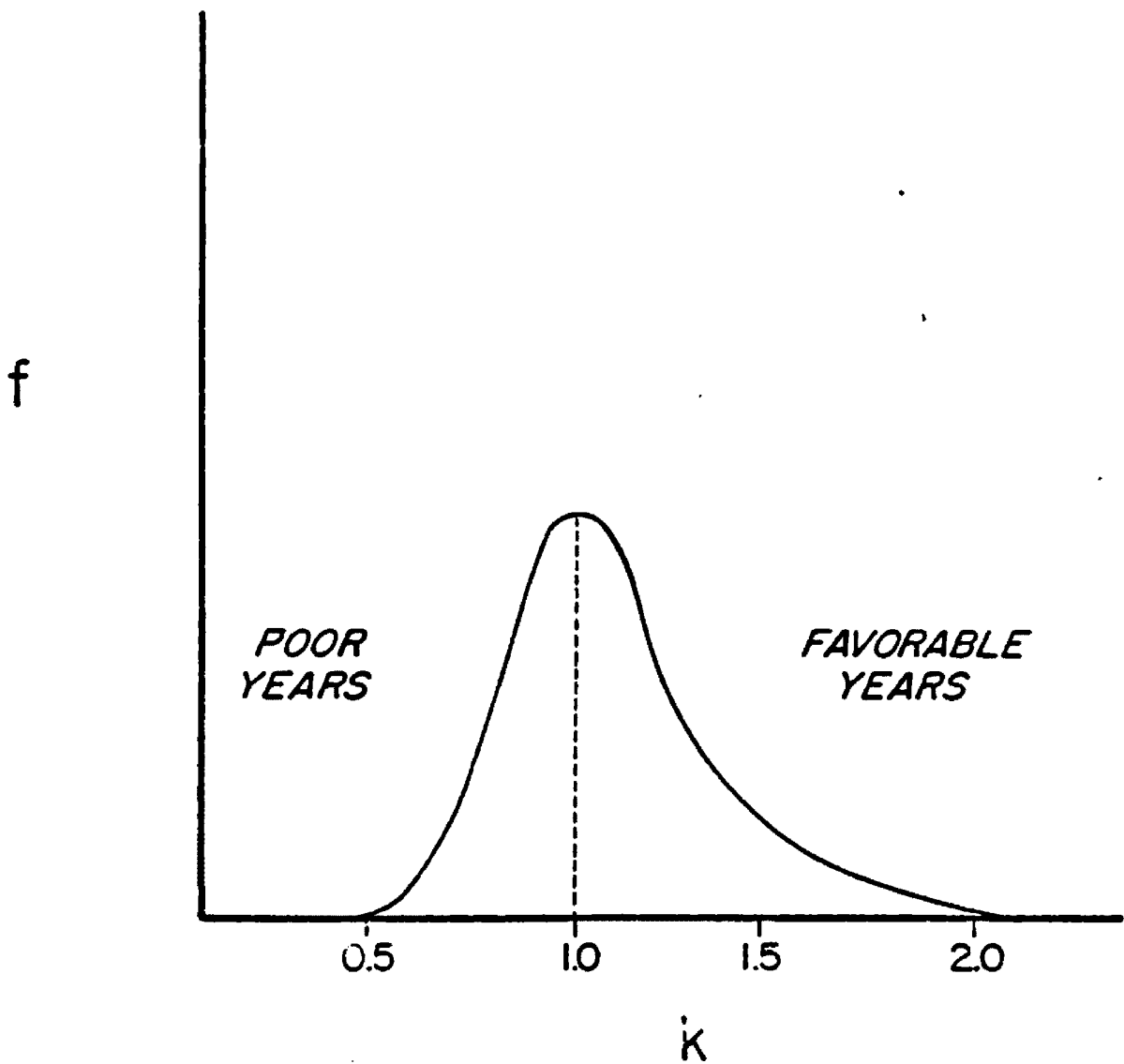


Fig. 7. A generalized distribution of K values, showing the log-normal distribution used in the simulation. Poor years and favorable years occur with equal frequency, although the distribution is skewed to the right. The variability of K displayed is greater than was used in the model; see text.

determined by specifying the proportion of the median K within which 95% of yearly K_i values will fall.

The inclusion of environmental stochasticity directly within K rather than separately in each rate function has an important biological interpretation. Because K remains constant within each simulation year, survival and density-dependent natality rates for that year are dependent on the same value of N_i/K_i . Thus, when K_i deviates negatively from its median value, (i.e. the carrying capacity is lower than average), survival and natality both decline. When K_i deviates positively, both survival and natality increase. This procedure simulates the effect of good and poor years of food availability simultaneously on survival and reproduction.

Sequence of Events

Within each simulation year, each life-history event takes place only once, and is placed in the sequence most nearly resembling nature (Fig. 5).

Initial Population

The simulation can be initiated in 2 ways. A population structure consisting of males and females aged 0 through 24 may be specified. In this case, each animal is considered unrelated to any others, and all are assigned identification numbers, beginning with the oldest animals. Alternatively, the simulation can be initiated with a population generated by a previous run. In this case, the family history of each animal from the previous run is preserved, so

female-juvenile relationships and prior breedings are known. Using an initial population generated by a previous run eliminates the influence of an arbitrary initial age-structure on the resultant simulation. It also enables simulating an abrupt change in birth and survival rates, by using a population that had been generated under a different set of rates.

Breeding

If a starting population structure of independent animals is used, breeding is the first process encountered. This allows the first year of the run to include pregnant females. If the starting population has been generated by a previous run, breeding is skipped in the first year only because the population has already been "bred" during the last year of the previous run. In either case, the breeding process is applied only to females that are unaccompanied by juveniles.

Breeding rates are age-specific. Thus, the age at first breeding may be modeled either as a step function, by assigning zero breeding rates to pre-reproductive age-classes, or as a continuous function, by gradually increasing the breeding rate over a range of years. For each female breeding, an adult (age 4+) male is randomly selected to be the "father" of her cubs. If no adult males are present, no females breed.

Census

The census is a complete head count of the entire population. The placement of the census after breeding and before the fall hunt comes close to the circumstances under which biologists most commonly observe bears. Cubs are identifiable in the field and family groups

travel together.

The mid-summer census provides all data on numbers and age-structure for the total population. It also provides a reference point against which the hunted sample can be compared.

Fall Hunt

The population is subjected to a fall hunt that removes any desired number of animals, up to and including the total population. The sex and age of each individual killed is recorded, enabling the hunt to serve as a sampling of the population age-structure, as well as a life-history event.

Individuals are killed or survive the hunt according to the same type of Bernoulli process used for natural mortality and reproductive components. Each animal is exposed to the hunt sequentially by order of its identification number, and the process is continued until the desired number of animals is removed. Because older bears have higher identification numbers than younger bears, they are exposed to the hunt first. This procedure biases the age distribution of the hunt in favor of older animals if the desired harvest is reached before all animals have been examined. To minimize this bias, the program first executes an algorithm that re-calculates the relative vulnerabilities of each life-history/age-class proportionally, to insure that, on average, 10 passes through the entire population are required before the desired number are killed. This algorithm effectively reduces to inconsequential the bias for older animals in the harvest.

The model allows for assignment of relative vulnerability rates by age, and by the life-history categories of lone male, lone female,

mother with juveniles, and juveniles with mother. It also allows for a change in a bear's life-history category during the hunt, if needed. For example, a yearling juvenile becomes a sub-adult yearling if its mother is killed. This enables the simulation of increased vulnerability of juveniles to hunting following the death of their mother. Similarly, a female whose only juvenile (or juveniles) is killed becomes a lone female for the remainder of the hunt.

Natural mortality

Data from wild populations on timing of natural mortality is lacking. In the model it is placed after the fall hunt. When using a density-dependent rate, the variable N/K is calculated using the post-hunt population size.

No distinction is made between natural mortality rates for adult females with and without juveniles. As in the hunt, individuals are examined in order of their identification codes, and any juvenile whose mother dies during that run is automatically transferred from the juvenile-with-mother category to the lone male or lone female category. However, unlike the hunt, an absolute number of deaths is not specified. Thus all individuals are exposed to natural mortality, the sequence ending only when every individual has been exposed, and no potential exists for bias in the age-structure of those dying.

Births

The birth process is applied only to females pregnant from the previous breeding event. No mortality occurs between birth and the following census, so the birth rate is more accurately considered a recruitment rate to age 0.5. Consequently, the litter size at "birth"

is really the litter size seen at mid-summer.

Litter sizes vary from 0 to 3 and are determined from probabilities that are age-specific. A litter size of 0 simulates mortality of all cubs in the den. A female losing all of her cubs is thus a candidate for breeding again during the following spring. Relative probabilities for each litter size are specified, and the program executes an algorithm that re-calculates each so that the cumulative probability equals 1.0.

Expected sex ratios of cubs at birth can be assumed 1:1 or held constant at any other ratio. Litter size and sex ratio probabilities are calculated with the MM equations described above, and thus may be functions of N_i/K_i or K/K_i .

Family Breakup

Prior to the spring breeding period, family groups enter the dispersal period, during which the mother may cast-off her juveniles. Probabilities of family breakup are specific to the age of the juveniles. If the mother casts-off her juveniles, she becomes a lone female and enters the subsequent breeding period. If she retains her juveniles, she does not participate in the subsequent breeding period. Thus, the age at which juveniles are cast-off largely determines the length of the breeding cycle of mature females.

Specific Models

The flexibility of the general model structure allows the creation of specific models reflecting slightly different assumptions

regarding the natural regulation of grizzly bear populations. Although biologists share a general consensus that unexploited bear populations stabilize in some density-related fashion, they propose alternative mechanisms by which density-dependence manifests itself. I use specific models for 4 contrasting mechanisms:

(1) Model DDALL (Density-dependent for all functions): All mortality is density-dependent, as are the 3 natality components; breeding (age at first reproduction), birth (litter size), and family breakup (breeding interval). The variable N_i used in the MM equations includes the entire population. The biological interpretation of this model is that competition among all individuals regulates the population through decreasing survival and natality as resources per individual diminish.

(2) Model DM (Density-dependent mortality only): All mortality functions are density-dependent, as in Model DDALL, but all natality functions are independent of density, varying only in response to environmental fluctuations. This model follows Bunnell and Tait (1981), who suggested that natality of female grizzlies is nutrition-based, and that nutritional status is not substantially affected by population density. In biological terms, population regulation occurs solely through the competitive effects of density on mortality rates of all age-classes.

(3) Model ADM (Adult males influence mortality of sub-adult males): Birth rates and adult mortality rates are density-dependent as in Model DDALL, but mortality rates of sub-adult males (age 4 or less) are functions of the number of adult males present (i.e., the MM

equations use N_m/K_m rather than N/K).

Many biologists have concluded that adult males contribute disproportionately toward the suppression of cub and sub-adult recruitment in bears. McCullough (1981), using data from Craighead et al. (1974), demonstrated this for grizzlies in Yellowstone National Park, although he did not distinguish between recruitment suppression of males and females. He did, however, find a higher mortality rate among sub-adult males than among sub-adult females. Stringham (1980, 1983) used slightly different analyses and came to similar conclusions. Bunnell and Tait (1981) suggested that suppression of recruitment by adult male bears is felt primarily by sub-adult males. Such was the case in a relatively stable, un hunted black bear (*Ursus americanus*) population in Alberta (Kemp 1972, 1976; Young and Ruff 1982), in which experimental removal of adult males led to increased recruitment of sub-adult males. A few years after the removal, when the newly recruited males had themselves become adults, recruitment of sub-adult males again declined. Young and Ruff (1982) believed that sub-adult males were forced to disperse from the population in the presence of adult males. Other authors (Stringham 1983, Bunnell and Tait 1981, Craighead and Craighead 1967, Troyer and Hensel 1962, Rogers 1977) have discussed killing of male sub-adults and cubs by adult males. It is presently not clear whether suppression of male recruitment is caused more by forced dispersal of sub-adults from the population, or by direct killing by older males. However, as Model ADM treats only a single closed population, dispersal and death of sub-adult males are functionally equivalent, both leading to permanent removal from the

population.

Model DMADM (Density-dependent mortality, influenced by adult males): This model combines the density-independent natality functions of Model DM and the sub-adult male mortality functions of Model ADM. It closely models the pattern of population regulation suggested by Burnell and Tait (1981).

Common to all 4 Specific Models are the following:

(1) Environmental stochasticity affecting all rates: For Models ADM and DMADM, environmental fluctuations within each year have the same proportional effect on sub-adult male survival as on all other rates.

(2) A 50:50 sex ratio of cubs at birth: Craighead et al. (1974) found an imbalanced sex ratio of cubs favoring males, although they assumed a 50:50 birth sex ratio in their population projection model. McCullough (1981) hypothesized that a male-biased sex ratio at conception could be the result of higher mortality rates of sub-adult males (Fisher 1958). Although this is intriguing, and potentially important, the overall data are presently inadequate to model the response of sex ratio at birth to differential mortality patterns. Therefore, equal sex ratios at birth are used throughout.

Life-History Rates Used in the Simulations

Grizzly bear populations in North America can be grouped into 3 types: coastal, northern interior and southern interior. Although not genetically isolated from each other, these groups show relatively

distinct trends in productivity. The lowest productivity occurs among northern interior populations in Yukon and Alaska (Pearson 1975, Reynolds 1976); the highest occurs in the coastal populations of British Columbia, southeastern Alaska, Kodiak Island, and the Alaska Peninsula (Glenn 1973,1975; Glenn et al. 1976, Hensel et al. 1969).

The natality and survival rates used in this thesis are those of a generalized southern interior population, i.e., a population from the area bounded by the national parks of the Canadian Rockies on the north and Yellowstone National Park on the south. The intent was not to mimic the behavior of a particular population, but rather to create a "typical" population by combining the best available data from similar areas. Data came from un hunted populations in Glacier National Park, B.C. (Mundy and Flook 1973), Glacier National Park, Montana (Martinka 1974; pers. comm. 1984), and Yellowstone National Park (Craighead et al. 1969, 1974; Knight et al. 1983, Knight and Eberhardt, unpubl.); as well as hunted populations in southeastern B.C. (McClellan 1983), and northwestern Montana (Jonkel 1982, Aune and Stivers 1983, K. Aune, pers. comm.). Additional reference was made to the summaries of population dynamics by Stirling et al. (1976), McCullough (1981), and Bunnell and Tait (1980, 1981).

Although differences in mortality and natality among these data were evident, broad patterns that emerged were incorporated into the rates. During preliminary simulations, mortality and natality rates were adjusted until they (i) agreed generally with the data, and (ii) resulted in populations that, on average, equilibrated at K.

There were no data upon which to base the exact forms of the

response of mortality and natality to changing environmental conditions or density. Shapes of the density-dependent λ rate functions generally followed Fowler (1981). He suggested that natality and mortality rates of large mammals show little response until population densities near K , but then break sharply.

The survival and natality rate schedules are tabulated in Appendix A; the relative vulnerabilities to hunting in Appendix B. The general patterns and biological interpretations of the life-history rates used are summarized below:

Survival. Adult survival rates are highest for ages 5 through 12, lower for ages 13 through 20, and lower yet for the oldest age-classes, 21 through 24. Female survival is slightly higher than male survival across all adult age-classes because of the security afforded by their generally smaller home ranges. Male survival is depressed more quickly by high densities or poor environmental conditions than is female survival, because males are assumed to respond to adverse conditions by dispersal or aggressive encounters more readily.

Sub-adults are assigned substantially lower survival rates than adults because of their lack of status and secure home range. Survival is particularly low for sub-adult males, especially at high densities or poor conditions, due to dispersal and/or cannibalism. Sub-adult male survival remains low until age 5, but sub-adult females attain nearly the rates of adult females by age 3 or 4. Survival of sub-adults is more responsive to density and environmental conditions than any other

group of rates.

Juveniles of both sexes are assigned high survival rates so long as they are accompanied by their mothers, but suffer high mortality if their mother dies, or if they are cast-off during or before their 2nd summer.

Natality. Age at first reproduction of females depends largely on the probability of breeding for each age-class. The variability of breeding probability due to the variability in K in the early reproductive years (ages 5,6, and 7) is considerably greater than in later years. Thus, poor conditions are assumed to impact inexperienced females disproportionately. After reaching age 8, females remain reproductively active, with no decline in their age-specific natality rates until they die.

Average litter size at equilibrium is set at about 2 cubs, and average breeding interval set at about 3 years. Litter size and breeding cycle are given less range of variation than other rates. Good conditions produce slightly more 3-cub litters and 2-year breeding intervals, while poor conditions produce slightly more 1-cub litters and 4-year breeding intervals.

Relative Vulnerability to Hunting. In lieu of quantitative data, rates for relative hunting vulnerabilities were inferred from general knowledge of grizzly bear biology and grizzly bear hunters. The hunt as simulated is opportunistic rather than oriented towards trophy animals. Hunters are assumed to kill the first grizzly they see rather than to pass up small animals in hopes of killing a large trophy. Thus for example, sub-adult males are considered vulnerable even when small

in size. No increase in vulnerability is given to very old (and presumably large) adult males. Adult males are arbitrarily assigned a vulnerability of 1, and all other sex/age-classes are considered relative to them. Adult females without juveniles are assigned a slightly lower vulnerability (0.8) than adult males because of the protection afforded by smaller home range size (Bunnell and Tait 1980). Sub-adults are given the highest vulnerability rates, 2 for females and 7 for males, because of their lack of experience and secure home ranges, and, particularly for males, their extensive wanderings. Both mothers-with-juveniles, and juveniles-with-mothers are considered to be only one-fifth (0.2) as vulnerable as adult males, due primarily to protection by law (regulations in some states protect only cubs; these rates simulated the protection of all juveniles accompanied by mothers). However, a few legally protected animals are considered likely to be killed either deliberately or due to mis-identification. The lowest vulnerability is assigned to cubs, under the assumption that even hunter mis-identification is unlikely for such small animals.

Environmental variability. With the exception of preliminary diagnostic runs, all simulations assume that 95% of yearly K values vary from 0.8 to 1.25 of the pre-specified carrying capacity. This variability is equivalent to a coefficient of variation of approximately 13%. For example, for a specified carrying capacity of 600, 95% of yearly K_i 's fall within the range 480 to 750 and approximately 68% fall within the range 540 to 675.

Review of Assumptions

At this stage, it is appropriate to briefly review the important assumptions and simplifications of the simulation model.

The model considers only a single, isolated population. Because no ingress or egress is possible, dispersal is equivalent to death. The environment in which the population exists is abstracted into the single variable K . All biotic and abiotic factors that affect the potential size of the population (e.g. prey species, competing species, availability of denning sites, berries, carrion, etc.) are subsumed by K . Further, variation in K is considered independent of population size, that is, populations are incapable of reducing their carrying capacity (e.g. by overgrazing). The carrying capacity varies each year independently of previous years, i.e. serial correlation and cycles are not modeled. As well, the variability in K is assumed proportional to K (i.e. distributed log-normally), with relatively good and poor years equally likely. Finally, the 13% coefficient of variation for yearly K is assumed representative of ecosystems for southern interior grizzly populations.

All hunting occurs in the fall, no spring hunt is modeled. The number killed, rather than the effort expended, is considered constant each year. The implicit assumption is that, at least over a broad range of bear densities, grizzly bear hunters exhibit no functional response. The hunt modeled is opportunistic rather than trophy-oriented. Relative vulnerabilities by age/sex class are determined by inherent behavioral properties of bears, as opposed to conscious selection by hunters (except for legal protection of family groups). Age/sex specific

behaviors that result in different relative vulnerabilities are also assumed independent of both bear population density and hunting pressure.

Life-history events that actually occur over a period of time are condensed into essentially instantaneous events, each occurring only once per year, and always in the same order. In nature, deaths probably occur at all times of the year; the model condenses natural mortality into the period between fall hunting and spring family breakup. This order creates a small amount of compensatory natural survival following a hunt, because mortality is lower when acting on a slightly smaller post-hunt population than an un hunted population.

Responses of density-dependent rates are assumed to follow the general pattern for large-mammals described by Fowler (1981). Thus, populations below the level at which density effects are felt have intrinsic growth rates close to the maximum biologically possible. Specific birth, death, and vulnerability to hunting rates are based as closely as possible on empirical data. In some cases, the best available data are weak or non-existent. Rates with the weakest supporting data include survival rates (particularly for orphaned cubs and sub-adults), relative hunting vulnerabilities, and values for all rates when the population is greater than K .

Finally, genetics is not treated. Inbreeding depression, as well as founder and bottleneck effects leading to loss of genetic diversity, while important considerations for conservation of the species, are assumed not to materially affect the age-structures of hunted samples.

METHODS

Definition of Terms

In this thesis, terminology is defined as follows:

Age-class. The category of age (by years 0-24) and sex (male or female) to which an animal belongs. Age-classes take only integer values; for example, an animal which in summer is 2.5 years old is a member of age-class 2. Having "age-class" refer to the entire sex by age (2 X 25) matrix eliminates the awkward "sex/age" terminology.

Age-structure. The sex by age (2 X 25) matrix of frequencies (or percentages) in each age-class.

Age-distribution. An age-structure for only 1 sex (1 X 25 matrix).

Standing age-structure. The age-structure of the entire population, existing at the census period of the model.

Harvest age-structure. The age-structure of those animals killed in a hunt; synonymous with **hunter-kill** and **hunted sample**.

Sustained yield curve (SYC). The curve made up of all the

points on a 2-dimensional graph of sustained harvest against standing population size that denote combinations resulting in zero net growth of the population.

Maximum sustained yield (MSY). The peak of the SYC; the highest harvest level on the curve.

N_{msy} . The population level at which MSY occurs.

Stable equilibrium. The level that a population subjected to a sustainable harvest tends toward, and returns to after being displaced, i.e. a point along the SYC to the right of N_{msy} .

Declining population. A population being harvested at a rate greater than sustainable; i.e. whose net growth after hunting is negative. Declining populations exist above and/or to the left of the SYC.

Stable population. A harvested population that tends to return to a stable equilibrium after displacement.

Stable harvest. A harvest level that can be applied to a given population indefinitely, that is, one that leads eventually to a stable equilibrium.

Overharvest. A harvest level that cannot be sustained by a

given population indefinitely, that is, one that leads eventually to extinction.

Declining region. The portion of the population size-harvest level graph in which overharvested populations are found (Fig 8).

Stable region. The portion of the population size-harvest level graph in which stable populations are found (Fig. 8).

Unstable portion of the SYC. The portion of the SYC that separates the declining region from the stable region. Points along the unstable portion are sometimes referred to as "release points".

Population trajectory. The direction of travel of a harvested population. From a point on the unstable portion of the SYC, population trajectory is either decline toward extinction or increase toward stable equilibrium.

Unexploited Equilibrium. The level a population equilibrates at in the absence of hunting and other man-caused mortality; synonymous with K .

Behavior of the Model

Mean realized natality and mortality rates were calculated from simulations run at $K=600$ for 75 years each. Because simulations

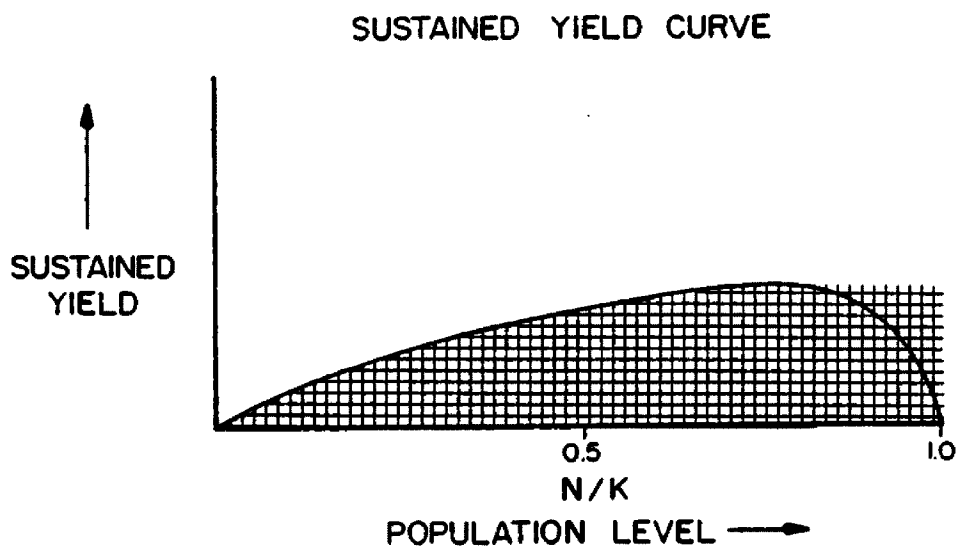


Fig. 8. A generalized sustained yield curve, showing the stable and declining region. The stable region is cross-hatched. All points below the curve are stable; additionally, points above the curve are stable when harvest is less than MSY and population level is greater than N_{msy} .

retained particularly strong and weak cohorts for many years, mean statistics from a 75 year run were often highly influenced by chance events. Thus, I ran no fewer than 3 independent 75 year runs to calculate each statistic. Specific formulae used for calculating realized natality and mortality rates are presented in the Results.

Population variability was defined as the coefficient of variation (CV) around the equilibrium value. Relative equilibrium value was defined as the mean value attained during a long simulation run as a proportion of the simulation's expected value, K . To examine the effects of stochastic carrying capacity and of population size on population variability and equilibrium level, 3 independent runs of 75 years were performed at each of 5 carrying capacities ($K=50$, $K=100$, $K=200$, $K=600$ and $K=900$), and 2 magnitudes of environmental stochasticity (no variability and $CV(K) = 13\%$). The amount of variability around equilibrium levels was tested first by comparing CVs from the different runs using 2-way ANOVA. Because they were significantly different (see Results), comparisons of relative equilibrium level could not be made with ANOVA. That is, the first test confirmed that runs with different amounts of environmental variability, as well as at different carrying capacities, had significantly different variances. Thus, an important assumption of ANOVA was violated for any further tests. To test for differences in relative equilibrium values, pairwise comparisons were made using the approximate t-test assuming unequal variances (Sokal and Rohlf 1981). To test for differences of relative equilibrium value among the 5 carrying capacities, the Games and Howell method was used (Sokal and Rohlf 1981).

Population growth form was examined by performing runs at a carrying capacity of 600 beginning with a population of 50 whose age-structure was arbitrarily defined. Increment curves were generated by plotting each yearly increment against the number in the population at the beginning of the year.

Sustained Yield Curves

Before an age-structure based index of decline could be developed, it was necessary to identify harvest-population combinations that caused decline. To do this, sustained yield curves under each Specific Model were located. Locating sustained yield curves (SYCs) enabled simulation runs used for developing the index to have known dynamics and trajectories. Portions of the SYC were generated for each of the 4 Specific Models at large and small carrying capacities of 600 and 200 animals. Ideally, simulations covering the complete range of population-harvest combinations would have been run, generating the entire curve. Unfortunately, such an effort was well beyond the constraints of budgeted computer time. In lieu of the entire SYC, vertical cross-sections at 40% and 70% of K were chosen for analysis. Both $0.4K$ and $0.7K$ are in the unstable portion of the SYC. The $0.7K$ cross-section is adjacent to N_{msy} , and therefore was considered an appropriate place to examine the dynamics of a population kept intentionally at or near N_{msy} . The $0.4K$ cross-section was chosen to represent a severely overharvested population.

The locations of the curves at these cross-sections were

determined by a 4 step process (Fig. 9). The process assured that populations subjected to experimental harvests (for locating SYCs) had age-structures that reflected a history of heavy harvest.

1. **Initial populations.** For each Specific Model and for both carrying capacities, I created 10 independent population age-structures at approximately K . These were considered "initial populations". Although all were generated from a common starting point, independence among the 10 was insured by running each from 11 to 20 years from its predecessor. This way, an excessively weak or strong cohort that appeared by chance in 1 initial population was unlikely to be retained by the next to be generated.

2. **Overharvest.** Each initial population was deliberately overharvested from approximately K until it reached $0.4K$. The overharvest rate (determined by trial and error) was the lowest harvest that always produced decline to extinction. This slow decline allowed the population to pass through many intermediate levels before reaching $0.4K$.

3. **Cross-section populations.** For simulations using $K=200$, the targeted cross-section population levels were 140 ($0.7K$) and 80 ($0.4K$). As each initial population was overharvested, each years' total census was compared to these target values. When overharvesting first reduced a population below 140, that years' census and the previous years' census (temporarily retained in computer memory) were compared, and whichever population was closest to 140 was retained as the $0.7K$ cross-section. The overharvest then continued to 80, at which point the procedure was repeated. For simulations using $K=600$, computer disk

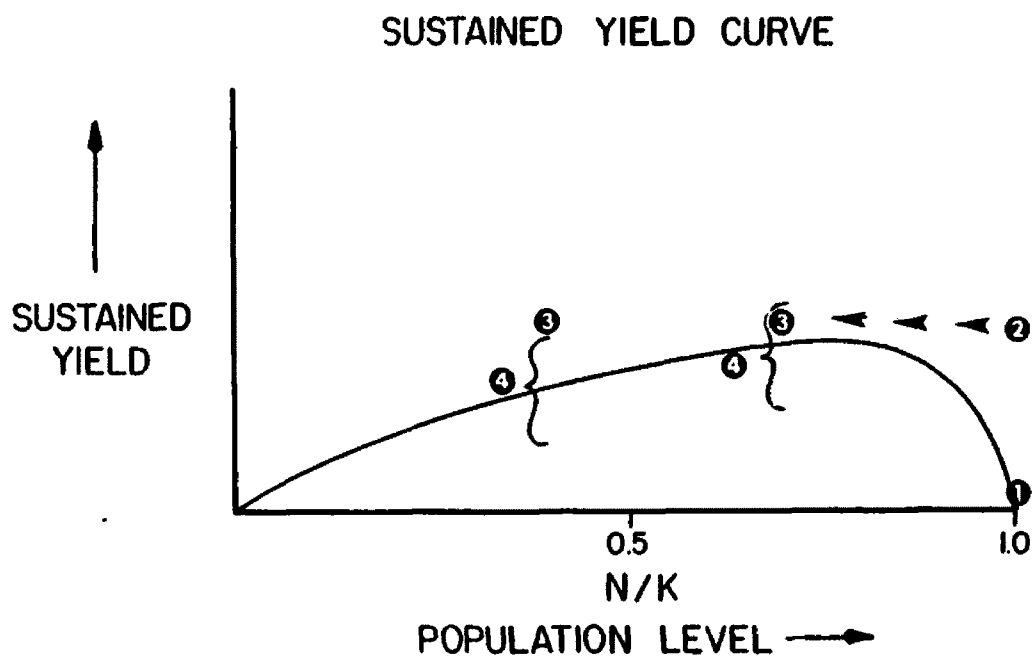


Fig. 9. A schematic diagram of the process by which sustained yields were located. 1. Initial (unharvested) population. 2. Populations are subjected to harvest greater than MSY (arrows indicate trajectory). 3. Populations at approximately $0.7K$ and $0.4K$ are retained for trial harvests. 4. Trial harvests, including those above and below the expected location of the curve, are applied. The brackets represent approximate locations of the 10 harvest levels.

storage was insufficient to allow retention of 2 complete populations for comparison. Therefore, the population structure in the first year in which the census fell below 420 (0.7 of 600) was retained as the 0.7K cross-section. Similarly, the 0.4K cross-section was taken as the population in the first year the census fell below 240 (0.4 of 600). This procedure caused the selected cross-sections for $K=600$ populations to be consistently less than their targeted values. The mean realized cross-sections for $K=600$ populations were 0.654K and 0.356K. For simplicity, these are referred to throughout as 0.7K and 0.4K.

4. **Trial Harvests.** Each 0.4K and 0.7K population was run for 30 years at each of 10 different trial harvest levels. For years 1 through 10, age-structure data from both the standing population and the hunted sample were recorded. Only the annual census totals were recorded for the subsequent 20 years. Trial harvest levels were chosen to bracket the regions where I hypothesized the population trajectories changed from stability to decline (Table 1).

Table 1. The 10 trial harvest levels applied to each cross-section population. The numbers in parentheses are the mean population sizes at each cross-section.

Population K	Cross- Section	Low Harvest	High Harvest	Increment
200	0.4K (80)	5	14	1
	0.7K (140)	8	17	1
600	0.4K (213)	15	42	3
	0.7K (392)	24	51	3

To differentiate declining from stable populations, the natural logarithm of each year's census was regressed against time, yielding r , the instantaneous rate of change. If r was significantly ($p < 0.01$) negative, the population was categorized as declining. At the 0.7K cross-section, near N_{msy} , all other populations were considered stable. However, at the 0.4K cross-section, only those populations with a significantly ($p < 0.01$) positive r were categorized as stable. Populations with r insignificantly different from zero were considered ambiguous; that is, although their long-term dynamic was either decline or stability, they exhibited neither dynamic during the time-span examined. Ambiguous populations were treated as missing data. The significance of r was examined separately for both the 10-year period of age-structure data collection, and the entire 30-year run.

To compare sustainable yields the following procedure was used. All data were divided into subsets by carrying capacity (200 or 600), Specific Model, 0.4K or 0.7K, and length of time for which population trajectory was calculated. Mean sustainable harvests for each subset were calculated by multiplying each harvest rate (expressed as a percentage of the mean number in the cross-section population) by the percentage of trials at that rate resulting in stability, and dividing the sum by the sum of the stable trial percentages:

$$[(H_i/N)p_i] / \sum p_i$$

where:

H = number harvested in trial i

N = mean number in cross-section population

p = percentage of trials at rate i resulting in stability

Differences among mean harvest rates were tested using a series of fixed-treatment 2-way analyses of variance (ANOVA). Three treatments were defined: (i) K, (ii) Specific Model, and (iii) length of time for which sustained yield was calculated. I examined the source of differences among the 4 Specific Models using planned orthogonal contrasts (Sokal and Rohlf 1981). The 4 Models were grouped in pairs according to their birth-rate functions (density-dependent or -independent), and their sub-adult male mortality functions (adult male dependent or population dependent). The ANOVA's assumed normality and homoscedasticity of the mean harvest rates of each data subset. Additionally, because interaction between treatments could not be tested, all treatments were assumed to be additive.

Description of Age-Structures

I used 2 basic approaches to describe age-structures of harvested grizzly bear populations: (i) examining age-structures directly, and (ii) computing statistics that summarized information about the age-structures.

Unweighted mean proportion in each age-class was computed by considering the number in each age-class as a percent of the total population each year. Means were computed as the summed percentages divided by the number of years considered. Age-distributions for a single sex were computed similarly, with the number in each age considered as a percentage of the total in that sex. Age-classes 5-9, 10-14, 15-19 and 20-24 were lumped to condense age-structures when it made interpretation easier.

Ten descriptive statistics for each age-structure were computed (Table 2). They were chosen for the information they conveyed about the age-structures, and for their ease of computation. The arc-sine transformation was applied to all proportions to adjust them toward normality, and to stabilize variances (Zar 1974). The 10 statistics were plotted against population size or time, or were used as variables for further analyses (see next section).

The behavior of age-structures under 3 sets of circumstances was considered:

1. **Harvested populations initially at K.** Ten independently generated Model DMADM populations were allowed to equilibrate with no harvest at approximately $K=600$. Each was then subjected for 20 years to 5 different hunt levels: 10,20,30,40 and 50 animals/year. The lower 2 harvest levels were below MSY and resulted in stable equilibria. The upper 2 levels were greater than MSY and gradually drove the populations to extinction. Age-structures and the 10 summary statistics were examined as these populations declined.

2. **Harvested populations initially at cross-sections $0.7K$ and**

Table 2. Ten descriptive statistics computed for each data sample. .

Abbreviation	Description	Computation		
MXBAR	Mean age of males	$\frac{24}{\sum_{i=0} im_i}$	$\frac{24}{\sum_{i=0} m_i}$	
FXBAR	Mean age of females	same, with m = f		
MMED	Median age of males	Age containing the $\frac{24}{((\sum_{i=0} m_i)+1)/2}$ individual, + age $\frac{24}{\sum_{i=0} m_i - ((\sum_{i=0} m_i)+1)/2}$ / m _{age}		
FMED	Median age of females	same, with m = f		
MSUBAD	Proportion of males in sub-adult ages	$\frac{3}{\sum_{i=0} m_i}$	$\frac{24}{\sum_{i=0} m_i}$	
FSUBAD	Proportion of females in sub-adult ages	same, with m = f		
M58JUV	Proportion of prime (5-8) males among those (0-2)+(5-8)	$\frac{8}{\sum_{i=5} m_i}$	$\frac{8}{\sum_{i=5} m_i} +$	$\frac{2}{\sum_{i=0} m_i}$
F58JUV	Proportion of prime (5-8) females among those (0-2)+(5-8)	same, with m = f		
MFALL	Proportion of males among all animals	$\frac{24}{\sum_{i=0} m_i}$	$\frac{24}{\sum_{i=0} m_i} +$	$\frac{24}{\sum_{i=0} f_i}$
MFAD	Proportion of males among adults (age 4+)	$\frac{24}{\sum_{i=4} m_i}$	$\frac{24}{\sum_{i=4} m_i} +$	$\frac{24}{\sum_{i=4} f_i}$

m = males, f = females, i = age, age = age containing the median individual

0.4K. Five independently generated Model DM populations were overharvested from $K=600$ down to 0.7K and 0.4K, the same procedure used in quantifying the 2 cross-sections of the SYC. At each cross-section, 2 harvest levels, 24 and 39 animals/year, were applied for 25 years each. The higher level produced declines at both 0.7K and 0.4K. The lower level always led to stable equilibria at 0.7K, but at 0.4K sometimes caused declines, sometimes stability. Age-structures and the 10 descriptive statistics were examined as declining and stable populations moved away from these release points on the SYC.

3. **Harvested populations growing in response to increased K.** Ten independently generated Model DDALL populations were allowed to equilibrate at $K=600$. Each was then run for 20 years under a harvest of 24 animals/year and with an increased K of 1000. Age-structures and descriptive statistics were examined as these populations increased.

Discrimination of Declining and Stable Age-Structures

Age-structures from the first 10 years of the simulation runs used for quantifying the SYCs were also used to develop indices for discriminating declining from stable populations. Each 10-year data set was considered in 2 ways: (i) as 10 separate samples, each consisting of age-class frequencies from a single year, and (ii) as 3 separate samples each consisting of summed age-class frequencies from 3 consecutive years. In the latter, year 1 was ignored, so the first year-group was from years 2-4, the second from years 5-7, and the third from years 8-10.

For each sample, the 10 statistics described in Table 2 were computed. No attempt was made to use raw age-class frequencies for discrimination because of their non-normality and large variances.

The 10 statistics for each sample were used as input variables to generate 2-group discriminant function equations. The known groups were 'decline' and 'stable', as determined during the SYC calculations for the 10-year period. I used SPSSX program DISCRIMINANT (Nie et al. 1975) to generate the discriminant functions. Variables were entered into the equation in stepwise order as they maximized the minimum D², the Mahalanobis distance, and its corresponding partial F value. Variables failing to make a significant ($p < 0.50$) contribution to the separation between group centroids were omitted.

The goal of 2-group discriminant function analysis (DFA) is generally to classify samples into pre-specified groups by maximizing their separation along a newly defined canonical axis. For prediction purposes, the overall mis-classification probability is minimized by taking the midpoint between the 2 group means as the critical decision point. This procedure assumes multivariate normality, equal variance-covariance matrices, and equal a priori probabilities of group membership. It also implicitly assumes that the objective of the analysis is minimization of the total error rate, i.e., that both mis-classification errors are of equal consequence. However, in discriminating declining from stable populations, the 2 types of mis-classification have different meanings and consequences. Classifying as a declining population one that is actually stable is a

relatively benign error for a manager. At most, the consequences of the erroneous classification will be unnecessarily conservative measures. But classifying as a stable population one that is actually in decline from excessive harvest is a serious error. The classification implies that all is well, when in fact, continuation of the status quo leads to extinction. Therefore, I chose as the critical decision point that value that would insure no greater than a specified probability of mis-classifying populations that were actually declining.

The critical point was determined in the following way. After discriminant function scores were computed for each sample, the mean and variance of the scores for the (known) declining group were computed. Each sample in the declining group was then coded with its associated standard z-score, indicating its standard deviation units from the mean score for decliners. Then, assuming normality along the canonical axis, the critical score that insured no greater than approximately 10% mis-classification of known decliners was that score corresponding to $z = 1.282$. The mis-classification probability for stable populations was then computed empirically by comparing actual vs. predicted group membership (Fig. 10). During this process, each discriminant function was tested against data other than those used in generation of the equation, including the 3 data sets used in the description of age-structures (see above).

I thus explicitly recognized 2 types of errors, analogous to Type I and Type II errors of standard statistical theory. Population decline was analogous to the null hypothesis. The probability of a Type I error, α was specified beforehand. The probability of a Type II

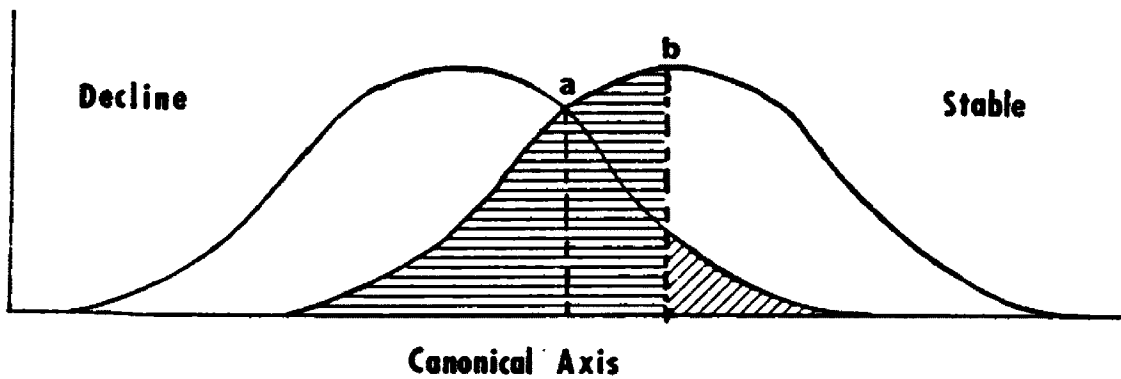


Fig. 10. A generalized distribution of discriminant scores along the canonical axis, showing the procedure used to calculate Type I and Type II errors. Age-structures from declining populations (left) received lower scores; age-structures from stable populations received higher scores (right). Both were distributed approximately normally along the canonical axis. Point 'a' would minimize the total probability of mis-classification. Point 'b' assures that declining populations will be mis-classified with probability 10%. Slanted hatching represents Type I errors; horizontal hatching represents Type II errors.

error, β , could not be predicted, but the power of the test, $(1 - \beta)$ was determined empirically. The basic question of DFA was thereby modified from "how accurately can this procedure predict group membership?", to "given that it will mis-classify declining populations with probability α (10%), how much power to correctly classify stable populations does this procedure have?". Overall and Klett (1972) present a similar method for calculating a critical point using standard z-scores.

I also tested the power of each of the 7 discriminating variables separately to determine how well differentiation between age-structures of declining and stable populations could be accomplished without the discriminant function. The procedure described for estimating Type I errors and power under the discriminant function was used for individual variables, simply substituting 1 variable at a time for the discriminant function score.

RESULTS

Results are presented in 4 parts. The first is a description of behaviors of the simulation model relevant to subsequent age-structure analyses. The second presents properties of sustained yields. The third is a general treatment of age-structures, both of stable and declining populations, as seen both in the standing population and in the harvest. In the final section, a discriminant index is developed, and its sensitivity is estimated under a variety of circumstances.

Behavior of the Model

Experiments performed on the simulated population were valid only to the degree that the simulation behaved like a real grizzly bear population. This section describes the behavior of the simulated population when not exploited. Average life-history rates of the unexploited population are presented and compared to published values from studied populations. Later, I describe some general dynamics of the modeled populations that have implications for the subsequent sections on harvested populations.

Natality and Survival Rates at Equilibrium

At equilibrium, natality and survival rates of the simulated population were similar to published figures from southern interior grizzly bear populations.

Natality Rates. Mean litter size at approximately equilibrium conditions was 2.066 cubs, computed as the weighted mean:

$$N_{0j} / \sum b_j$$

where:

N_0 = total number of cubs in year j

b = total number of birth events in year
 j

Published mean litter sizes for southern interior grizzly populations vary from 1.7 (Martinka 1974) to 2.26 (Aune and Stivers 1983). Bunnell and Tait (1981), in summarizing grizzly bear natality from all 3 sub-populations, found a mean of 2.12 cubs among 1042 family groups. The distribution of 1-, 2- and 3-cub litters in the simulation was also similar to published figures (Table 3).

Mean breeding interval at approximate equilibrium was 3.091 years, computed as the weighted mean:

$$\sum y / \sum B$$

where:

y = years between successive breedings of females that gave birth more than once during a simulation

B = successive breedings by the same female

Table 3. Litter sizes in this simulation and other published figures. All values are percent frequency.

Litter size			Source
1	2	3	
19%	55%	26%	This simulation
24%	52%	24%	Mundy and Flook 1973
43%	46%	11%	Martinka 1974 ¹
33%	53%	14%	Martinka 1974 ²

¹ Cubs-of-the-year only

² Yearlings; greater numbers of larger litters are apparently due to sampling error.

Table 4. Breeding intervals in this simulation and other published figures. All figures are percent frequency.

Breeding Interval (Years)					Source
2	3	4	5	6	
14%	63%	20%	2%	-	This simulation
26%	47%	15%	6%	2%	Craighead et al. 1974
32%	45%	21%	3%	-	Knight and Eberhardt (in press)

Most published reports of mean breeding interval are about 3 years (Bunnell and Tait 1981). The mean distribution of breeding intervals was also similar to published reports (Table 4).

The simulated age-at-first-reproduction for females averaged 5.502, calculated as the unweighted mean:

$$\Sigma a_j/j$$

where:

a = the mean age-at-first-reproduction
for all females in year j

j = number of years in the simulation

Mean age-at-first-reproduction for each year ranged from 5.0 to 6.2 (Table 5). Knight and Eberhardt (in press) calculated mean age-at-first-reproduction in Yellowstone National Park as 5.62 during 1959-1970, and 6.06 during 1974-1980. Bunnell and Tait (1981) concluded that mean age-at-first-reproduction was commonly between 5 and 6 years of age.

The percentage of the total population in the cub class at equilibrium conditions averaged 16.4%, calculated using the unweighted mean:

Table 5. Ages at first reproduction in this simulation and other published figures. All figures are percent frequency.

Ages at first reproduction (females)				
5	6	7	8	Source
65%	26%	9%	1%	This simulation
69%	6%	19%	6%	Craighead et al. 1976
15%	62%	15%		Best and Eberhardt (1976)

$$\Sigma (N_{0j}/N_j) / j$$

where: N_0 = number of cubs in year j

N = total population in year j

Percent cubs was a highly variable statistic. Due largely to synchrony of breeding (see below), the model generally produced "strong" and "weak" cohorts, causing the percentage cubs to vary from 8.6% to 26.8%. Published figures for percent cubs include 17% (Martinka 1974), 18% (Mundy and Flook 1973), and 19% (Craighead et al. 1974).

Survival Rates. Simulated mean survival rates were similar to those reported by Knight et al. (1983) and Craighead et al. (1973). Mean male survival was less than mean female survival, as reflected in the survival curves at equilibrium (Fig. 11).

Although the mean age distribution (Fig. 12) appears smooth and stable, yearly differences in the distribution of ages were great. Older age-classes frequently outnumbered the adjacent younger age-class as strong and weak cohorts alternately made their way through the population (Fig. 13).

Population Variability and Equilibrium

Unexploited populations were variable, but always equilibrated near their carrying capacities, K (Fig. 14). Females usually outnumbered males because they were assigned lower mortality rates. The number of males in a population was slightly more variable than the

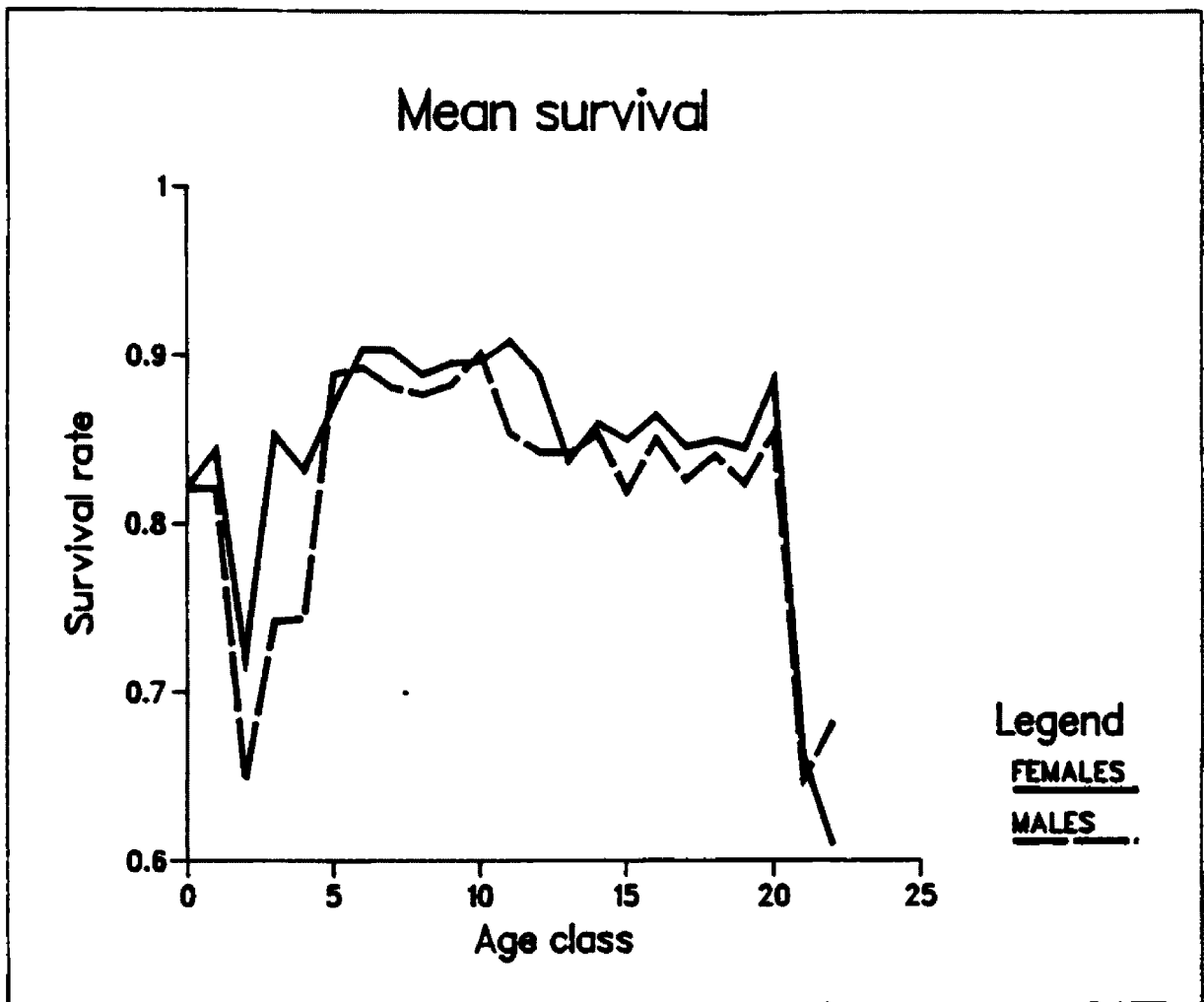


Fig. 11. Mean survival rates of males and females in the simulated population at unharvested equilibrium (K).

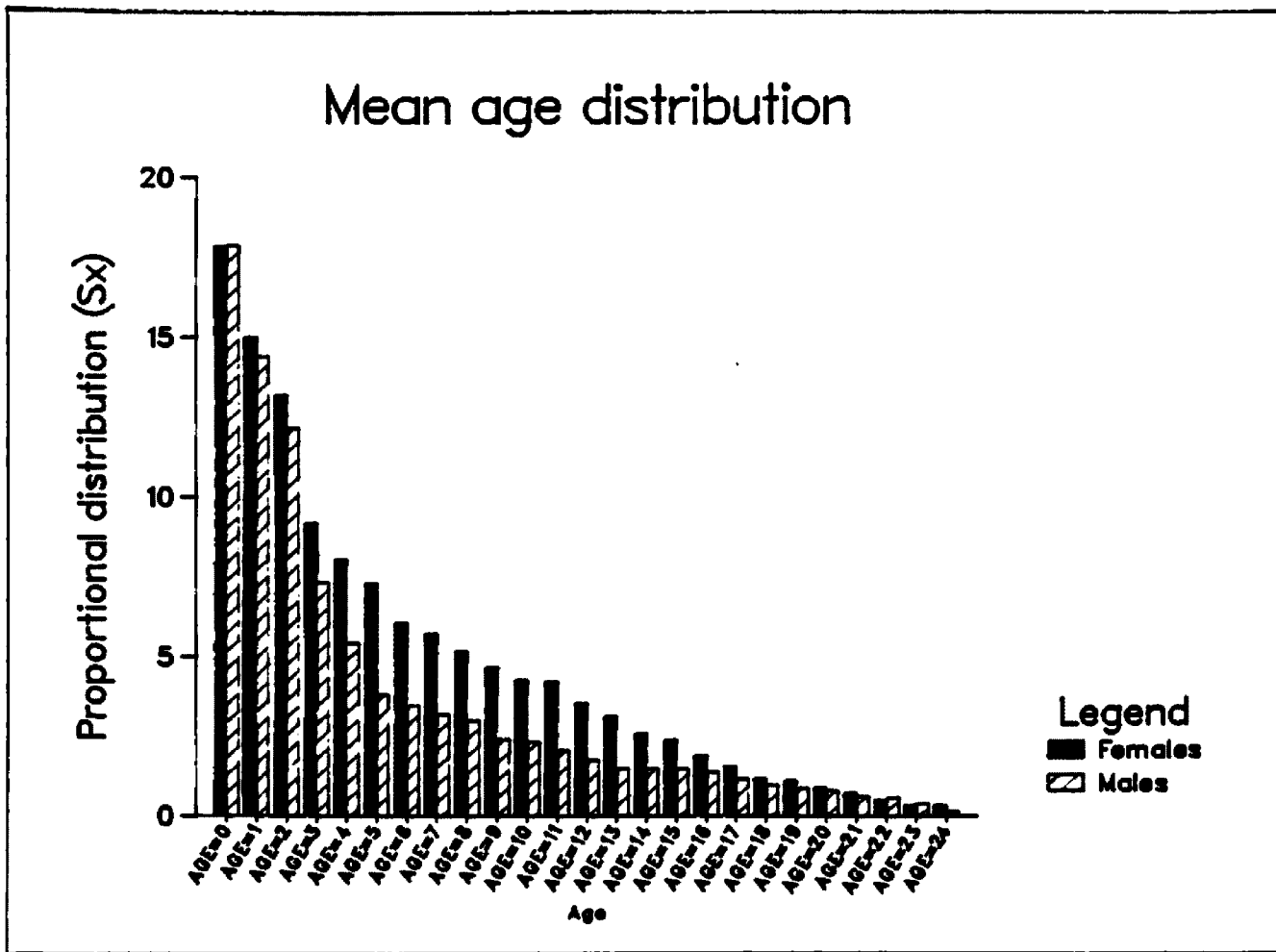


Fig. 12. The mean age-structure of the simulated population at K.

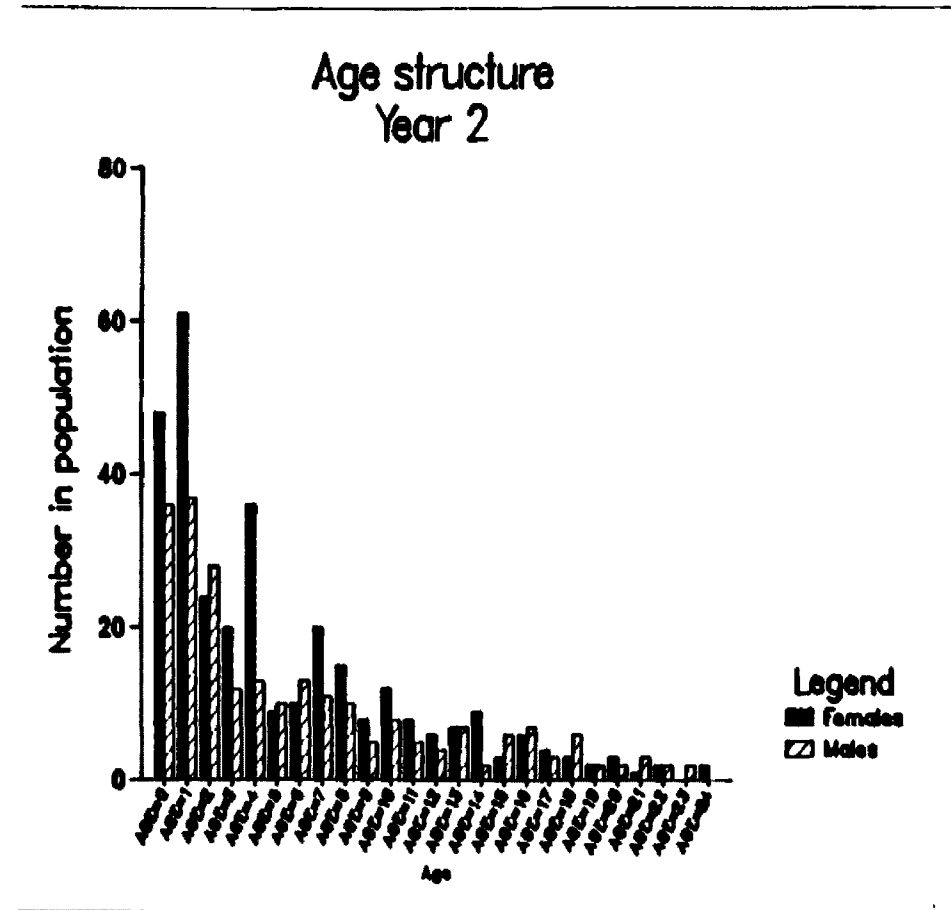
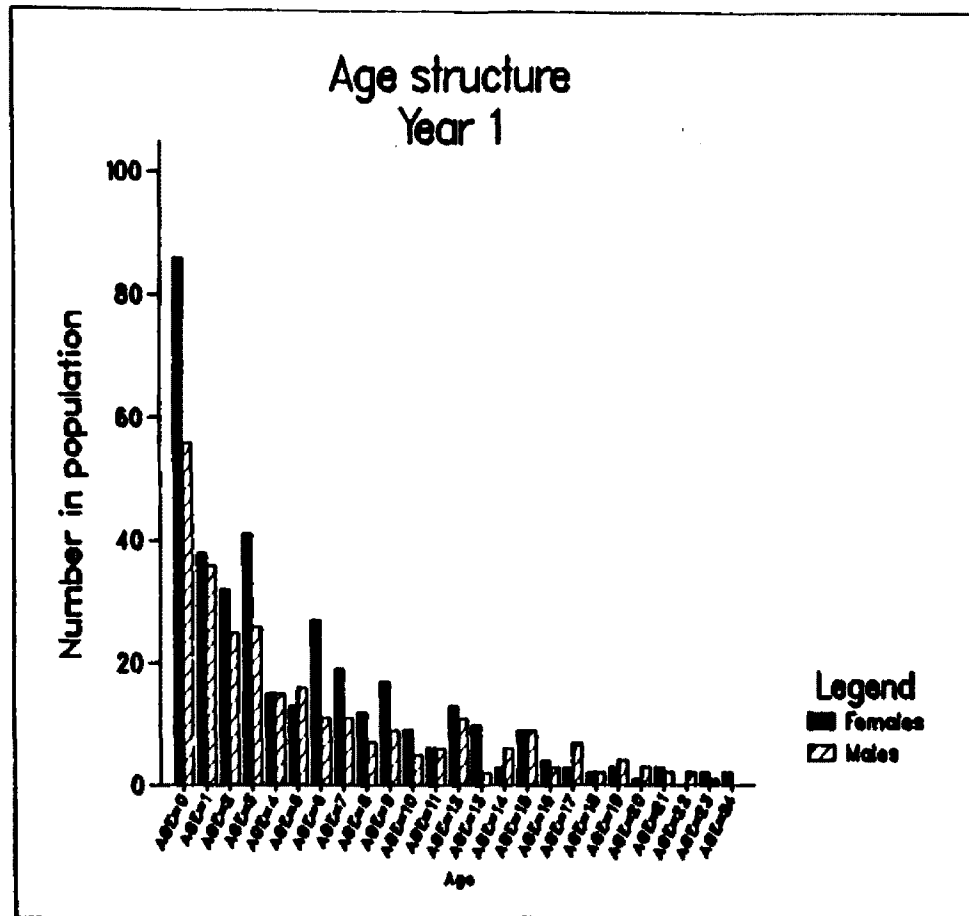


Fig. 13. Age-structures from 2 consecutive years, selected randomly. Note that particularly large and small cohorts in year 1 (e.g. female cubs, age-class 4) can be seen a year older in year 2. Note also that strong and weak cohorts result in older age-classes frequently outnumbering younger age-classes.

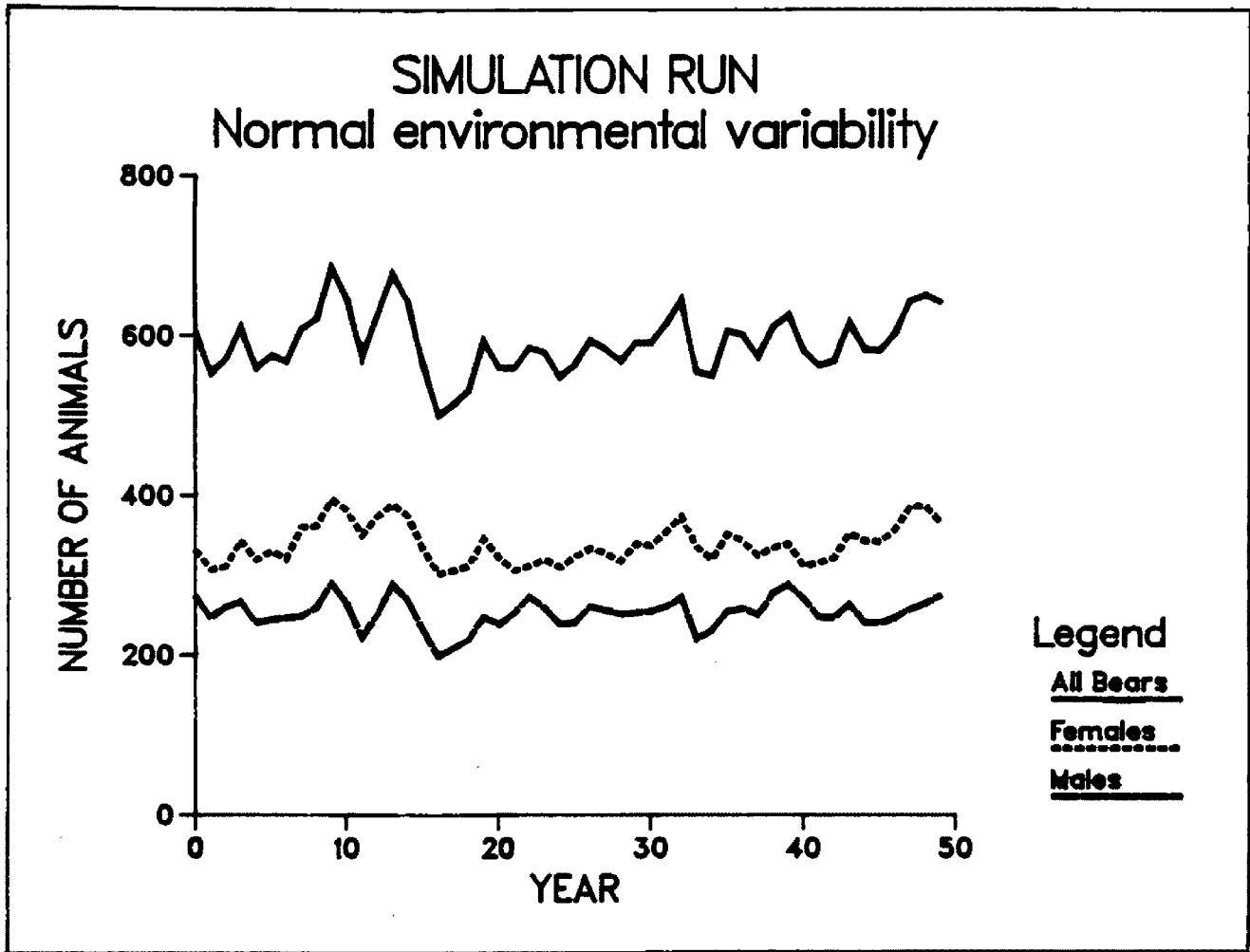


Fig. 14. A typical 50-year simulation run at $K=600$ with environmental variability.

number of females. In a set of simulations with $K=600$ and no added environmental variation, number of males had a coefficient of variation (CV) of 4.7%; the CV for females was 3.8%.

The amount of fluctuation while at unexploited equilibrium was a function of both demographic and environmental stochasticity. Variability was significantly reduced ($p<0.01$) when environmental variability was removed by holding K constant (Table 6). The relative magnitude of fluctuations caused by environmental variability was similar at all carrying capacities tested (Fig. 15).

Given the same magnitude of environmental variability, fluctuations were relatively greater ($p<0.01$) at smaller populations than at larger populations (Fig. 16). The most variable populations at unexploited equilibrium were those that were both small, and subject to environmental stochasticity (Fig. 17, Table 6).

Variability in number of cubs was far greater than in of any other segment of the population (Fig. 18). Coefficients of variation for cubs at equilibrium varied from 16% at $K=600$ to 40% at $K=100$, and to 71% at $K=50$. Interestingly, environmental stochasticity accounted for little of the variability in cub numbers (Fig. 19). Keeping K constant resulted in only a slight decrease in the CV of cubs, to 15% at $K=600$ and to 34% at $K=100$. At $K=50$, cub variability was essentially unaffected by environmental stochasticity; CVs from simulations with no environmental variation were often higher than those from simulations with environmental variability.

The high variability of the cub class was a function of the female reproductive cycle. Numbers of cubs followed roughly a 3-year

Table 6. Variability of population equilibrium as a function of environmental stochasticity and population size at K.

a. Average coefficients of variation at 2 population sizes (expected K), with and without environmental stochasticity. Each value is a mean of 3 replicates, each replicate containing 75 years.

K	Coefficients of Variation	
	Variability of K (CV)	
	0%	13%
50	11.31%	13.53%
100	7.75%	10.20%

b. ANOVA table

Source	df	MS	F	p
Population Size	1	35.39	12.2	<0.01
Variability of K	1	16.31	5.6	<0.05
Interaction	1	0.04	0.1	ns
Error	8	2.91		

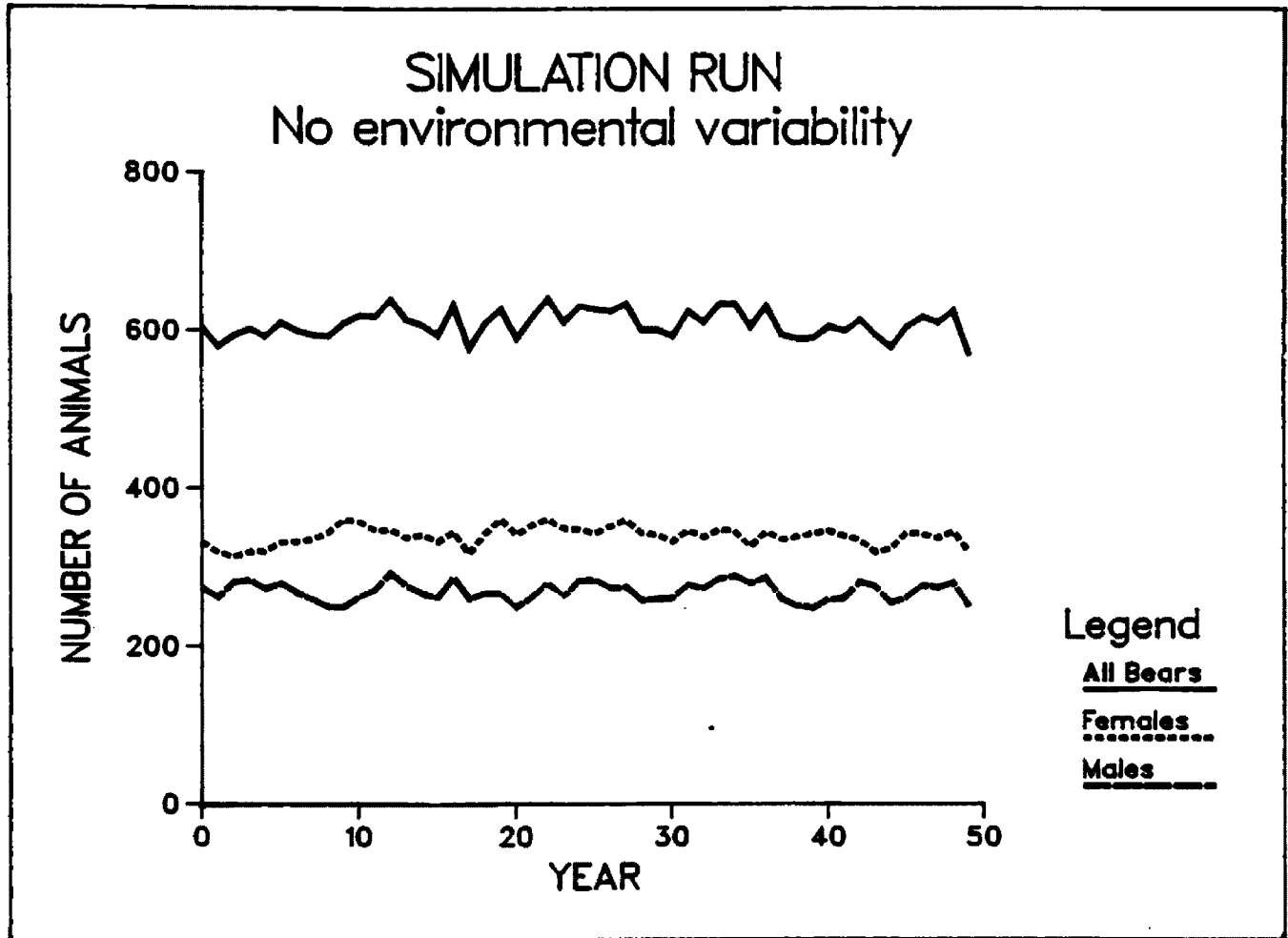


Fig. 15. A typical 50-year simulation run at $K=600$ with environmental variability removed. The fluctuations remaining are due to demographic stochasticity.

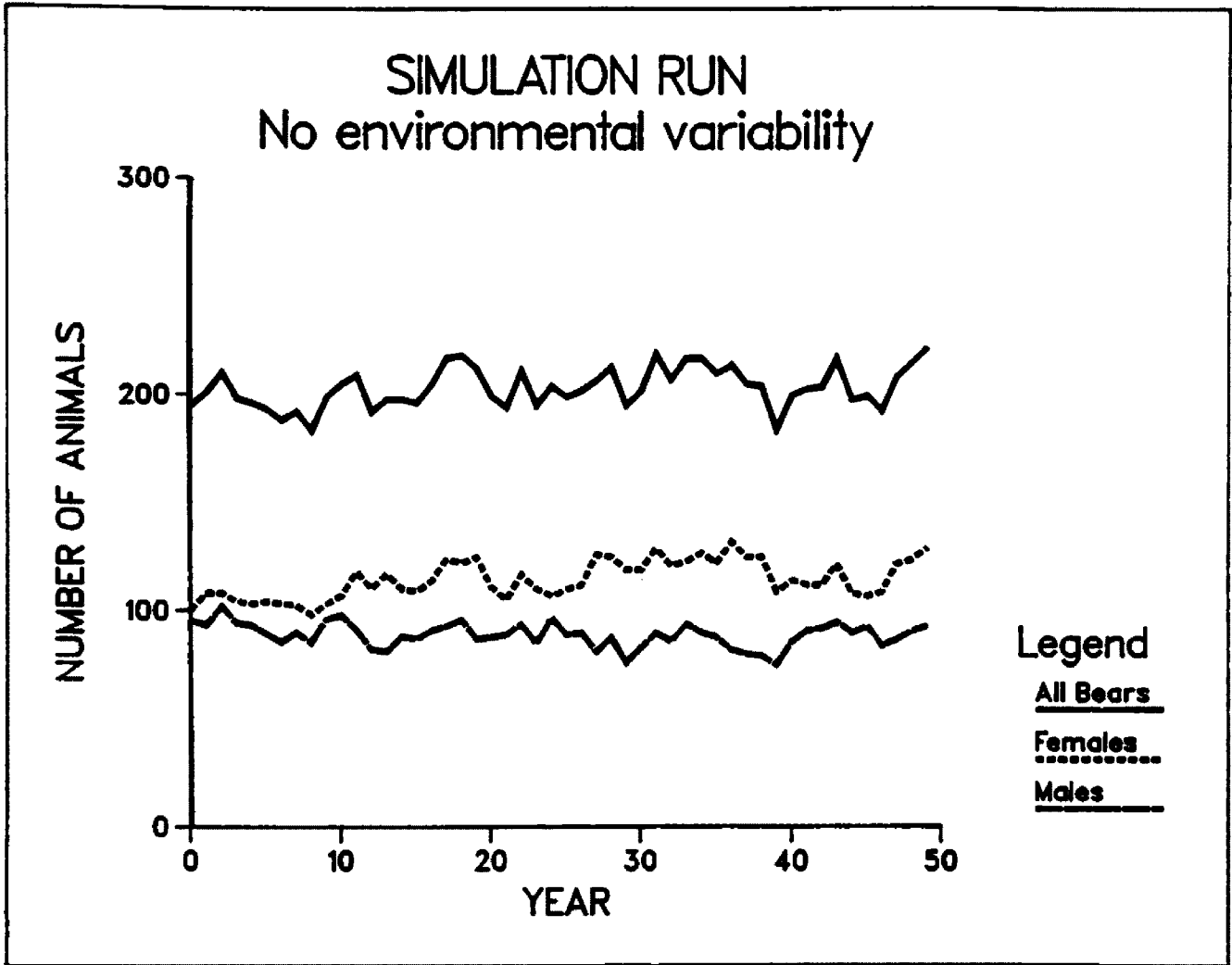


Fig. 16. A typical 50-year simulation run at $K=200$ with environmental variability removed. The fluctuations are due to demographic stochasticity; note that they are relatively greater than seen in Fig. 15.

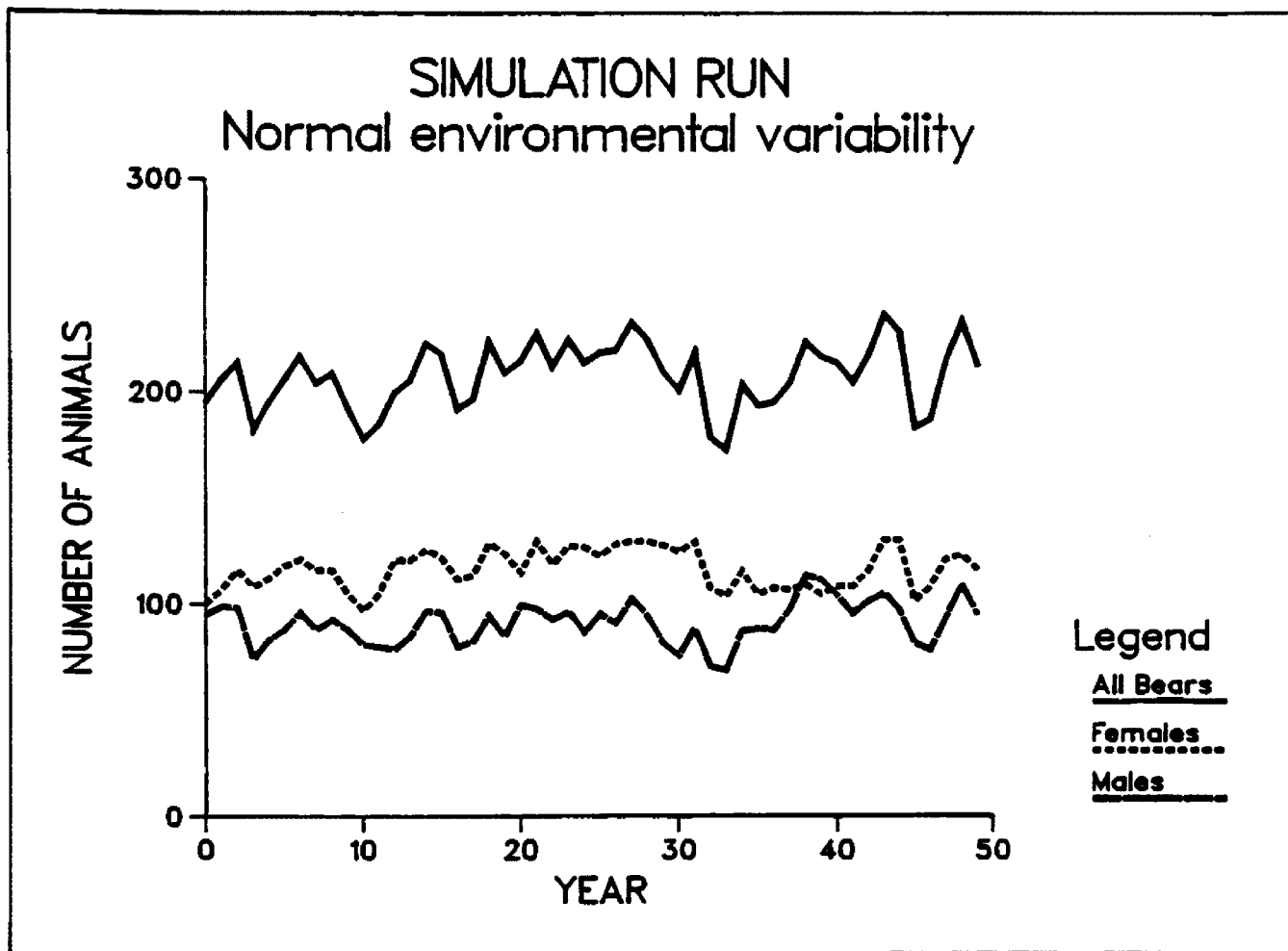


Fig. 17. A typical 50-year simulation run at $K=200$ with environmental variability. Note that, at 1 point, males outnumber females.

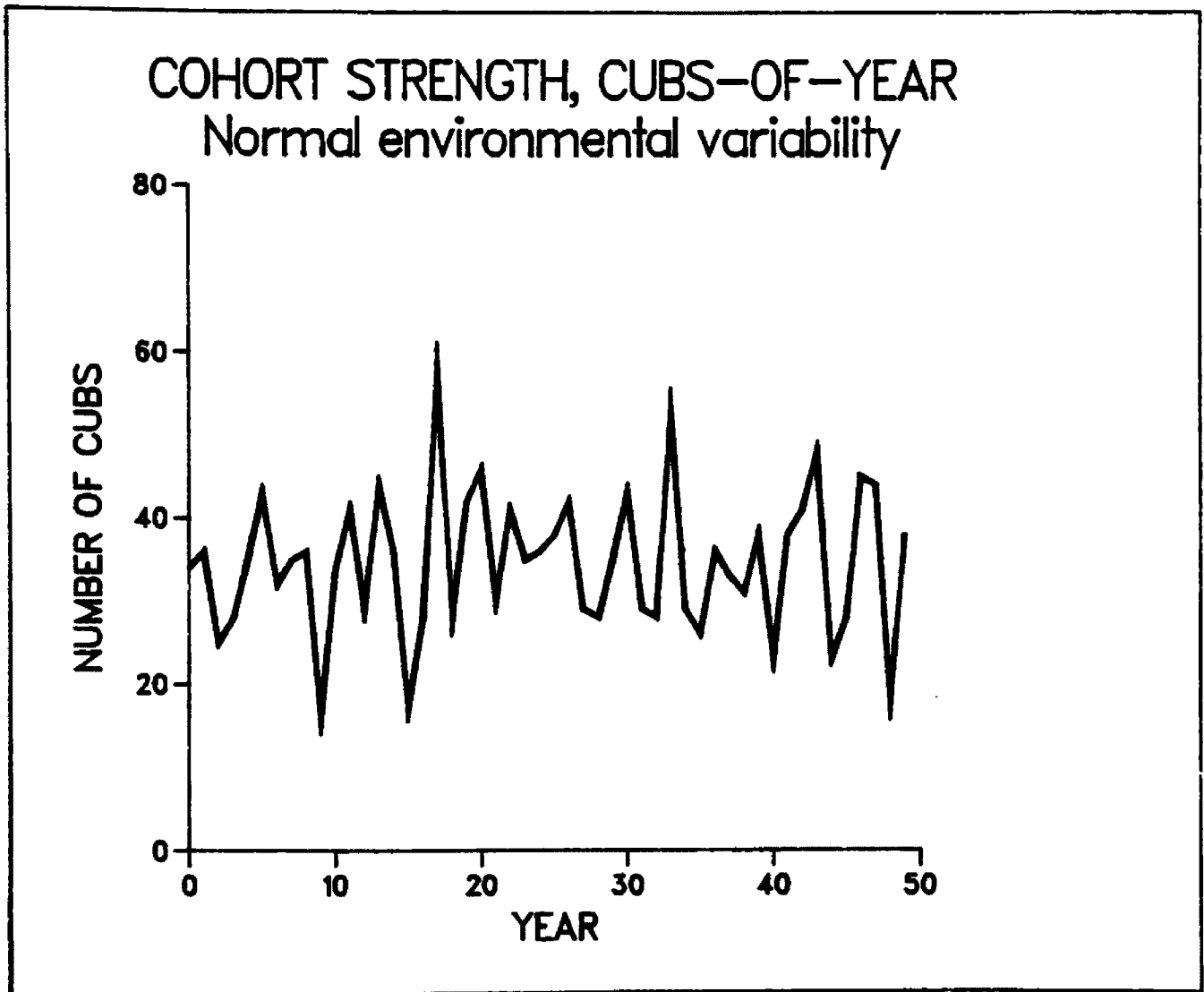


Fig. 18. A typical 50-year simulation run at $K=200$ with environmental variability, showing the number of cubs each year. Highs and lows are most often at 3-year intervals.

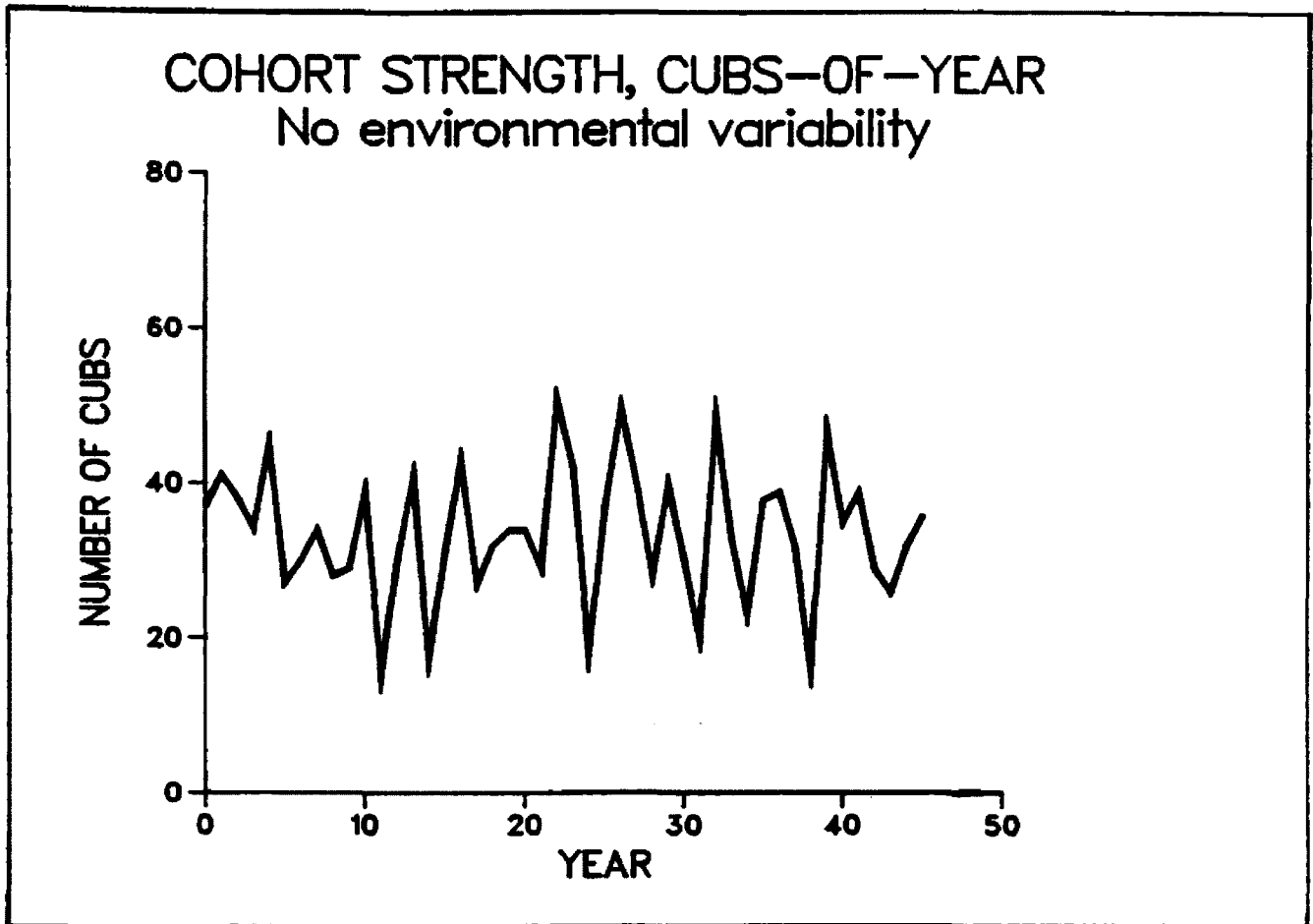


Fig. 19. A typical 50-year simulation run at $K=200$ with environmental variability removed, showing the number of cubs each year. Fluctuations are only slightly less severe than with environmental variability.

cycle in response to mature females' synchronous breeding. This can be seen in Fig. 18 and Fig. 19, and more clearly when the correlation coefficients of cub numbers between years are plotted against year intervals in a correlogram (Fig. 20). The highest correlation was at 3 years. Low correlations also occurred in 3 year intervals, at 2,5,8 and 11 years.

Cole (1951) demonstrated that a series of random numbers exhibited "cycles", with a mean length of about 3 years. However, the 3-year cycles of cub abundance in this model were much more regular than predicted by Cole's random model. The CV of cub cycle length was about 15%; Cole's random model predicted a cycle length with a CV of about 37%. It should be noted that synchronous breeding was not modeled deliberately; rather it resulted inevitably from the interaction of the age-at-first breeding and breeding cycle length functions.

Mean equilibrium values attained by populations relative to their expected values (i.e., median K) were also functions of both environmental and demographic stochasticity. Adding environmental variability significantly reduced ($p < 0.01$) mean population levels. Populations that equilibrated at K in the absence of environmental stochasticity equilibrated roughly 5% lower when K was allowed to vary log-normally with a CV of about 13% (Table 7).

With environmental variability removed or kept constant, mean equilibrium values relative to their expected values were weakly related to the magnitude of their expected K. The rate functions used in the model were calibrated using populations with $K=200$. Populations with $K=900$ equilibrated at slightly above K (mean 905.0, standard error =

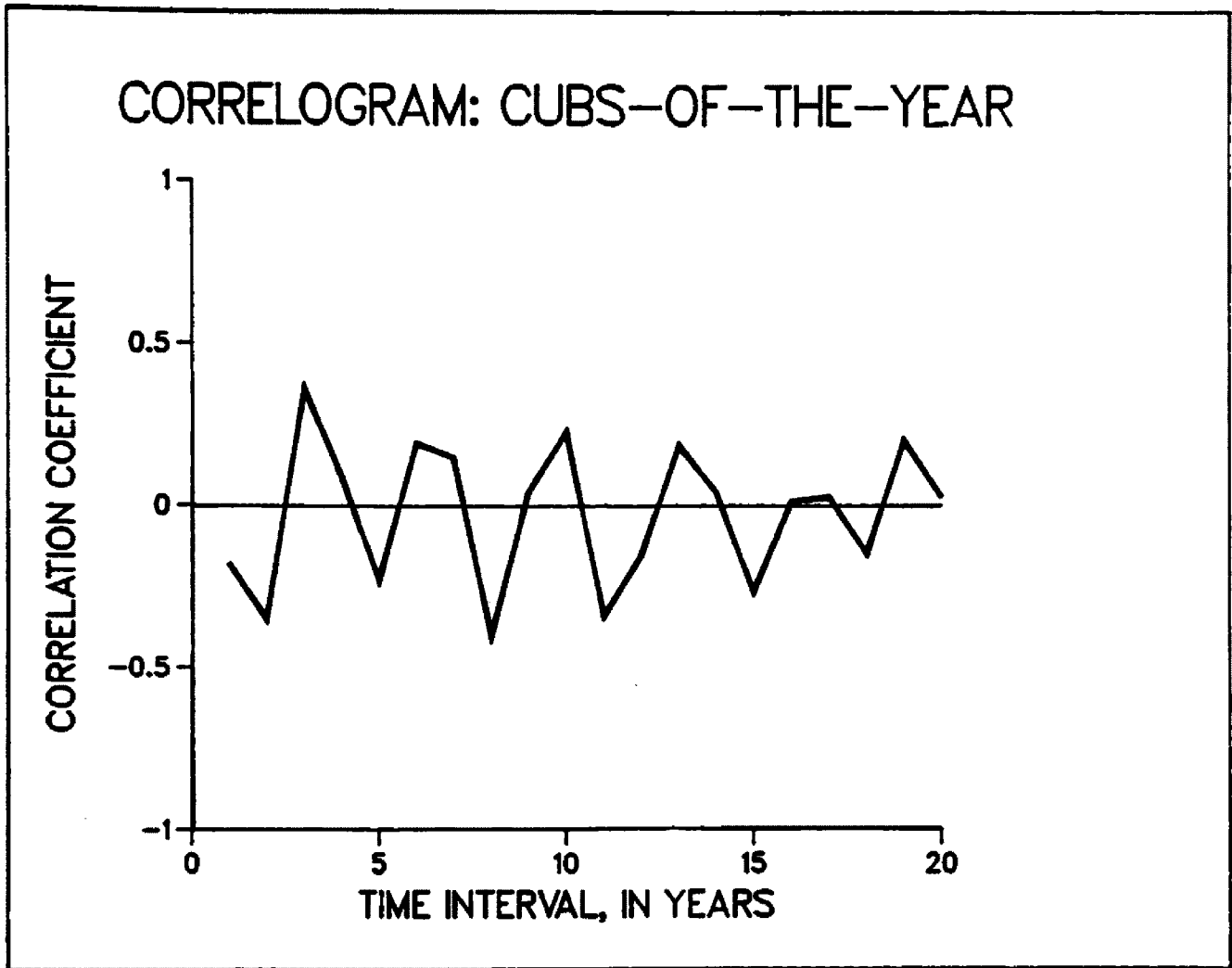


Fig. 20. Correlation coefficients (r) of the number of cubs in year 0 with the number of cubs a specified time interval later, plotted against the time interval. The highest correlation is at 3 years; low correlations also occur in 3 year intervals.

Table 7. Mean equilibrium values of 6 simulations with expected K=100, 3 with 13% coefficient of variation for K, 3 with no environmental stochasticity. Each value represent 75 years.

Replicate	Variability of K (CV)	
	0%	13%
1	100.493	96.120
2	101.893	93.480
3	100.053	96.493
Grand Mean	100.813	95.364

$t = 4.9594, df = 8, p < 0.01$

1.74); populations with $K=50$ equilibrated at slightly below K (mean = 48.75, standard error = 1.39). No relationships between relative equilibrium value and the magnitude of K were statistically significant, but sample sizes were small, variability was great, and heteroscedasticity among populations with different K values necessitated using a conservative test, the Games and Howell method (Sokal and Rohlf 1981). However, plotting relative equilibrium values against the magnitude of expected K suggests that a highly non-linear relationship applied (Fig. 21). Relative equilibrium values were fairly constant in the range $K=100$ to 900, but dropped off sharply below 100 as demographic stochasticity became the dominant influence in the dynamics of the population.

Growth Form of Unexploited Populations

When initiated at an arbitrary small level, populations grew gradually until they reached their unexploited equilibria (Fig. 22). Occasional declines occurred during the growth phase despite the favorable conditions that prevailed at levels well below K . Growth curves were approximately sigmoid-shaped, with the inflection point at greater than $2/3 K$. Density-dependent factors were weak until numbers approached equilibrium, resulting in nearly exponential growth at low and intermediate densities. A plot of the natural logarithm of population against time was nearly linear over a broad range of densities (Fig. 23).

During growth from an arbitrary, initial population, yearly increments were variable (Fig. 24), but were generally small at low

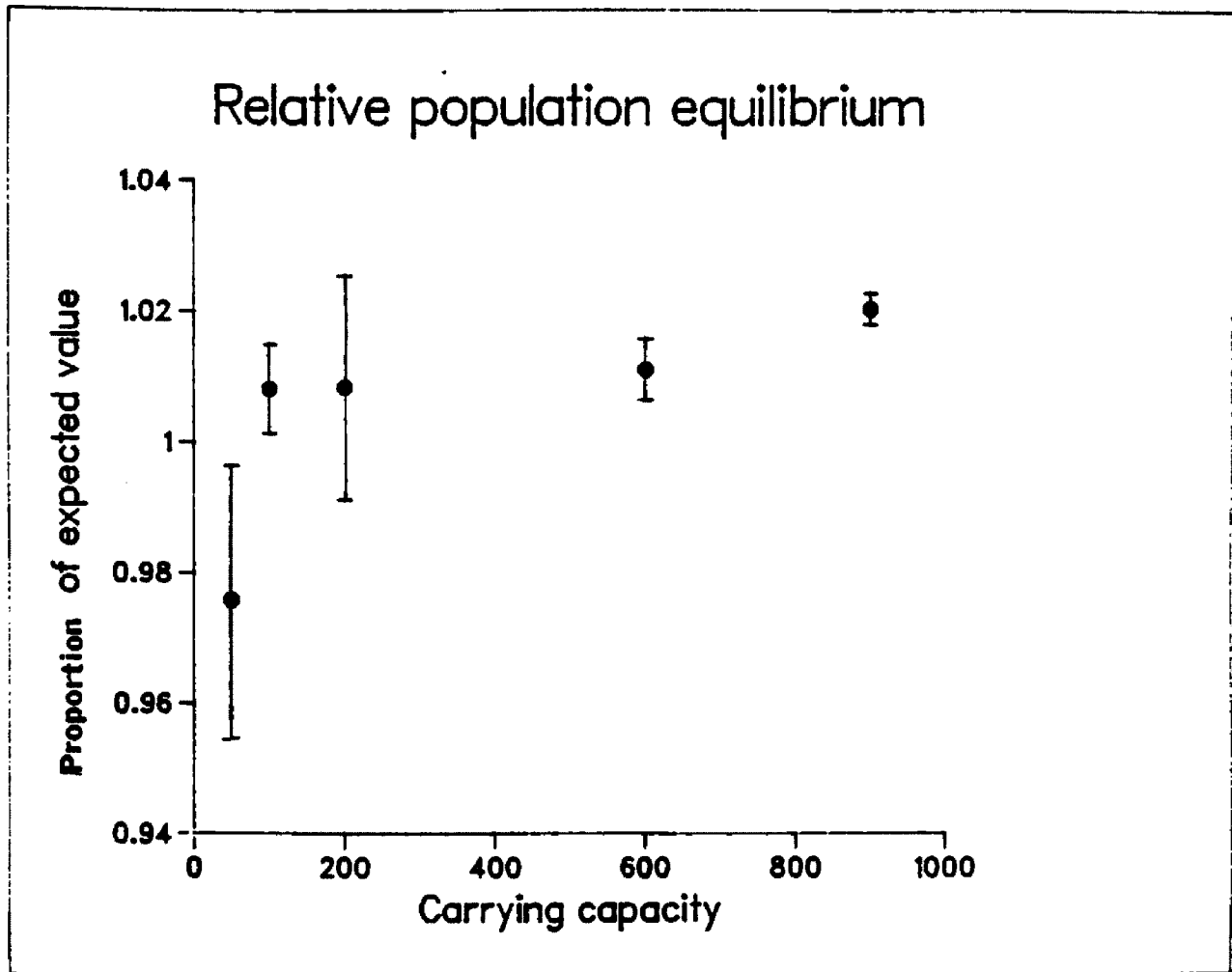


Fig. 21. Relative equilibrium values attained by simulated populations plotted against expected carrying capacities. Solid circles are means; bars represent 1 standard error from the mean.

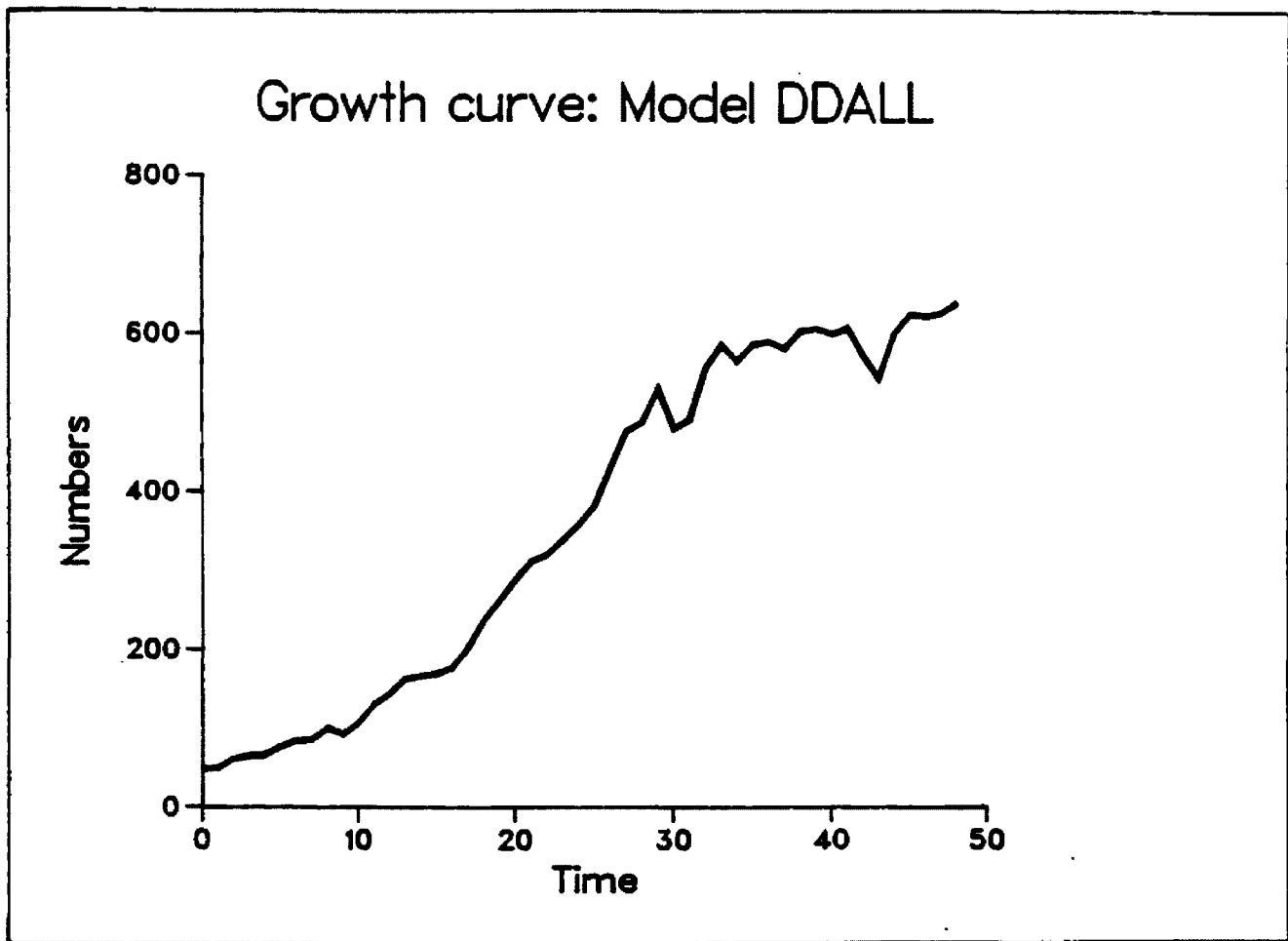


Fig. 22. A typical simulation run with $K=600$, starting from an arbitrary population of 50 animals. This illustration used Model DDALL.

GROWTH CURVE, LOG SCALE

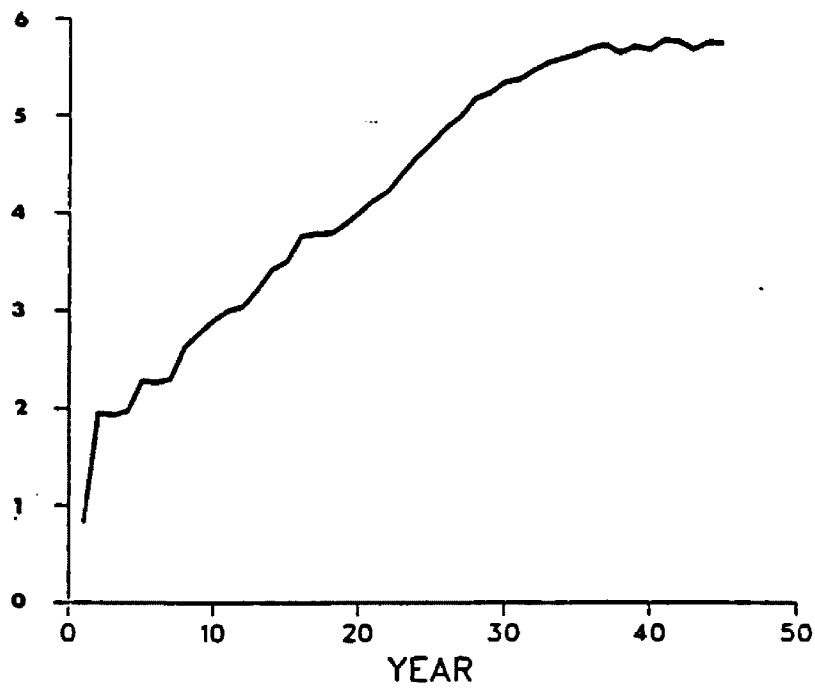


Fig. 23. The simulation run in Fig. 22 plotted with number of animals on a logarithmic scale.

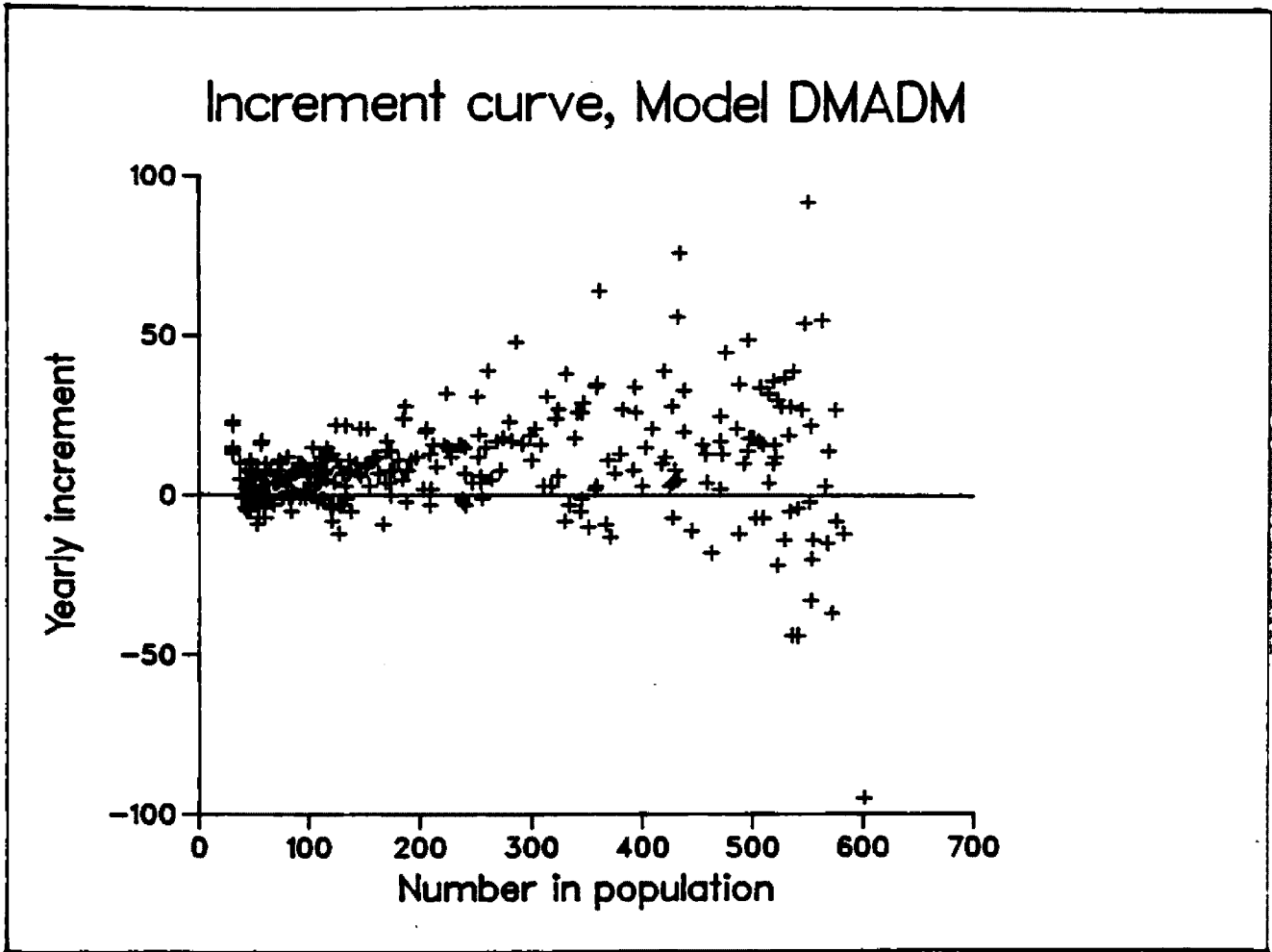


Fig. 24. A typical increment curve, as generated by a growing population. This illustration used Model DMADM with $K=600$.

densities, largest at populations slightly below K , and averaged 0 at K . The resulting increment curve tended toward the asymmetrical shape as presented in Fig. 1 (and in Fowler 1981), but zero and negative increments occurred during all phases of population growth.

Sustained Yield Curves

Sustained yield curves represent all the possible equilibrium combinations of population size and harvest rate. Deterministic models suggest that the portion of the SYC separating declining populations from those recovering toward stable equilibrium is a line of release points (Fig. 2). The curve has always been portrayed as a sharply defined dividing line. However, sustainable yields of grizzly bear populations were not accurately portrayed by 1-dimensional curves. Rather, at each cross-section population, sustained yields formed broad probability bands (Fig 25) that bracketed the high and low harvests leading toward decline and stable equilibrium (defined here as a stable harvest). **Above** the probability bands, harvests were excessive and always caused declines; **below** the bands, harvests were sustainable and populations always moved toward stable equilibria. Harvest levels **within** the probability bands were sometimes sustainable and sometimes not. The ambiguity usually peaked in the center of the band; harvest levels near the top or bottom of the bands resulted in more predictable population trajectories (Fig. 25, inset).

Probability of stability for a given harvest level was quantified as the number of times the population moved toward stable

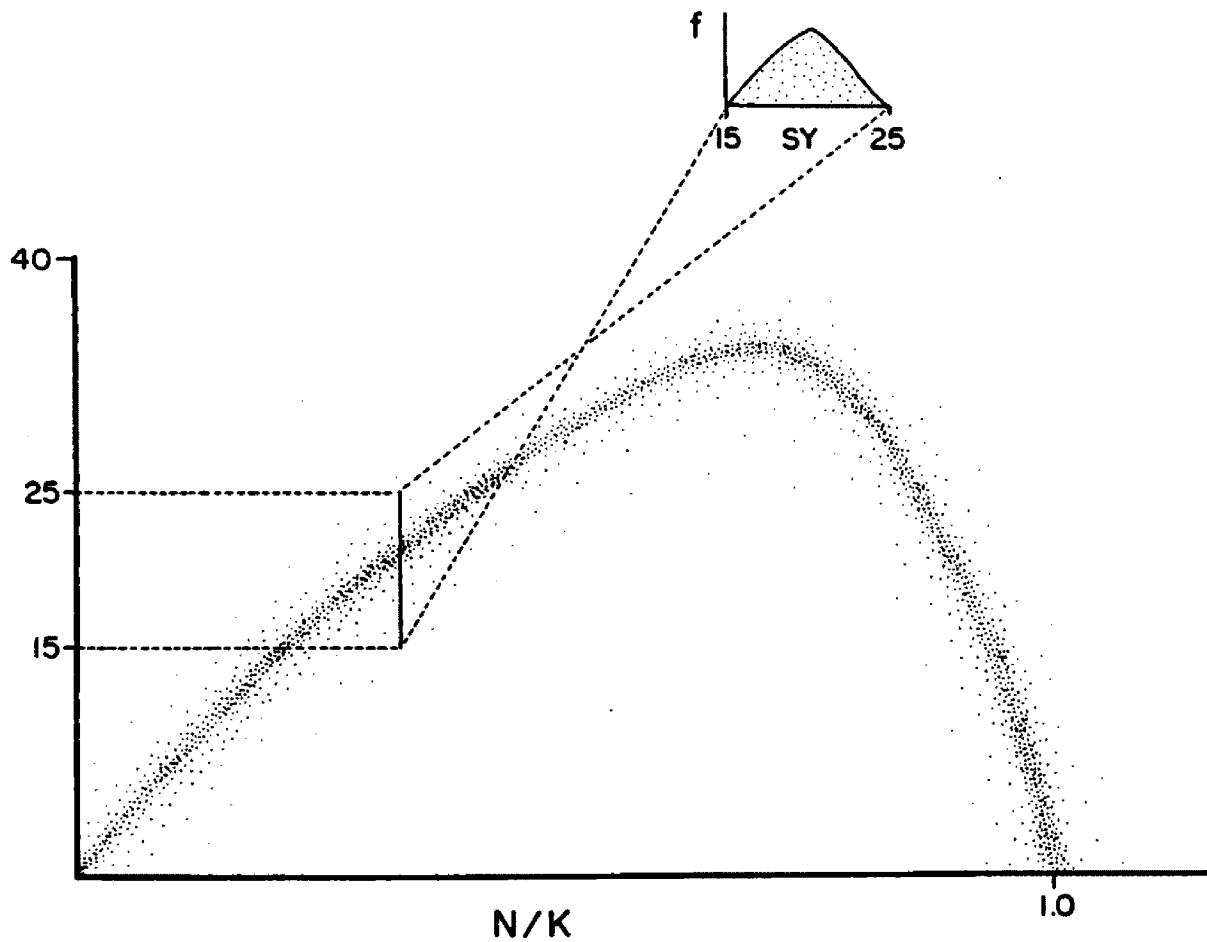


Fig. 25. A generalized sustained yield curve, showing the probability band of sustained yields. The band is most dense at its center, gradually becoming more diffuse at more extreme harvests for any given N/K level. The inset shows the probability distribution of sustained yield curve location at a cross-section of the curve, rotated 90 degrees.

equilibrium out of the 10 replicates at that harvest level (not including replicates in which population trajectory was ambiguous) (Tables 8 - 11). When plotted, probabilities of the dividing line between stability and decline for each of 10 harvest levels formed generally bell-shaped distributions (Fig. 26).

Factors influencing trajectories of individual populations.

At any given cross-section and harvest level, an expected trajectory existed that was a function of the harvest rate and stochastic events. Four stochastic factors influenced an individual population's trajectory: (i) the precise number of animals in the cross-section population prior to the trial harvests, (ii) the age-structure of the cross-section population prior to the trial harvests, (iii) the age-structure of the animals taken during the trial harvests, and (iv) random variation in natural birth and survival rates resulting from variation in K during the trial harvests. The first 3 were essentially demographic effects, the 4th was an environmental effect.

A specific case history, in which each of these factors came into play, will help to clarify their influence. To review the components within the 4 Specific Models: DDALL - Density-Dependent ALL (both natality and survival); DM - Density-dependent Mortality only; ADM - Adult Male dominated survival functions for sub-adult males, natality density-dependent; DMADM - Density-dependent Mortality only, Adult Males dominate survival functions of sub-adult males.

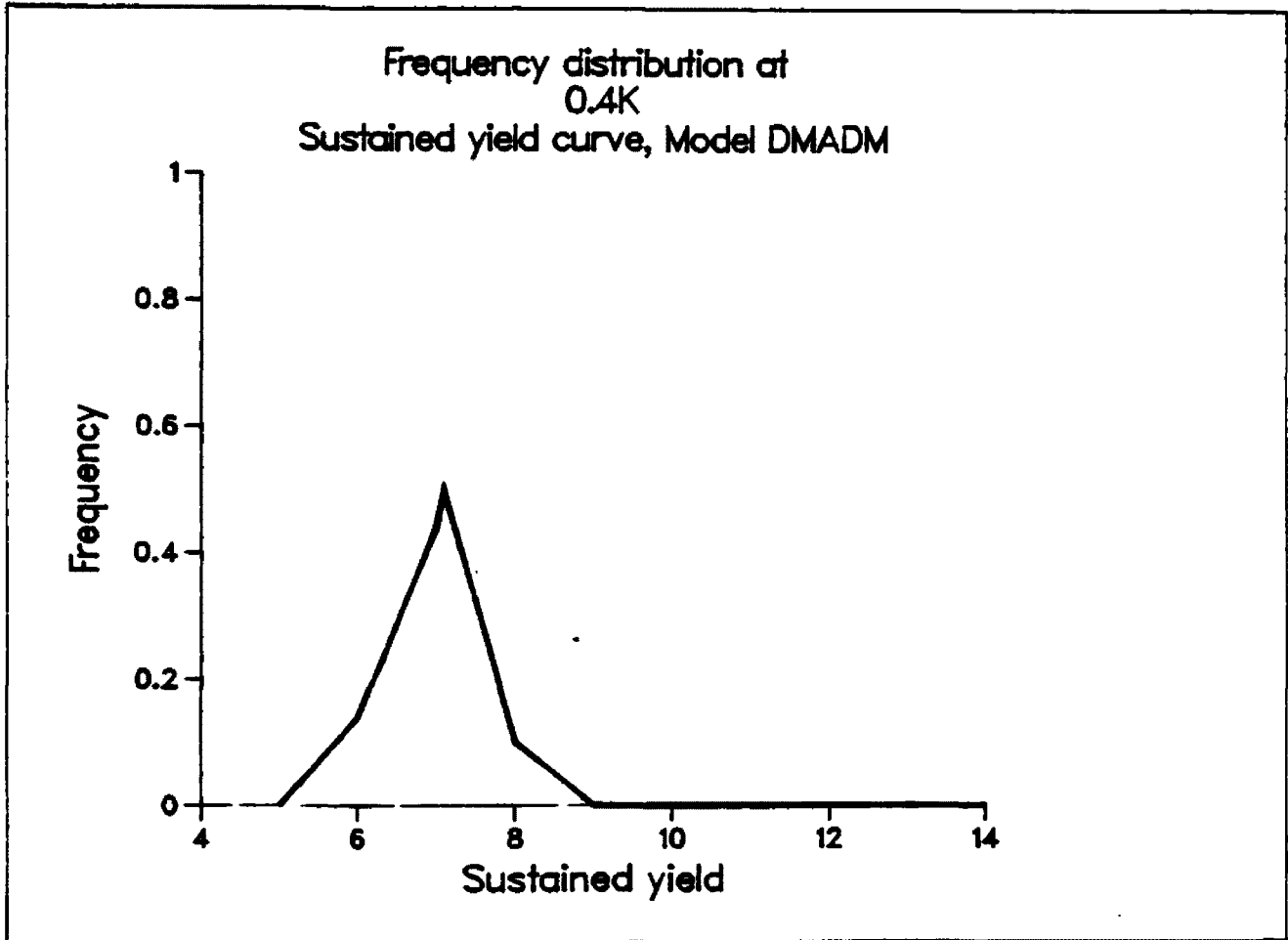


Fig. 26. A typical frequency distribution of sustainable yield, as seen schematically in the inset of Fig. 25. Illustrated is the probability that the sustained yield curve is located at each harvest (4-12) for the 0.4K cross-section of Model DMADM populations with a theoretical $K=200$, as calculated over 30 years.

Table 8. Stability of sustained harvests, as calculated over a 10-year period. Figures are the percentage of the 10 replicates in which population trajectory was positive, excluding those replicates in which trajectory was ambiguous. All simulations used a carrying capacity of 200.

Percentage of replicates resulting in stability					
Proportion Harvested	Hunt	Specific Model			
		DDALL	DM	ADM	DMADM
Cross-Section 0.4K					
.062	5	100	100	100	100
.075	6	100	71.4	100	71.4
.087	7	75	0	70	57.1
.100	8	100	16.7	75	22.2
.112	9	87.5	0	40	0
.125	10	0	0	37.5	0
.137	11	0	0	11.1	0
.150	12	0	0	10	0
.162	13	0	0	0	0
.175	14	0	0	0	0
Cross-Section 0.7K					
.057	8	100	90	100	100
.064	9	100	90	100	100
.071	10	100	80	100	77.8
.079	11	100	88.9	100	87.5
.086	12	100	50	90	62.5
.093	13	100	57.1	100	55.6
.100	14	87.5	11.1	88.9	10
.107	15	33.3	12.5	75	11.1
.114	16	22.2	12.5	66.7	11.1
.121	17	25.0	0	28.6	0

Table 9. Stability of sustained harvests, as calculated over a 30-year period. Figures are the percentage of the 10 replicates in which population trajectory was positive, excluding those replicates in which trajectory was ambiguous. All simulations used a carrying capacity of 200.

Percentage of replicates resulting in stability					
Proportion Harvested	Hunt	Specific Model			
		DDALL	DM	ADM	DMADM
Cross-section 0.4K					
.062	5	100	100	100	100
.075	6	100	70	100	86
.087	7	100	12.5	70	55.5
.100	8	55.5	11.1	60	10
.112	9	10	0	30	0
.125	10	20	0	0	0
.137	11	0	0	10	0
.150	12	0	0	10	0
.162	13	0	0	0	0
.175	14	0	0	0	0
Cross-section 0.7K					
.057	8	100	90	100	90
.064	9	100	60	100	90
.071	10	90	70	100	70
.079	11	70	30.9	90	60
.086	12	80	10	90	30
.093	13	40	0	70	20
.100	14	30	0	66.7	10
.107	15	0	0	0	0
.114	16	0	0	0	0
.121	17	0	0	0	0

Table 10. Stability of sustained harvests, as calculated over a 10-year period. Figures are the percentage of the 10 replicates in which population trajectory was positive, excluding those replicates in which trajectory was ambiguous. All simulations used a carrying capacity of 600.

Percentage of replicates resulting in stability					
Proprtion Harvested	Hunt	Specific Model			
		DDALL	DM	ADM	DMADM
Cross-section 0.4K					
.070	15	100	100	100	100
.084	18	100	66.7	100	80
.098	21	62.5	57.1	87.5	40
.112	24	0	0	37.5	22.2
.126	27	0	0	11.1	0
.140	30	10	0	0	0
.155	33	0	0	0	0
.169	36	0	0	0	0
.183	39	0	0	0	0
.197	42	0	0	0	0
Cross-section 0.7K					
.061	24	100	100	100	100
.069	27	100	90	100	100
.076	30	100	100	100	100
.084	33	100	60	100	100
.092	36	90	60	100	80
.099	39	50	10	100	30
.107	42	50	0	70	20
.115	45	10	0	22.2	0
.122	48	0	0	11.1	0
.130	51	0	0	11.1	0

Table 11. Stability of sustained harvests, as calculated over a 30-year period. Figures are the percentage of the 10 replicates in which population trajectory was positive, excluding those replicates in which trajectory was ambiguous. All simulations used a carrying capacity of 600.

		Percentage of replicates resulting in stability			

Proportion Harvested	Hunt	Specific Model			
		DDALL	DM	ADM	DMADM

Cross-section 0.4K					
.0703	15	100	90	100	100
.0843	18	90	54.5	100	60
.0984	21	44.4	0	80	22.2
.1124	24	0	0	40	0
.1265	27	0	0	0	0
.1405	30	0	0	0	0
.1546	33	0	0	0	0
.1686	36	0	0	0	0
.1827	39	0	0	0	0
.1967	42	0	0	0	0
Cross-section 0.7K					
.0612	24	100	100	100	100
.0688	27	100	90	100	100
.0765	30	100	40	100	100
.0841	33	70	10	100	60
.0918	36	70	0	70	20
.0994	39	10	0	50	10
.1071	42	0	0	20	0
.1147	45	0	0	0	0
.1224	48	0	0	0	0
.1300	51	0	0	0	0

-(i). For Model ADM simulations with $K=200$, 9 of 10 populations declined over 30 years when harvested from 0.4K at 12 animals/year (Table 9). The 9 that declined averaged 76 individuals (S.E.=0.972) at 0.4K. The 1 replicate that moved toward a stable equilibrium during the 30-year period began at a population size of 86. Further, the 9 declining populations averaged 42.11 females at 0.4K (S.E.=2.37), but the stable population contained 55 at the initiation of experimental harvesting. Clearly, the larger the number at the outset of trial harvests, the higher the probability of stability.

-(ii). Only 1 of the 10 Model DDALL $K=600$ 0.4K replicates was stable over 10 years when harvested at 30 animals/year (Table 10). It benefited from a favorable sex ratio at the initiation of harvesting: 58.9% females, compared to an average of just 50% females among the 9 populations that declined. The unusually large cohort produced in the 2nd year of experimental harvesting suggests that many of the females in the stable population were of breeding age. Thus, the 1 stable population had a greater than average proportion of reproductive females.

-(iii). Eight of 9 Model DM $K=200$ populations with unambiguous trajectories declined during the first 10 years of harvesting at 8 animals/year from 0.4K (Table 8). The 1 replicate that was stable benefited from a favorable sex ratio in the harvest. Although the standing population sex ratio approximated 1:1 at the initiation of experimental harvests, 15 of the 16 animals harvested during the 1st 2 years were males. This unusually skewed harvest sex ratio enabled

almost all of the young females to survive and produce young. In year 3, after the 2 years of favorable harvests, 25 cubs were born. The flush of recruits swelled the total numbers, and the population increased significantly during years 7,8, and 9, when the females among those 25 cubs had young of their own.

-(iv). At 0.7 of $K=600$, 9 of 10 Model DM populations exhibited stability over the 1st 10 years when harvested at 27 animals/year (Table 10). The population that declined suffered from 1 particularly bad year: during year 8, 53 of the 359 animals (almost 15%) died from natural causes in addition to the 27 killed by hunting. The carrying capacity during year 8 was only 472, or 79% of the median carrying capacity, an extremely poor year. This population never fully recovered.

Factors influencing average sustainable harvests.

Differences in probability distribution location and shape (i.e. height and width of the probability band) were caused by 4 factors.

1. The width of the probability distribution was related to the cross-section at which it was examined. Probability distributions at 0.7K were wider than those at 0.4K (compare Fig. 27 with Fig. 26). Under constant harvests, trajectories were horizontal. Because populations at 0.7K were near the peak of the SYC, their trajectories necessarily passed through more of the probability band than did populations at 0.4K (Fig. 28). Additionally, the shape of the SYC near 0.7K resulted in close proximity to the band, producing relatively slow

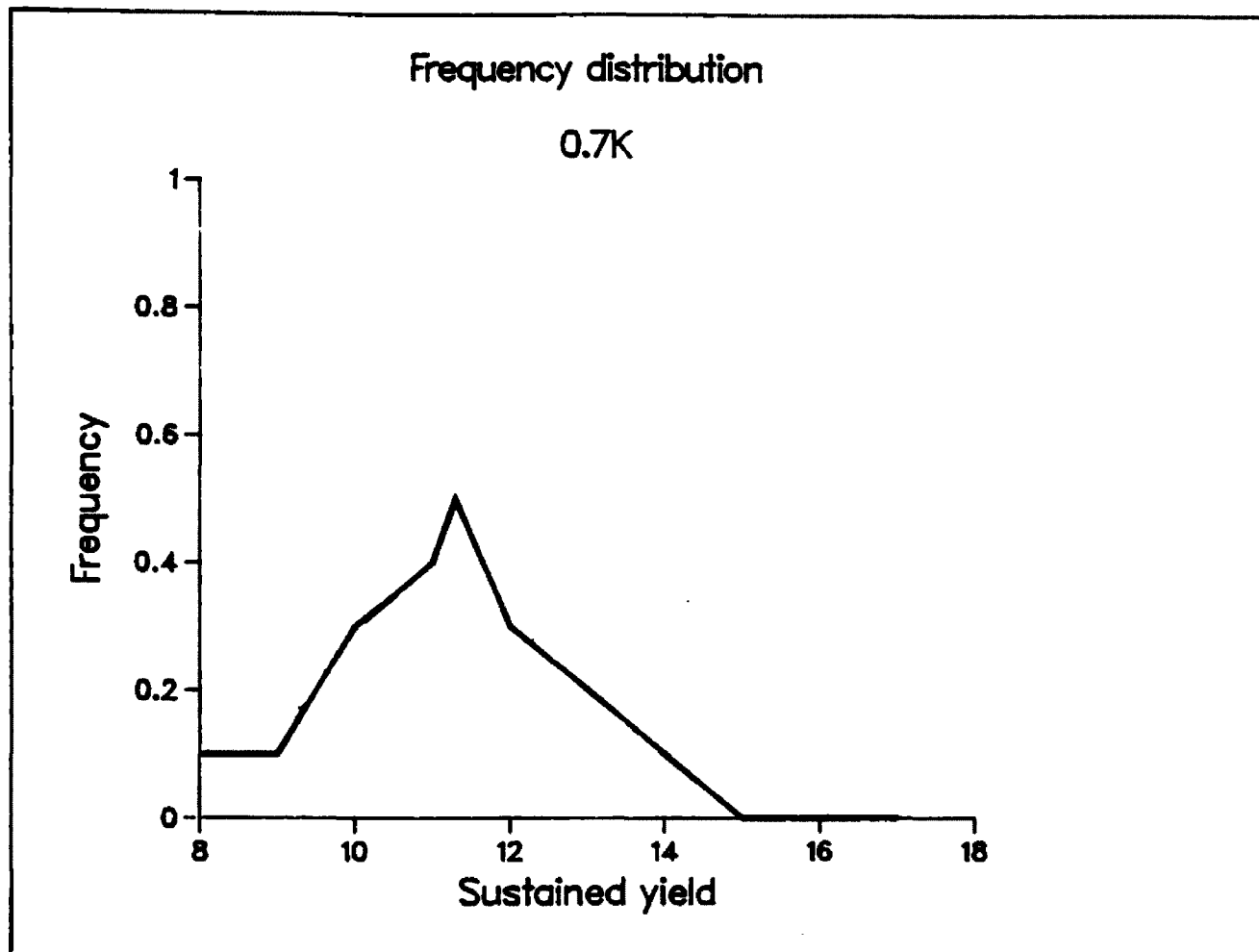


Fig. 27. The frequency distribution of sustained yield for the 0.7K cross-section of Model DMADM populations with a theoretical $K=200$, as calculated over 30 years.

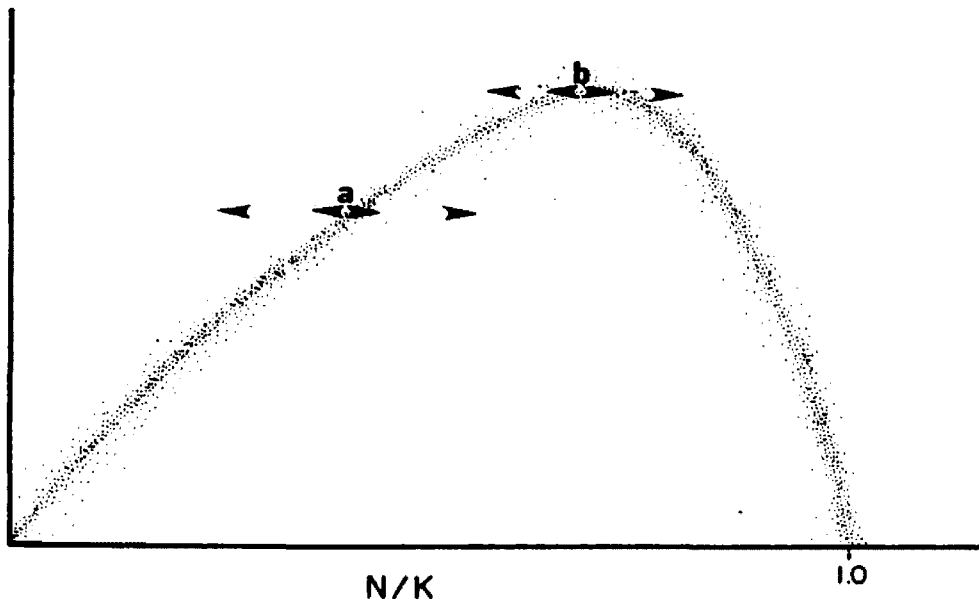


Fig. 28. Trajectories of harvested populations along the sustained yield curve. a. Trajectories from $0.4K$. b. Trajectories from $0.7K$. Note that trajectories at $0.7K$ pass through more of the probability band than do those at $0.4K$.

trajectories. Populations at 0.4K moved away from the band more quickly. The combined effect was that populations moving from 0.7K had a longer exposure to the probability band, increasing the chance that a random event could reverse an initial trajectory.

2. Sustainable yield was inversely related to the length of time simulations were run ($p < 0.01$, Table 12). Populations exposed to the same harvest level were more likely to decline when considered over 30 years than when considered over 10 years (Fig. 29). Of 673 populations that appeared stable during the 10 year analysis, 143 displayed downward trajectory for the 30 year analysis. However, none of the 870 populations exhibiting significant decline during the 1st 10 years reversed their trajectory toward stability in the subsequent 20 years. The difference in rates of reversal was significant (McNamer test for the significance of changes $G=198.2$, $p < < 0.001$). Thus, the height of a SYC was a function of time. The longer a harvest continued, the greater the probability that a random event would perturb the system out of the probability band into declining space.

3. The Specific Models used in the simulations resulted in different sustainable yields (Table 12). The Models differed in their mechanisms of population regulation and hence in their resilience to harvest.

The 2 Models that incorporated density-dependent birth rates, Models DDALL and ADM, were able to sustain heavier harvests than the 2 with density-independent birth rates ($F=79.3$, $df=1,3$, $p < 0.005$, Table 12). Probability bands generated with Models with density-dependent natality were higher (i.e. higher harvests were needed to induce

Table 12. Mean sustainable yield, comparing calculations over 10 years and 30 years. All values are expressed as proportions of the cross-section population, 0.7K, and all 4 Specific Models have theoretical K=600.

a. Mean sustainable yield, expressed as a proportion of pre-hunt population

Years of Calculation	Specific Model			
	DDALL	DM	ADM	DMADM
10	.0986	.0806	.1122	.0959
30	.0887	.0721	.0967	.0875

b. ANOVA table.

Source of Variation	df	MS	F	p
Years of Calculation	1	.000225	39.5	<0.01
Specific Model	3	.000268	47.0	<0.01
Density-depenent or -independent births	1	.000452	79.3	<0.005
Adult male mortality function	1	.000341	59.8	<0.005
Remainder	3	.000006		

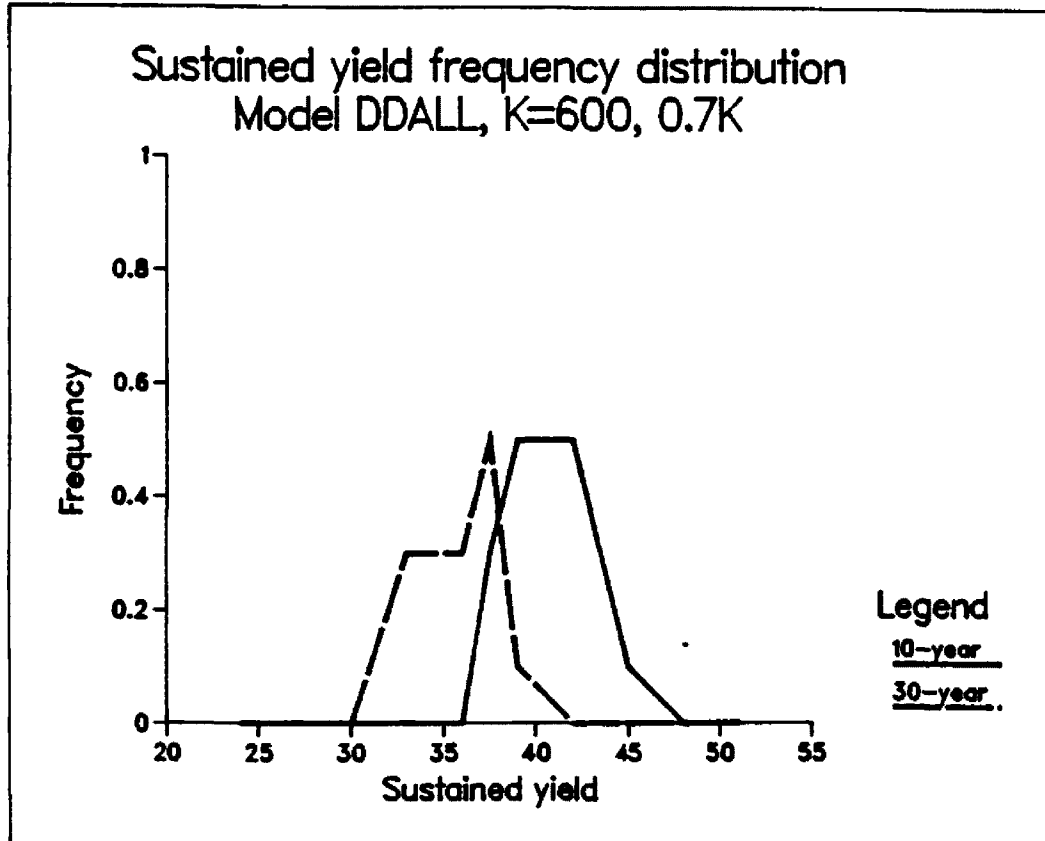


Fig. 29. Sustained yield frequency distribution, showing the difference between yields resulting in stability over 10 years and 30 years. Illustrated are the sustainable yields from the 0.7K cross-section of Model DDALL populations with a theoretical K=600.

declines) than probability bands generated with the later 2.

The inclusion of a separate, adult male-dependent mortality function for sub-adult males had a similar, although weaker effect. The Models with the adult male-dependent function, Models ADM and DM.ADM, had generally higher sustainable yields than did their respective Models without the adult male-dependent mortality function ($F=59.8$, $df=1,3$, $p<0.005$, Table 12). Consequently, the largest differences occurred between Models ADM and DM (Fig. 30). Model ADM had density-dependent birth rates and the adult male-dependent mortality rates for sub-adult males. Model DM had neither of these mechanisms, resulting in low ability to withstand harvests.

4. Sustainable yield, calculated as a percentage of the standing population at the initiation of harvest, increased with equilibrium population size (Table 13). Mean sustained percentage harvests were significantly lower ($F=13.3$, $df=1,1$, $p<0.05$) for populations with $K=200$ than for those with $K=600$. Thus, as the magnitude of demographic stochasticity increased with smaller populations, resilience to the same proportional harvest decreased.

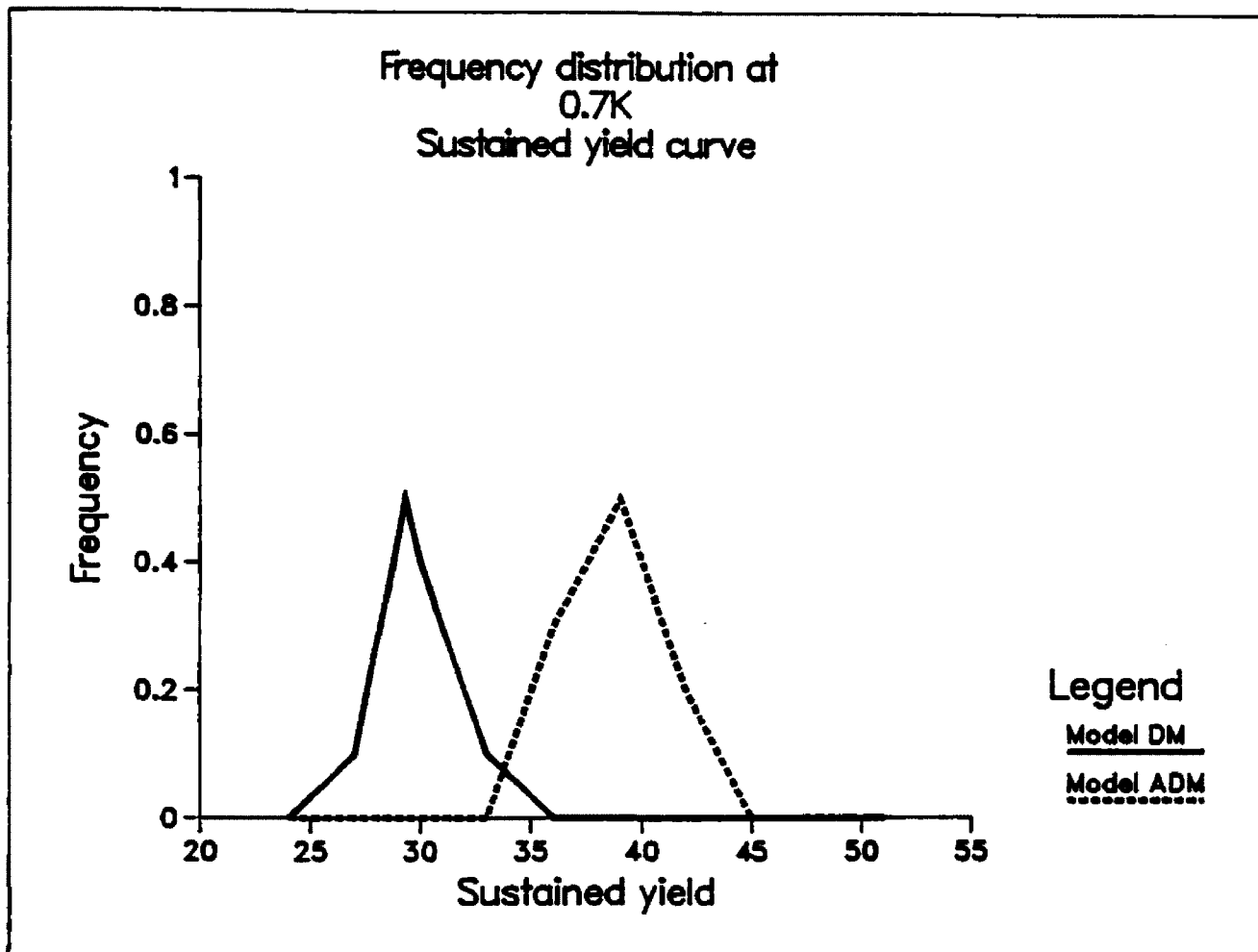


Fig. 30. Sustained yield frequency distributions for Models DM and ADM, showing the difference between the 2. Illustrated are sustainable yields from 0.7K of K=600 populations, as calculated over 30 years.

Table 13. Mean sustainable yield, comparing populations with theoretical $K=200$ and $K=600$. Yields are calculated for each of the 4 Specific Models over 30 years, and all values are expressed as percentages of the cross-section population, $0.7K$.

a. Mean sustainable yield, expressed as a proportion of pre-hunt population

Carrying capacity	Specific Model			
	DDALL	DM	ADM	DMADM
200	.0823	.0622	.0883	.0705
600	.0887	.0721	.0967	.0875

b. ANOVA table.

Source of Variation	df	MS	F	p
Carrying Capacity	1	.000178	13.3	<0.05
Specific Model	3	.000197	14.7	<0.05
Density-depenent or -independent births	1	.000445	33.2	<0.025
Adult male mortality function	1	.000142	10.6	<0.05
Remainder	3	.000013		

Caution must be used in interpreting Tables 12 and 13. They appear to indicate that harvesting as much as 10% of a grizzly bear population can lead to a stable equilibrium. However, these harvest rates are not compatible with stable management. All harvest rates in Tables 8-11 were applied to populations in the unstable region of the SYC; the region prudent management attempts to avoid. To calculate the proportion of the population that can be harvested indefinitely, trial harvests would have been applied to cross-sections in the stable portion of the SYC, to the right of N_{msy} . These cross-section populations would have been larger than those used here, and hence sustained harvest rates, viewed as percentages, would have been smaller.

Description of Grizzly Bear Age-structures

Harvested Populations Initially at K.

Standing Population Age-Structures. The mean age-structure for modeled grizzly bear populations at unexploited equilibrium is presented in Fig. 12. Under an initial, stable harvest, mean age-structures showed subtle changes from this equilibrium condition (Fig. 31). Males predominated in the hunt, increasing the bias towards females in the standing age-structure. The age-distribution of females showed little change from the unexploited distribution. Among males however, the sharp drop-off after age 2 became slightly more accentuated. When overharvested from an initially unexploited state, the same 2 changes occurred, but with greater magnitude (Fig. 32). In general, mean age-structures of overharvested populations differed only slightly from mean age-structures of populations under stable harvest.

Changes in population age-structures that occurred with chronic overharvest were most clearly seen in plots of descriptive age-structure statistics against the number in the population when the population was driven from K to extinction. These plots are presented here in a form often used to calibrate an index of abundance with known population size (Caughley 1977), but they should not be interpreted strictly as calibrations. As will be discussed below, numerous factors other than population size determine the value of a descriptive age-structure statistic. The plots serve here to indicate the general trend of

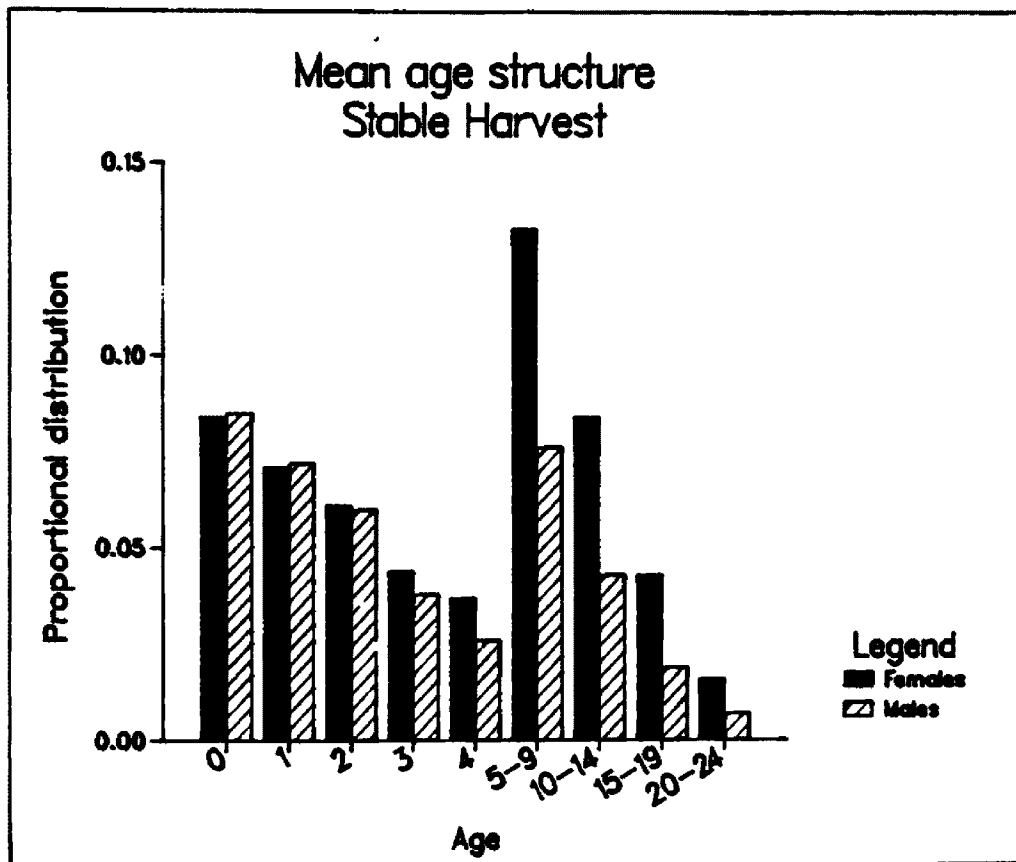


Fig. 31. The mean age-structure of the standing population when subjected to an initial, stable harvest. Age-classes 5-9, 10-14, 15-19 and 20-24 are lumped to show the differences more clearly. All values are proportions of the total number.

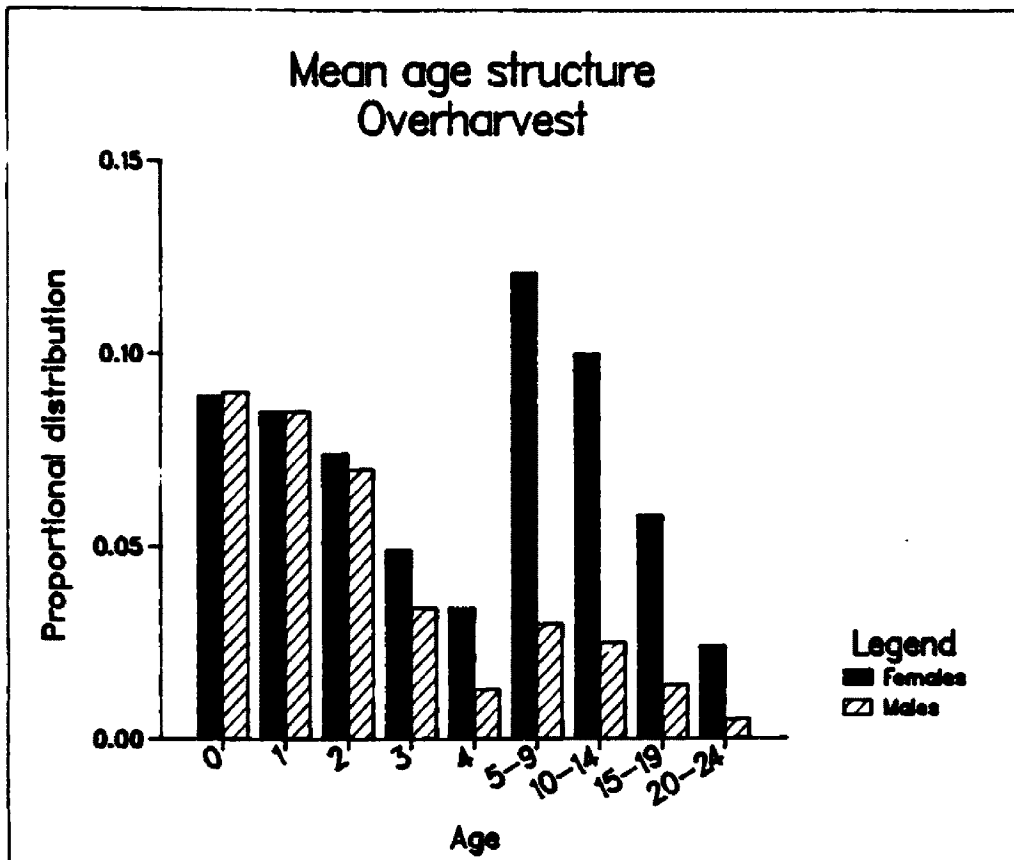


Fig. 32. The mean age-structure of the standing population when subjected to overharvesting from K.

age-structures on population size under the particular set of circumstances specified.

As populations of about 600 declined toward extinction because of overharvest, males in the population became, on average, younger (Fig. 33). From roughly 4 1/2 years at equilibrium, mean male age decreased to about 1 1/2 years at a population size of 50, at which point the population was considered extinct because only females remained. Note, however, that substantial variability characterized mean male age, especially during the early stages of population decline. For example, at population level 500 (or roughly 83% of carrying capacity), mean male age varied from about 2 1/2 to almost 5 1/2. A mean age of 3 characterized a population levels from 1/3 to almost 4/5 of carrying capacity (200 to almost 500).

Conversely, mean female age increased slightly as the population was driven to extinction, primarily because a few very old females were retained in the population despite the overall decline. The trend toward older females was weak, and the differences between mean female age in declining and stable populations was not evident until many years following initiation of harvesting (Fig. 34).

Females made up a continually increasing proportion of the age-structure as the equilibrium population was driven to extinction. Among adults (age 4+), this trend (Fig. 35) was particularly clear. (In Fig. 35, as well as all subsequent calibration-like plots, much of the actual variation has been removed by plotting only the mean statistic from 10 replicate simulations).

As in unexploited populations, age-structures of harvested

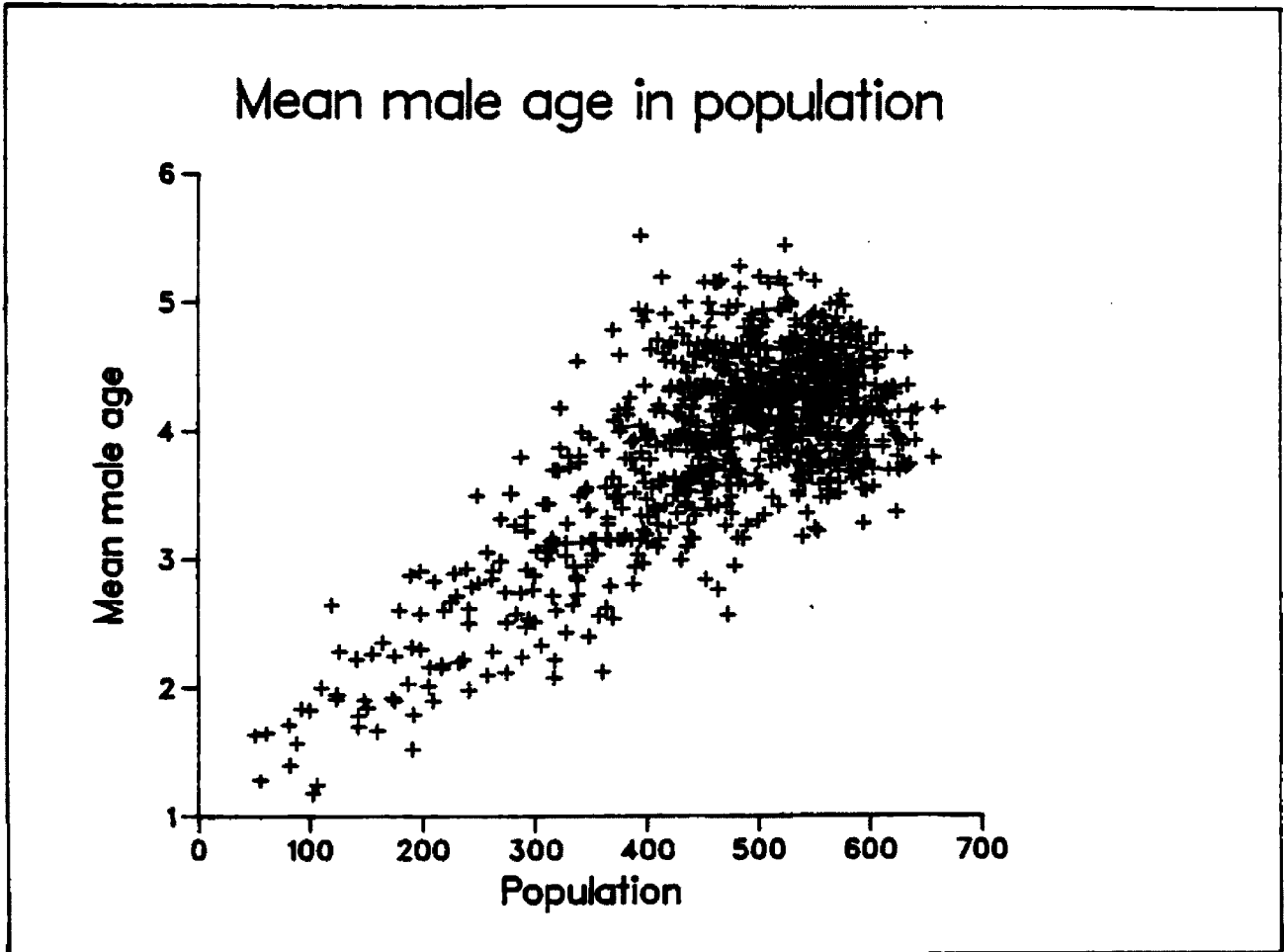


Fig. 33. Mean male age in the standing population age-structure, as a population at $K=600$ was overharvested to extinction.

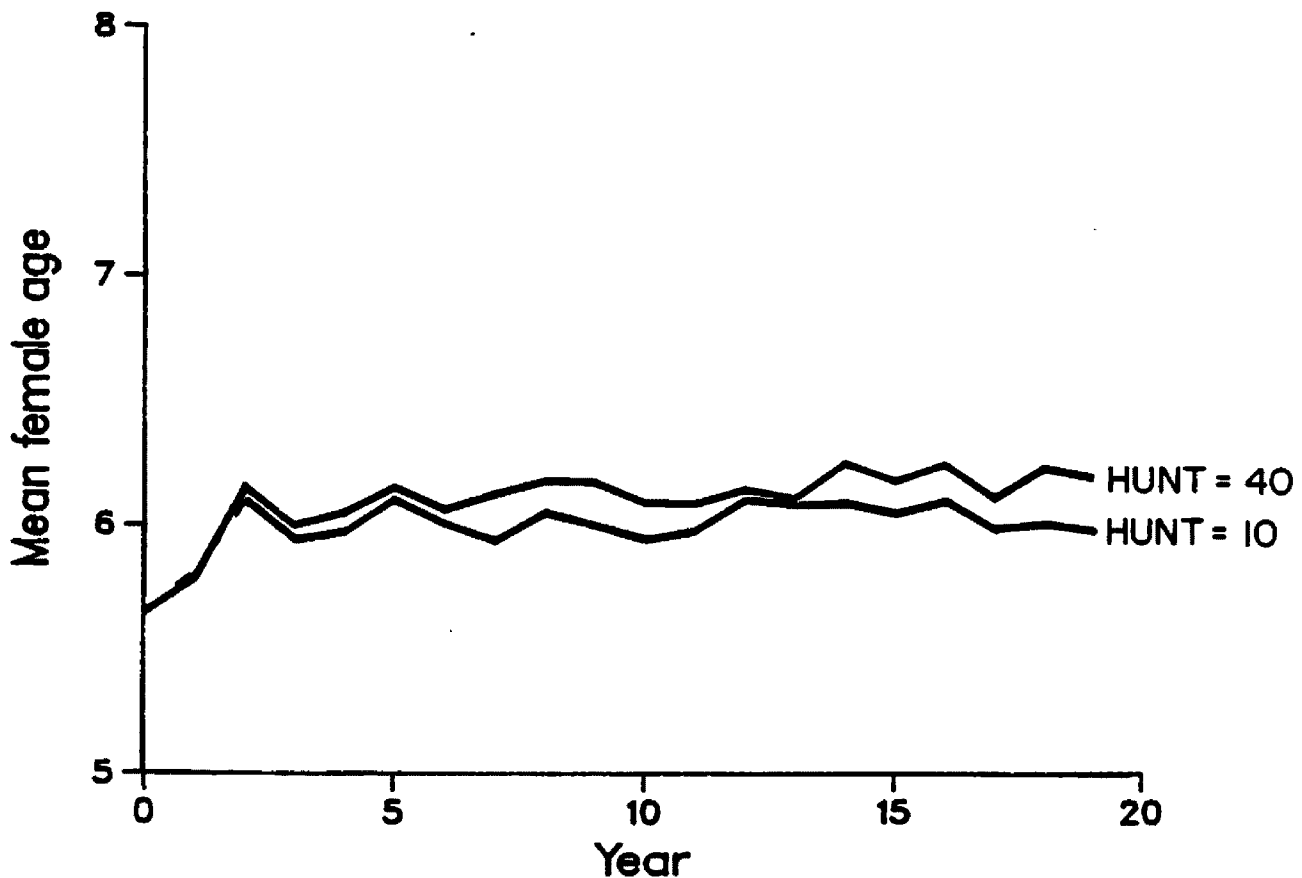


Fig. 34. Mean female age in the standing population from 2 differing sets of simulations, plotted against time. Each line represents the mean of 10 independent simulations; all 20 simulations had a common initial population structure. Harvest rates are the total number of animals (most of which were males). Harvesting 40/year drove all 10 simulations to extinction; harvesting 10/year allowed all 10 simulations to achieve stable equilibria.

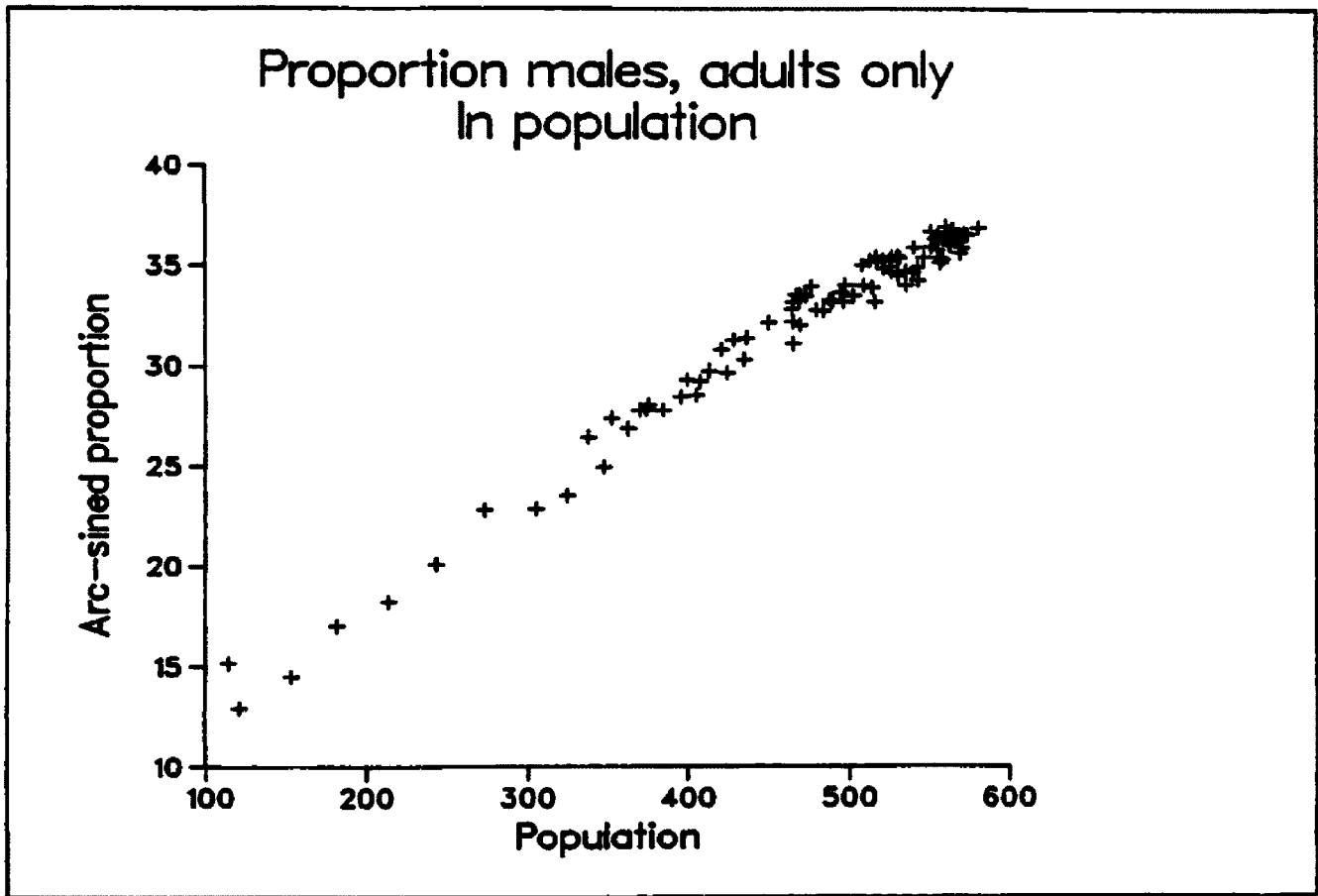


Fig. 35. The proportion males among adults in the standing age-structure as a population at $K=600$ was overharvested to extinction.

grizzly bear populations retained strong and weak cohorts for many years. Also, the effect on the age-structure produced by an abrupt change in harvest level was subject to a pronounced time-lag. For example, female age-structures showed great similarities to each other despite a 4-fold difference in overall harvest level (Fig. 34). Mean female age peaked in years 2 and 5 in both sets of simulations despite the independence among all 20 runs after year 0. The coincidental highs and lows in all runs reflected the persistence of strong and weak cohorts from within the common initial population prior to the first year of differential harvesting. Overharvesting (40 animals/year) did little to "smooth out" these ripples in female population structure. Not until year 7 did the marked difference in harvest rates overshadow the similarities among age-structures.

Table 14 summarizes the strength and direction of the relationships between all 10 age-structure statistics and population size, as populations were overharvested from K to extinction. The use of linear regression statistics is for descriptive purposes only; this is not properly a Model I regression problem. The relationships are not necessarily linear, variances are often not homoscedastic, each data point is a mean of 10 replicates (thus inflating the values of r^2), and population size is not an independent variable in the pure sense (Sokal and Rohlf 1981). Therefore, significance tests and confidence intervals are inappropriate. However, comparisons among variables can be made regarding the signs and magnitudes of slopes (β), and the relative "tightness" of the fits (r^2). In comparing slopes, note that means and medians are expressed in years, but (arc-sined) proportions are

expressed in degrees.

In all cases, descriptions of male age had stronger relations to population size than did the corresponding statistics for females (Table 14). Male ages (MXBAR, MMED) declined with the population; female ages (FXBAR, FMED) showed the opposite trend. For both sexes, means changed more with population than did medians. Sub-adults of both sexes constituted larger proportions of the age-structures as over-harvest proceeded. Also for both sexes, the ratio of prime-aged animals to cubs decreased as the population declined. Finally, the proportion males in the population declined with overharvest; the relationship being stronger when considering only adults.

Age-Structures of Hunted Samples. Male age structures from stable harvests were dominated by the vulnerable sub-adult age-classes. Harvested age-structures appeared truncated because cubs, and to a lesser extent yearlings, were generally protected from hunting. With increased harvest pressure, the less vulnerable older age-groups appeared in the harvest more frequently (Fig. 36). However, old males were eventually depleted entirely with overharvest, resulting in the appearance of more very young males (Fig. 37).

The 10 age-structure statistics computed from harvested samples showed the same general relationships to population size as they did when computed from standing population data. However, the small size of hunted samples resulted in greater variability within all 10 statistics. All r^2 values for hunter-kill age-structure statistics were less than their corresponding values when computed from standing population structures (Table 15).

Table 14. Summary of the relationships between 10 descriptive statistics of standing age-structure and population size as equilibrium populations are overharvested to extinction. Each statistic is regressed against total population size. See Table 2 for full explanation of statistics; see text for interpretation of regression statistics.

Statistic	Units	β	r^2
-----	-----	-----	-----
MXBAR	Years	0.00058	.933
MMED	Years	0.00032	.853
FXBAR	Years	-0.00023	.728
FMED	Years	-0.00005	.040
MSUBAD	Degrees	-0.05458	.967
M58JUV	Degrees	0.05344	.915
FSUBAD	Degrees	-0.00033	.259
F58JUV	Degrees	0.01961	.750
MFALL	Degrees	0.01362	.880
MFAD	Degrees	0.04974	.976

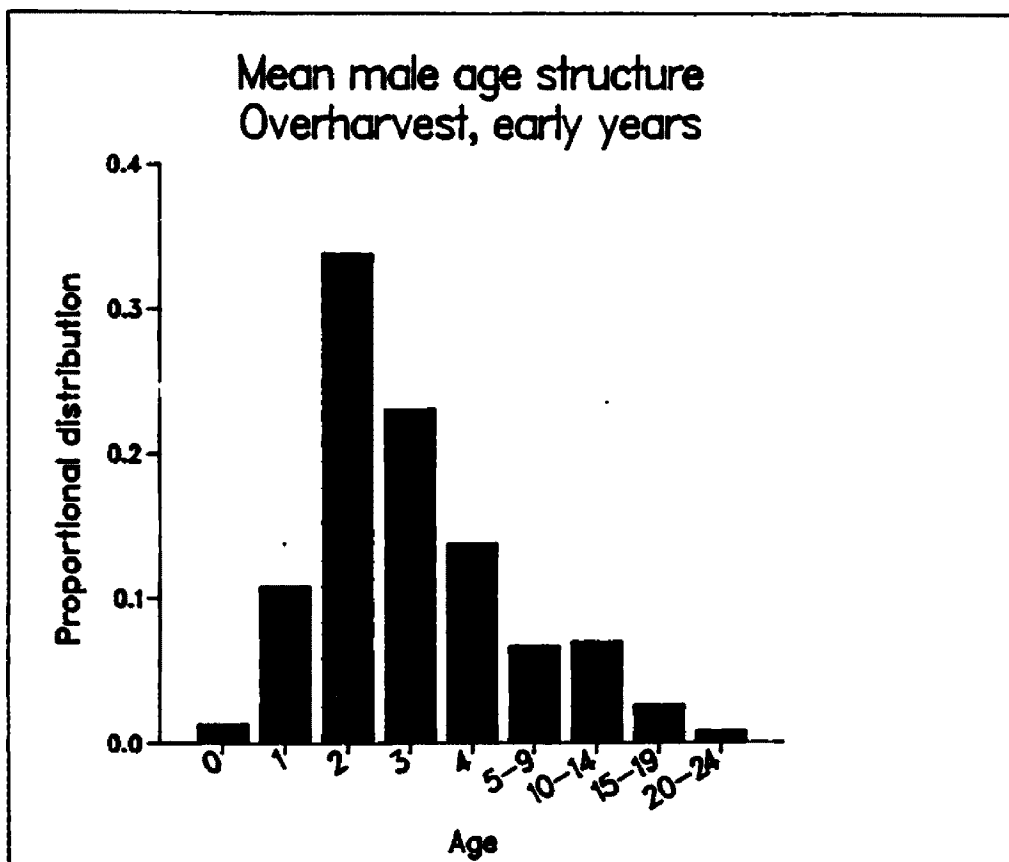


Fig. 36. Mean age-distribution of males in harvests that caused decline, pictured during the years 1-3 of the harvest. Age-classes 5-9 and 10-14 appear in the harvest despite their lower vulnerability because age-classes 2 and 3 are beginning to be depleted.

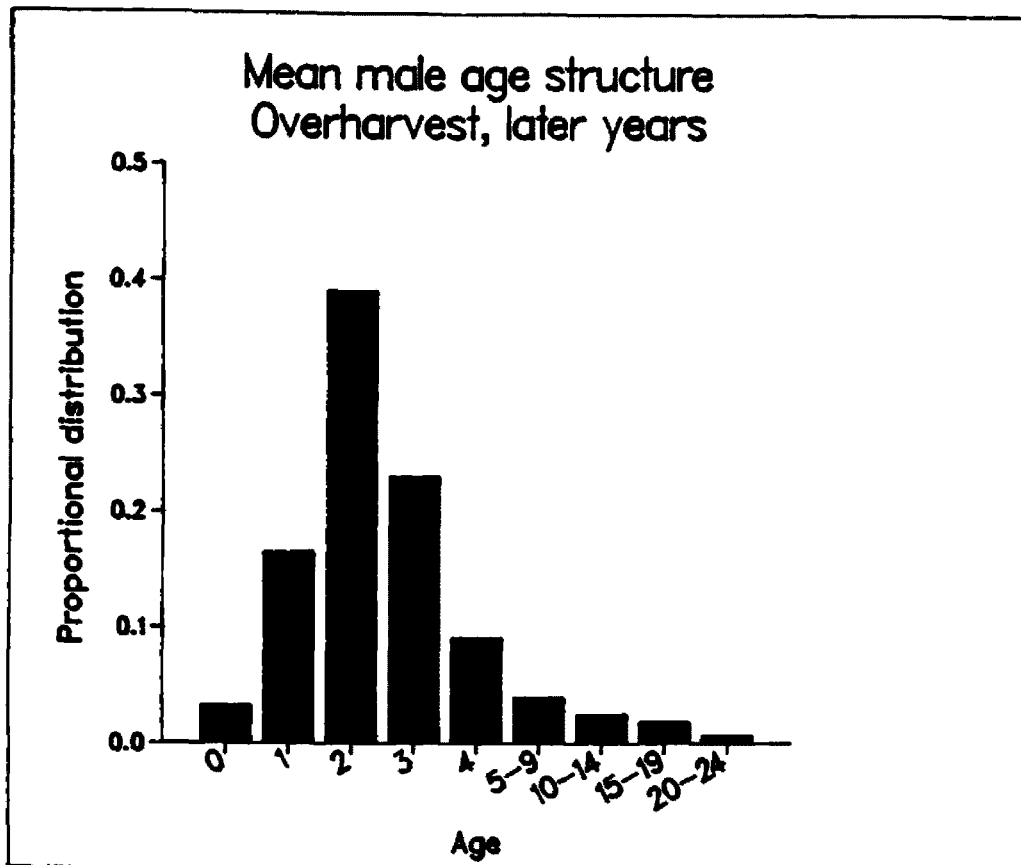


Fig. 37. Mean age-distribution of males in harvests that caused decline, pictured during years 8-10 of the harvest. Age-classes 5-9 and 10-14 are less abundant than in Fig. 36 because older males have now become depleted. Cubs and yearlings appear in increasing numbers despite their protection, because they are relatively numerous compared to the depleted older age-classes.

Table 15. Summary of the relationships between 10 descriptive statistics of harvest age-structure and population size as equilibrium populations are overharvested to extinction. Each statistic is regressed against total population size. See Table 2 for full explanation of statistics; see text for interpretation of regression statistics.

Statistic	Units	β	r^2
-----	-----	-----	-----
MXBAR	Years	0.00034	.540
MMED	Years	0.00032	.748
FXBAR	Years	-0.00024	.163
FMED	Years	-0.00025	.150
MSUBAD	Degrees	-0.04954	.745
M58JUV	Degrees	0.03545	.284
F58JUV	Degrees	0.00009	.001
MFALL	Degrees	0.03458	.662
MFAD	Degrees	0.07662	.779

For hunter-kill data, median male age (Fig. 38) varied less in its relationship to population size than did mean male age (Table 15). Among standing population age-structures, median male age varied more (compare MXBAR with MMED; Tables 14, 15). With small samples, mean age was highly sensitive to the occasional inclusion of 1 or a few very old animals. Female age in the hunted-sample was relatively unresponsive to population declines. As overharvest proceeded, females constituted a larger proportion of the hunt, and their larger representation in the harvest reduced the variability in their mean age (Fig. 39). Mean female age increased substantially only when the population verged on extinction. At this point, almost all males, as well as the younger, more vulnerable females had already been removed, leaving mostly old females for the final harvests.

As in the standing population, the proportion males declined continuously as overharvest progressed (Fig. 40). Although variation was greater, the proportion males statistics in the hunter-kill data responded to overharvest more sensitively than they did in the standing population data (compare Fig. 40 with Fig. 35). The magnitude of the change in proportion male among adults (MFAD) from harvest samples was roughly twice that seen in the standing population data.

Harvested Populations Initially at 2 Cross-sections of the SYC.

Standing Population Age-Structures. Populations at cross-sections 0.7K and 0.4K showed the effects of the overharvest that had reduced them to these levels from their initially unharvested state.

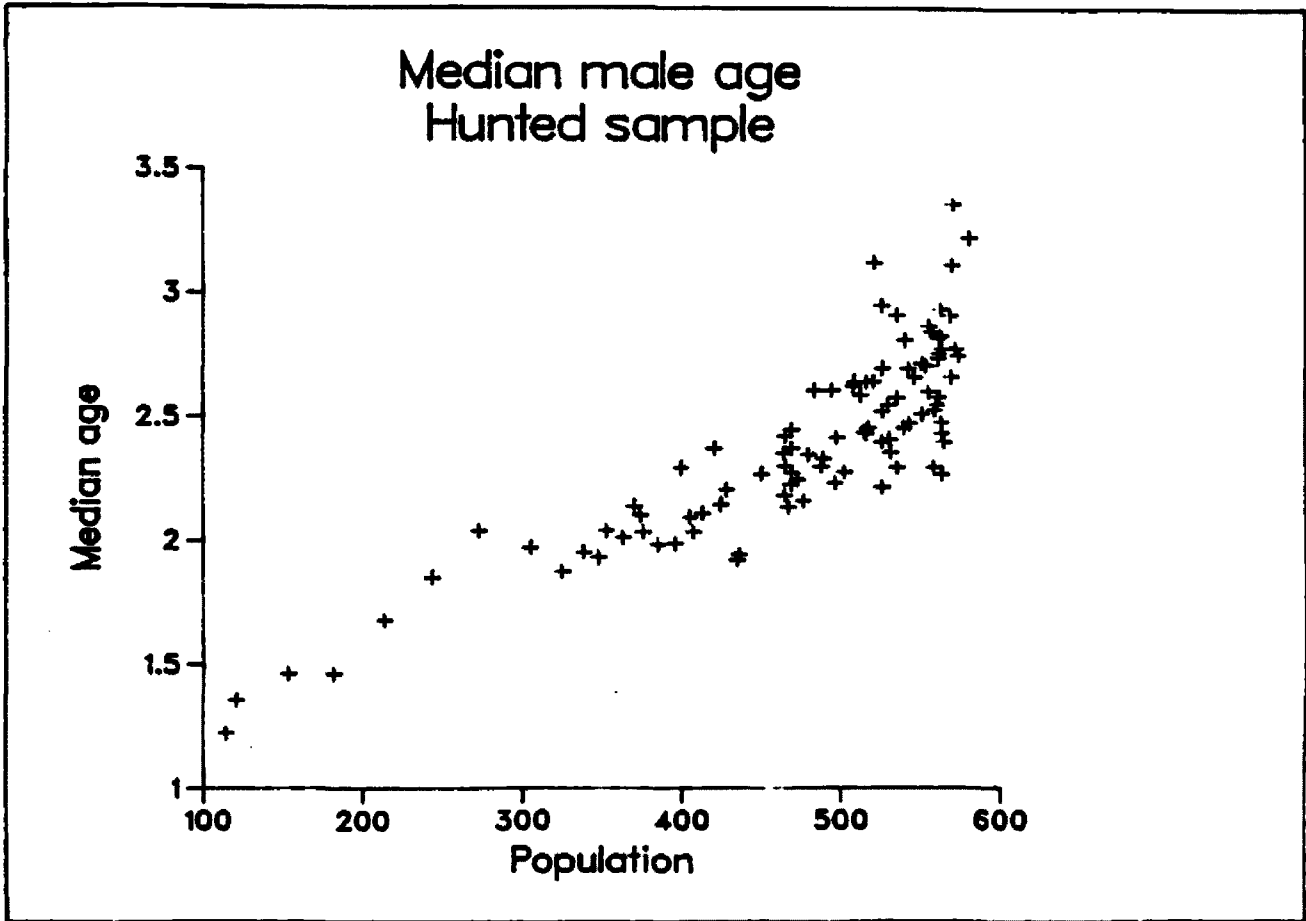


Fig. 38. Median male age in the harvest sample as a population initially at $K=600$ was overharvested to extinction.

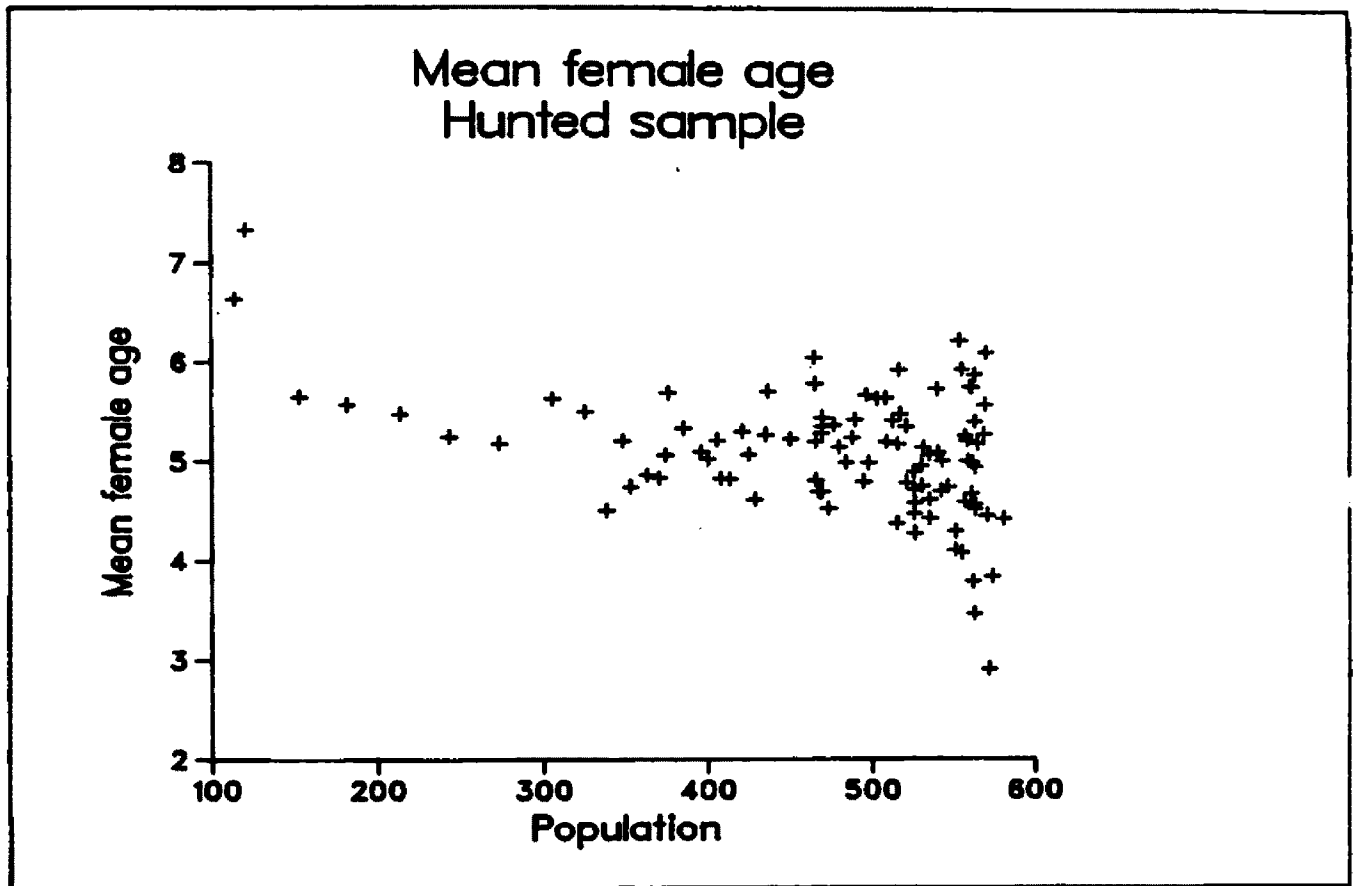


Fig. 39. Mean female age in the harvest sample as a population initially at $K=600$ was overharvested to extinction.

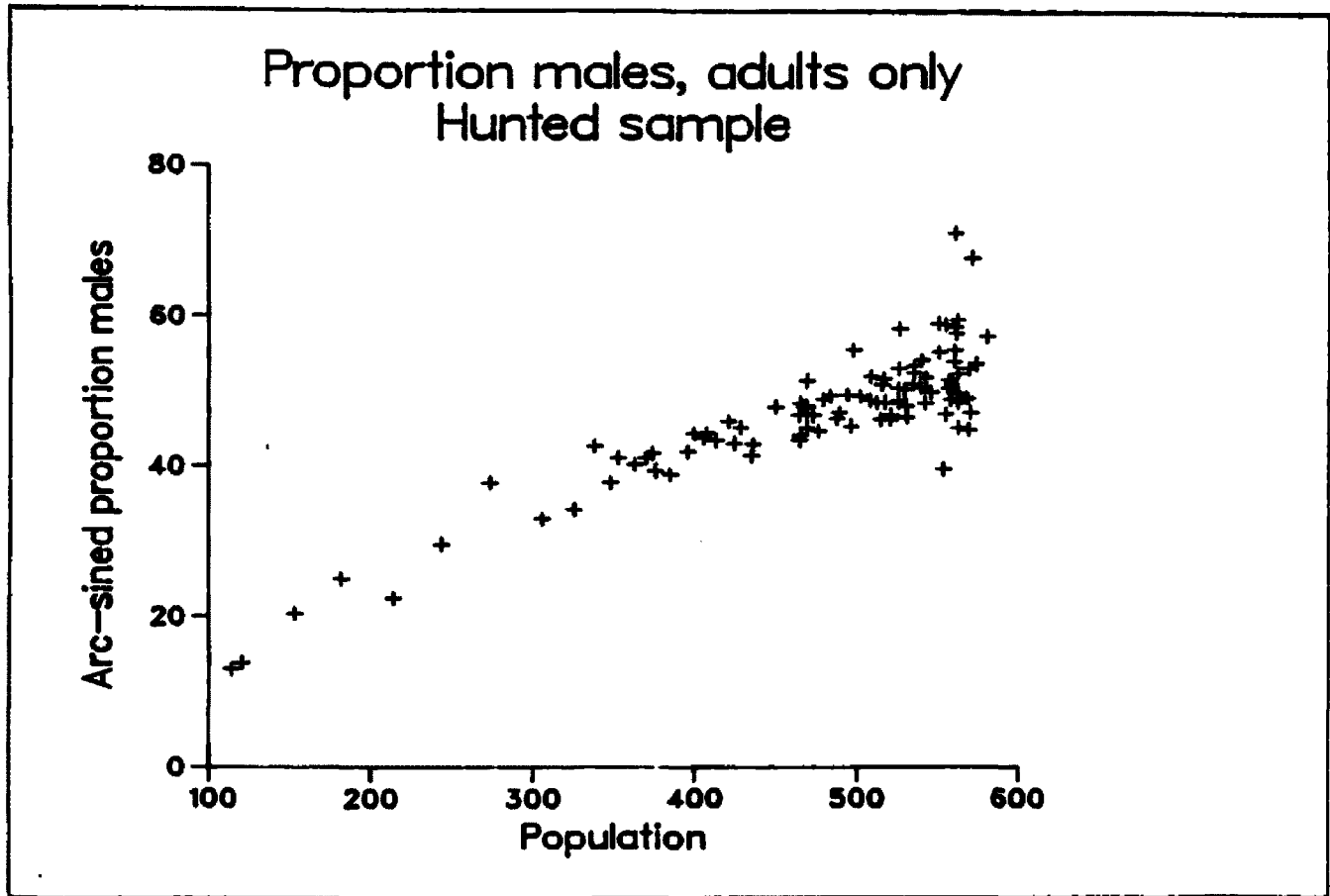


Fig. 40. Proportion males among adults in the harvest sample as a population initially at $K=600$ was overharvested to extinction.

Females far outnumbered males, and few old individuals of either sex survived (Fig. 41). Thus, age-structures characteristic of previously harvested populations formed the baseline from which differences between further declines and returns toward stable equilibria were measured.

At 0.7K, populations harvested at 24 animals/year returned slowly to stable equilibria while those harvested at 39 animals/year continued to decline toward extinction (Fig. 42).

Age distributions were never stable; rather they were complex mixtures of those that would theoretically result from survival schedules applying during that year as well as previous years. Thus, age-structures (S_x) lagged behind survival schedules (L_x).

Age-structures of Hunted Samples. Harvest age-structures similarly lagged behind the survival schedule of their parent populations. Age-structures from populations in which the hunt had been reduced to a stable level at 0.7K continued to appear overharvested for about 8 years (Fig. 43). By year 8, these age-structures had begun to achieve the stationary configuration characteristic of stable hunts. Between year 0 and year 8, age-structures reflected a mixture of past overharvest and present stability. Those populations subjected to continued overharvest from 0.7K also had harvest age-structures that resulted from mortality schedules that applied a few years before-hand. However, they did not achieve stationary configurations; rather they continued to shift as the overharvest exerted increasing pressure on the survivors (Fig. 44).

Age-structure "inertia" was also reflected in the response to

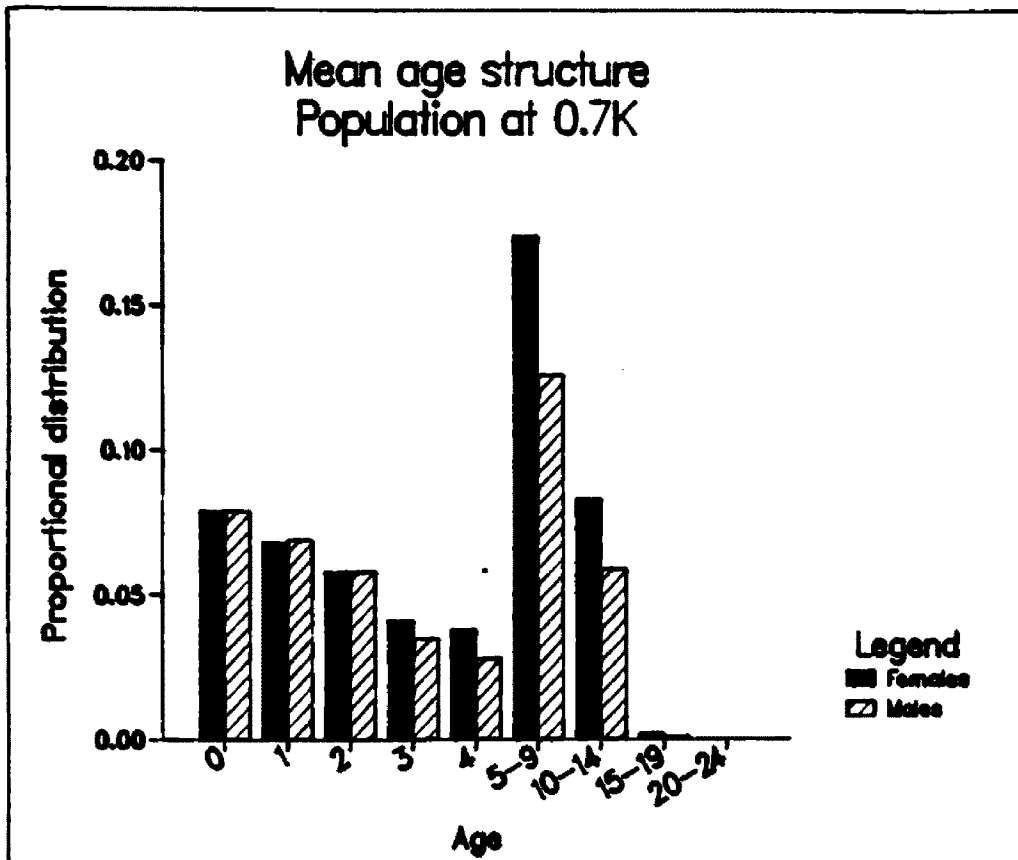


Fig. 41. Mean age-structure of a population when it arrives at 0.7K after being overharvested from K. Illustrated is an age-structure from a population with K=600.

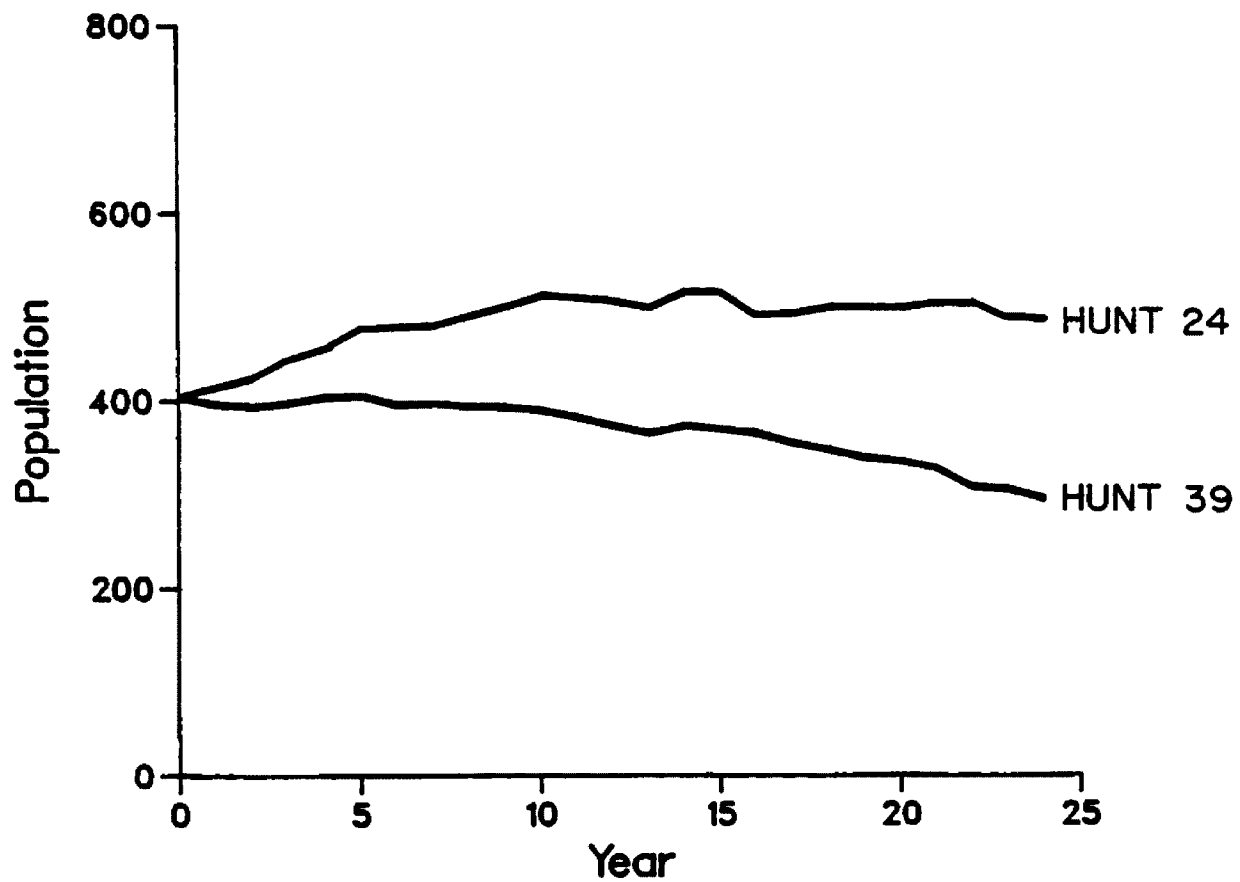


Fig. 42. Mean trajectories of populations initially at 0.7K from 2 different sets of simulations. Populations harvested at 24/year gradually achieved stable equilibria; those harvested at 39/year continued to decline from 0.7K. Each line represents the mean of 5 simulation runs.

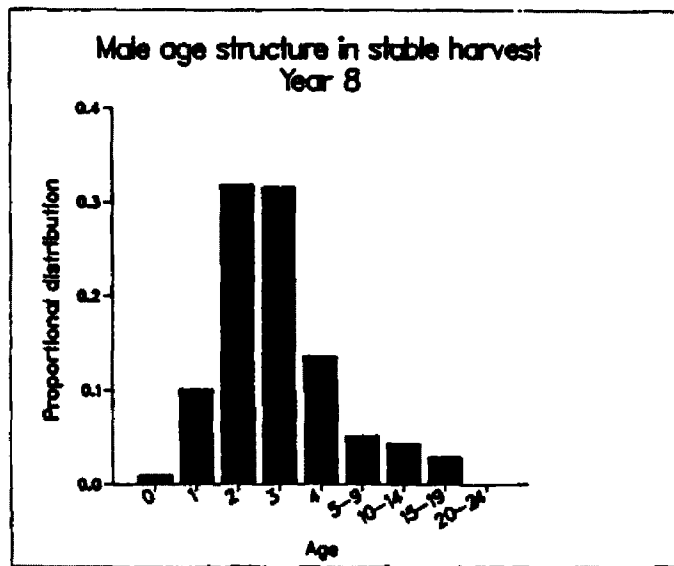
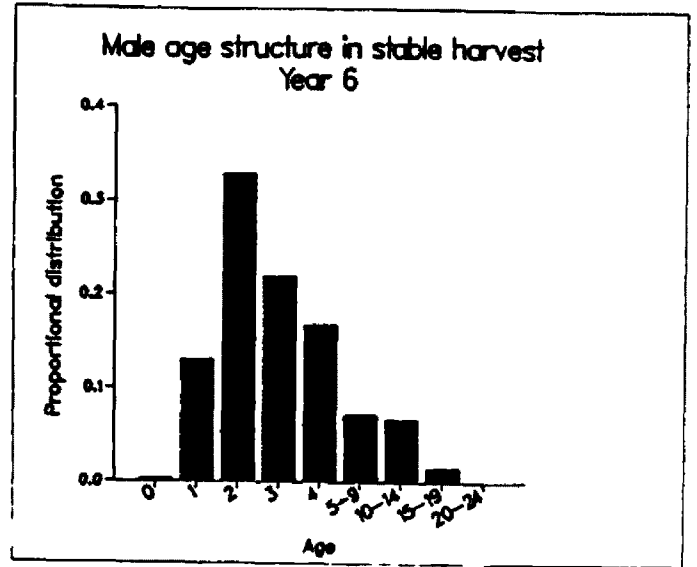
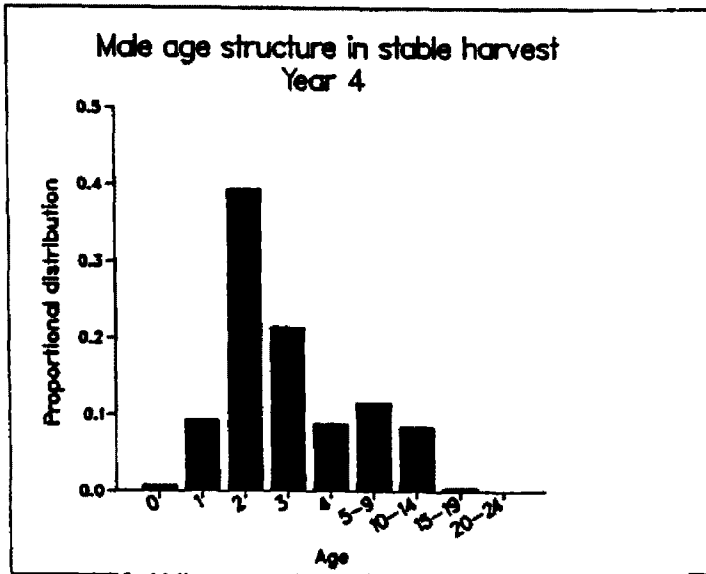


Fig. 43. Mean male harvest age-structures from populations at 0.7K subjected to stable harvesting. Illustrated are the means from years 4,6 and 8 of the 10 year runs.

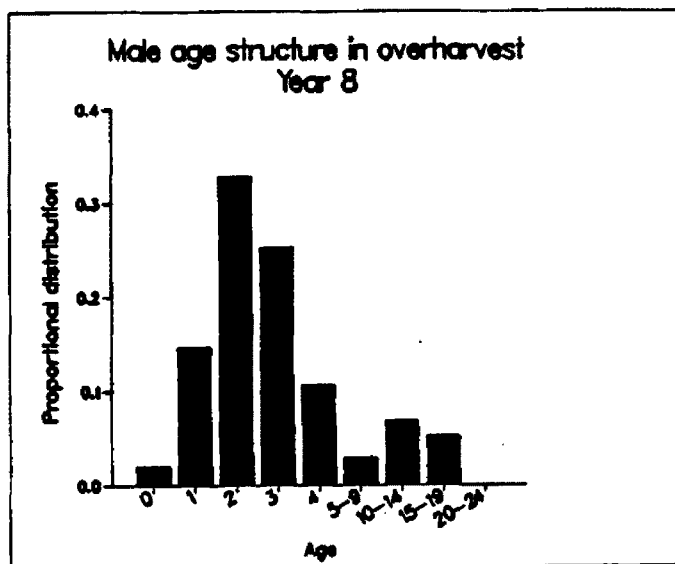
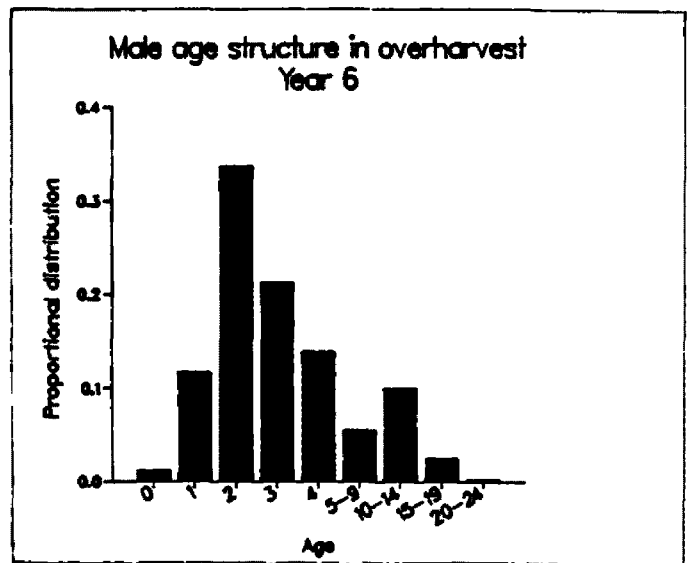
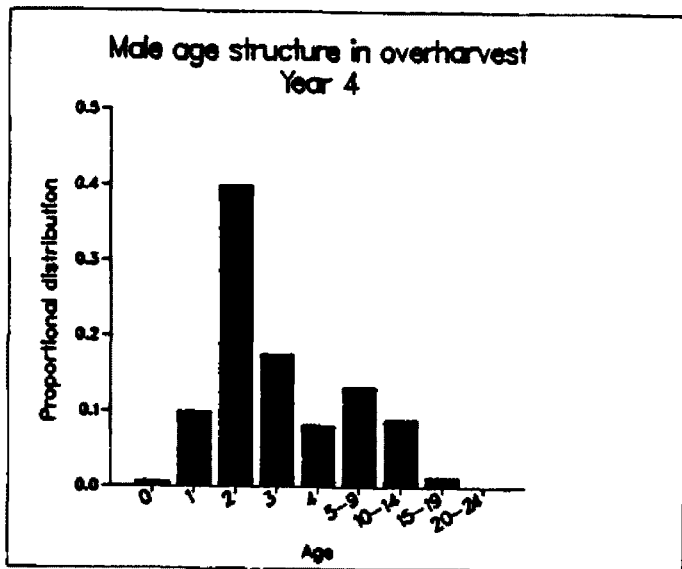


Fig. 44. Mean male harvest age-structures from populations at 0.7K subjected to an overharvest. Illustrated are the means from years 4,6 and 8 of the 10 year runs. 123

overharvest of the 10 descriptive statistics. For $K=600$ populations, the harvest rate used to bring populations down from K was 51 animals/year. Thus, while the stable hunt of 24/year at $0.7K$ was clearly an abrupt change, the newly applied overharvest rate of 39/year also caused a substantial reduction in average mortality. At year 0, harvest age-structures from both regimes responded similarly to the cessation of the 51/year overharvest (Fig. 45, Fig. 46). Only later did age-structures reflect the fundamentally different trajectories of their populations.

Additionally, because age-structures at $0.7K$ were already similar to those characteristic of overharvested populations, descriptive statistics from populations continuing to decline had little range of variation left open to them. For example, most of the old males had been removed prior to reaching $0.7K$, so male age statistics were no longer able to reflect the depletion of old males with overharvest, as they had done from unharvested equilibrium (Fig. 47).

The combined effects of time-lag and the limited range of response left open to indicators of decline at $0.7K$ blurred the already minor distinctions between declining and stable populations. Even the most powerful indicator of overharvest, the proportion male adults, was largely insensitive to the difference between stability and decline (Fig. 48).

At $0.4K$, indices of decline were more sensitive. However, populations that continued to decline from $0.4K$ usually went extinct within 10 years. Even so, the first few years were characterized by ambiguity. Only in the final years of these declines to extinction did

age-structures unambiguously reflect their population's status (Fig. 49).

Harvested Populations Growing in Response to Increased K.

When populations were allowed to grow despite a small harvest by abruptly increasing their carrying capacity, age-structures displayed little change. In general, the addition of harvest mortality to the equilibrium population was offset by the decrease in mortality associated with greater resources per capita. Average age among males and proportion males declined slightly as populations increased despite harvesting (Table 16).

However, even these weak patterns were not detectable in the harvest age-structures (Table 17). As populations increased from about 600 to over 900, neither of the most sensitive indicators of decline displayed any clear trends. Both mean male age and the proportion males among adults remained at levels characteristic of stable populations (Fig. 50, Fig. 51).

Differences among the 4 Specific Models

Age-structures from all 4 Specific Models followed the same general patterns of change in response to overharvest. Although differences among them were statistically significant, they would likely not be detectable in field data. Rather, the changes in age-structures caused by differing harvest intensities tended to overwhelm differences

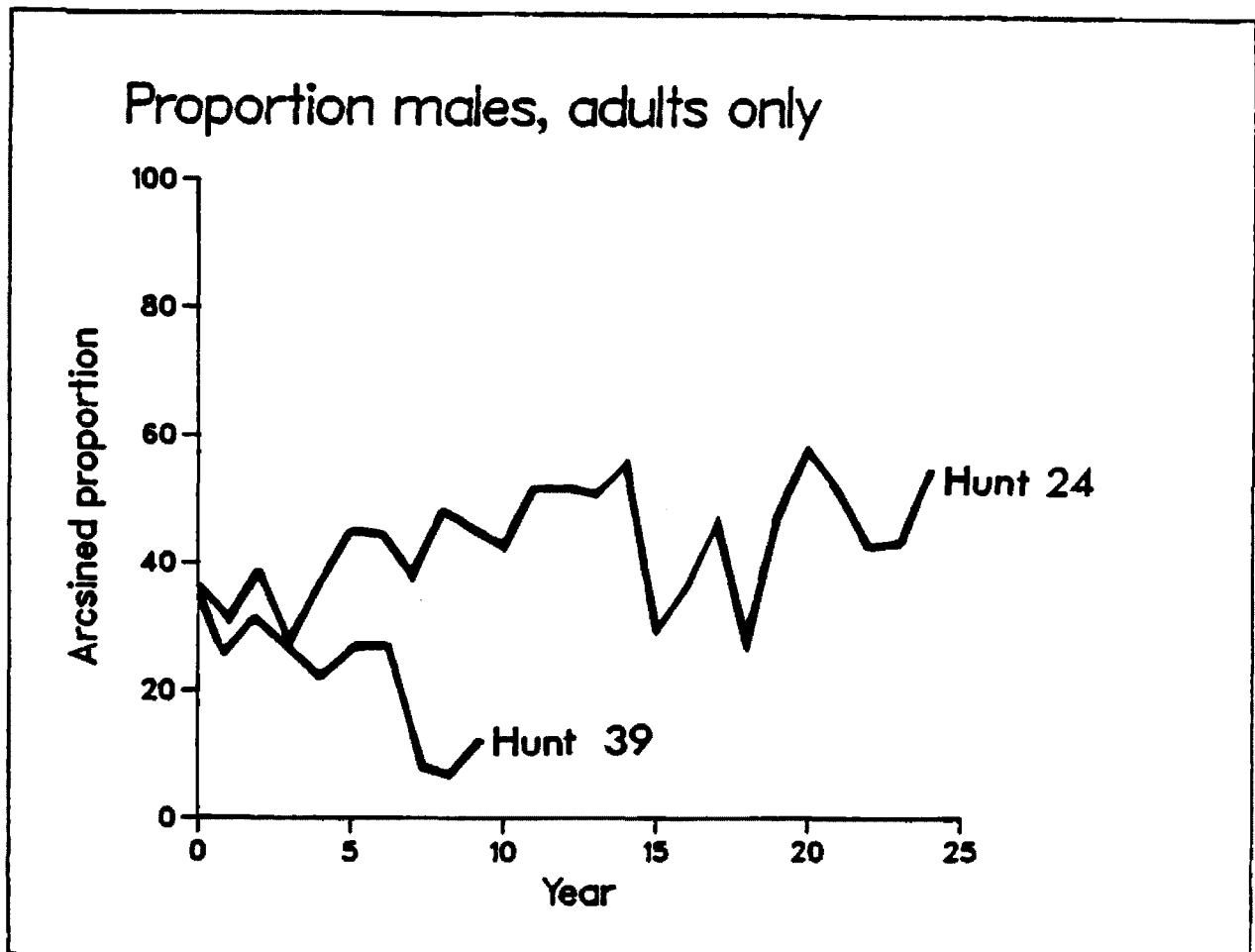


Fig. 49. The proportion male among adults in the harvest as populations at $0.4K$ decline to extinction or return to stable equilibria. Each line represents the mean of 5 independent simulations. Declining populations were harvested at 39/year, stable populations were harvested at 24/year. The line for the declining population stops at year 9 because populations began going extinct at that time.

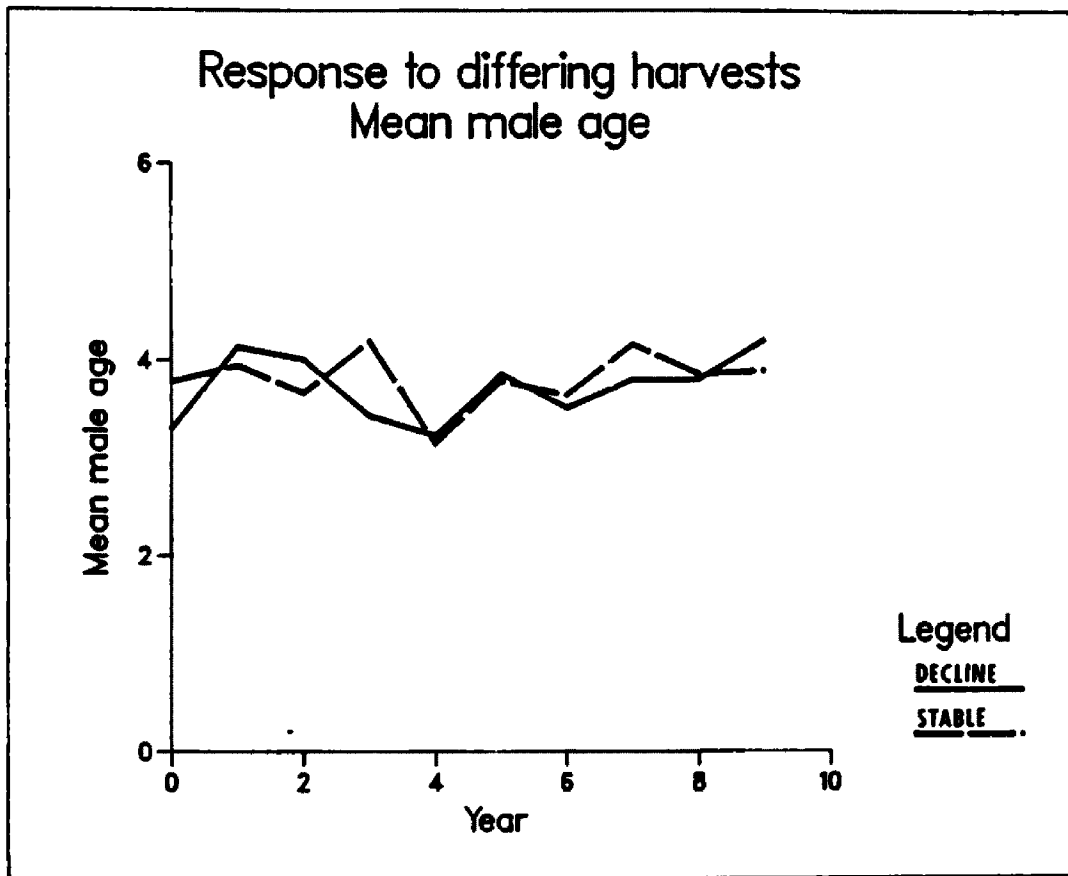


Fig. 45. Mean male age in the harvest as populations at 0.7K decline or return to stable equilibria. Each line represents the mean of 5 independent simulations. Declining populations were harvested at 39/year, stable populations were harvested at 24/year; corresponding population trajectories are illustrated in Fig. 42.

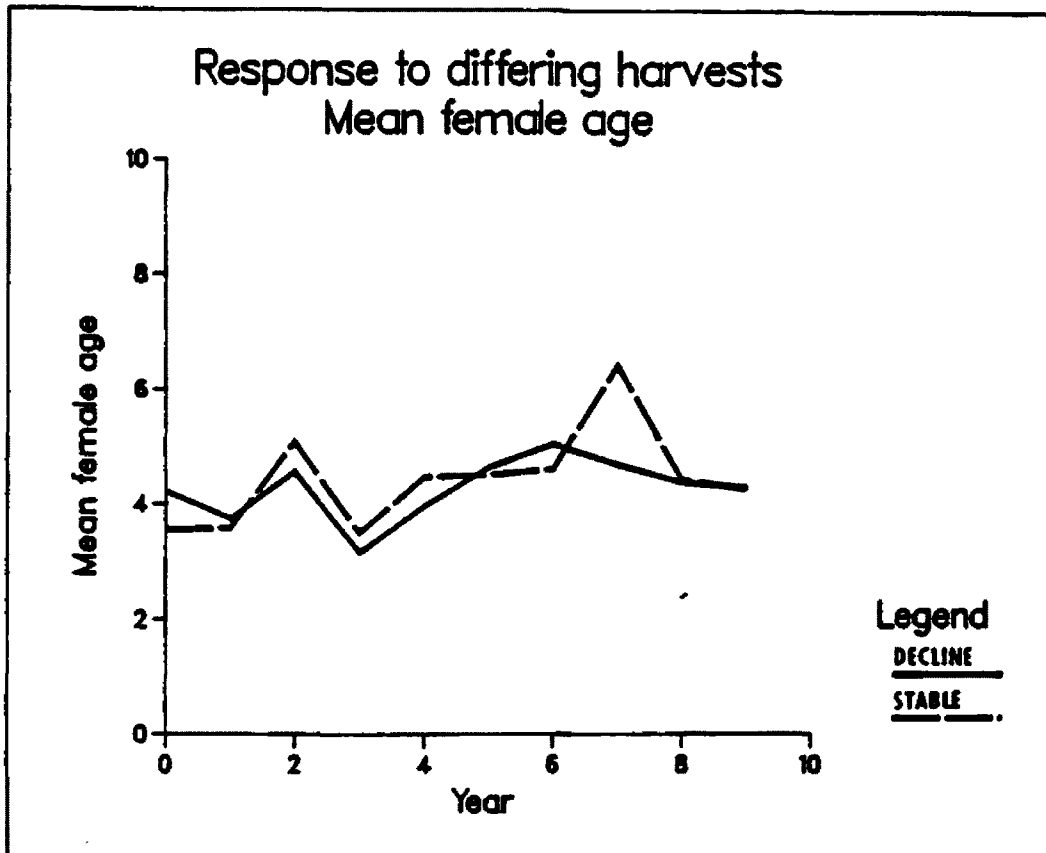


Fig. 46. Mean female age in the harvest as populations at 0.7K decline or return to stable equilibria. Each line represents the mean of 5 independent simulations. Declining populations were harvested at 39/year, stable populations were harvested at 24/year; corresponding population trajectories are illustrated in Fig. 42.

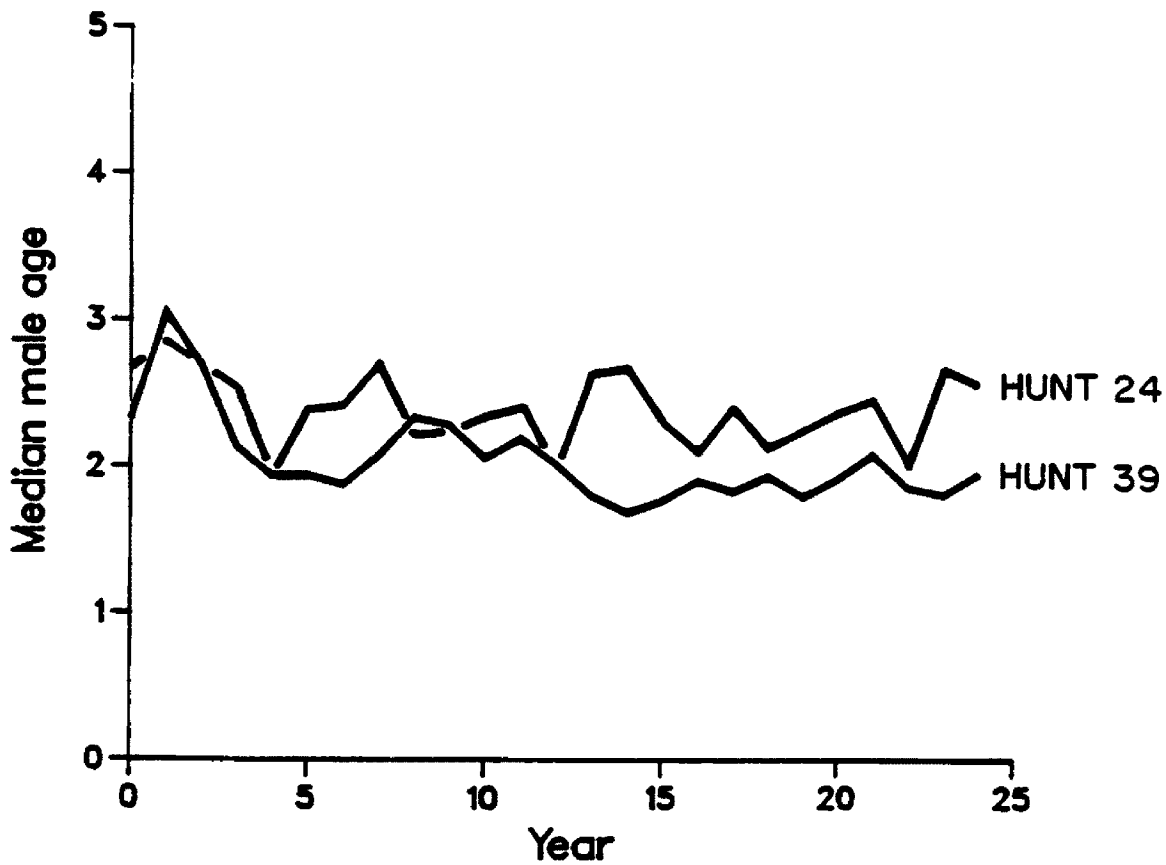


Fig. 47. Median male age in the harvest as populations at 0.7K decline or return to stable equilibria. Each line represents the mean of 5 independent simulations. Declining populations were harvested at 39/year, stable populations were harvested at 24/year; corresponding population trajectories are illustrated in Fig. 42.

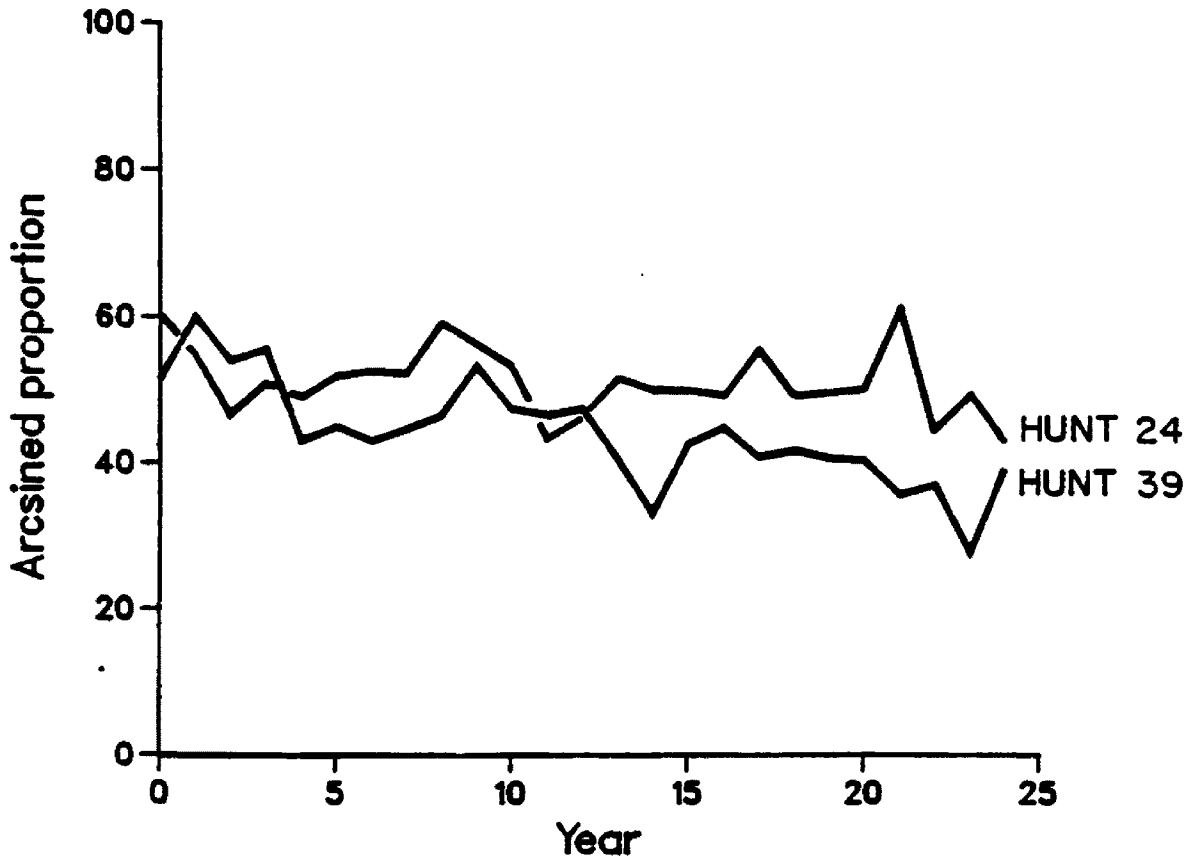


Fig. 48. Proportion male among adults in the harvest as populations at $0.7K$ decline or return to stable equilibria. Each line represents the mean of 5 independent simulations. Declining populations were harvested at 39/year, stable populations were harvested at 24/year; corresponding population trajectories are illustrated in Fig. 42.

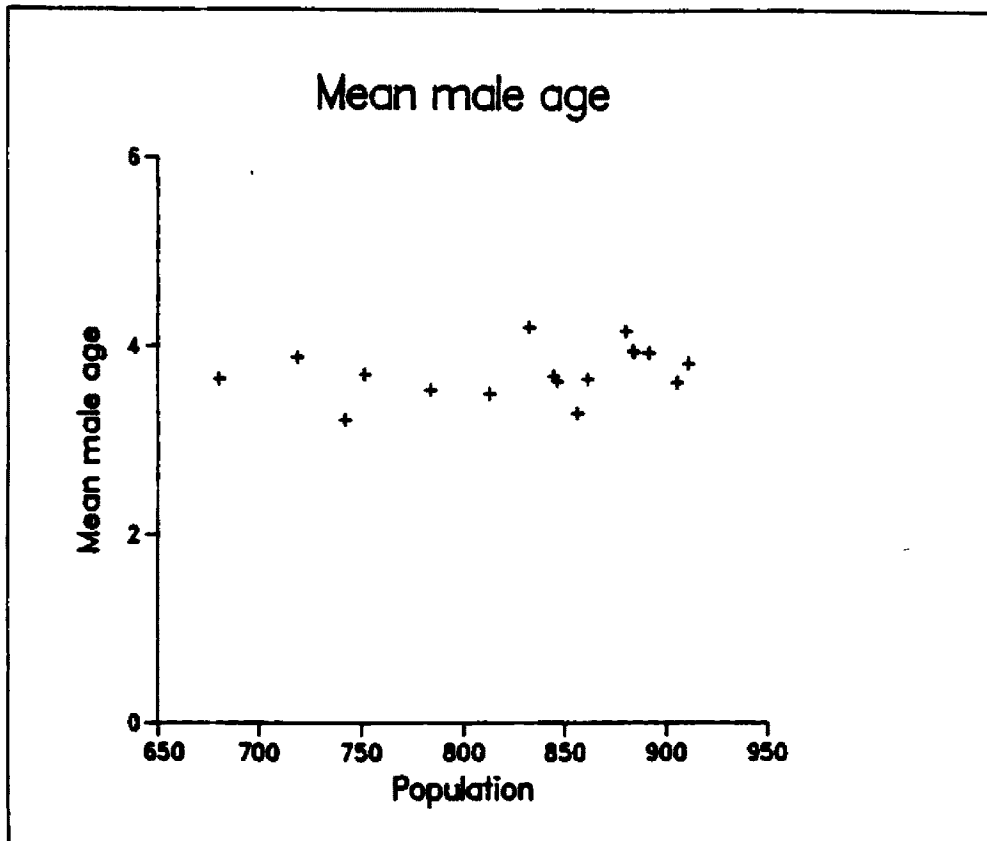


Fig. 50. Mean male age in the harvest sample from populations allowed to increase despite harvesting by increasing their carrying capacity. From an initial K of 600, K was changed to 1000. Each point represents the mean of 10 replicate simulations.

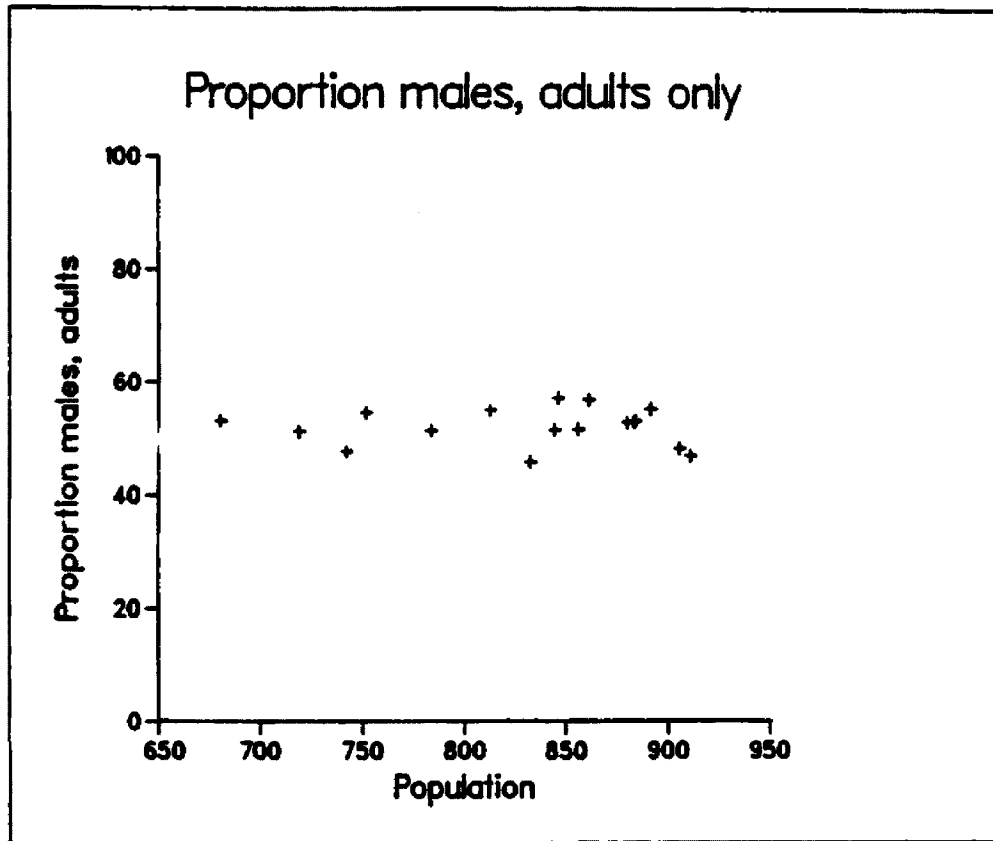


Fig. 51. Proportion males among adults in the harvest sample from populations allowed to increase despite harvesting by increasing their carrying capacity. From an initial K of 600, K was changed to 1000. Each point represents the mean of 10 replicate simulations.

among the Models.

Subtle differences that were exhibited in mean age-distributions of males (Fig. 52) corresponded to the differences in resilience to harvest, discussed earlier. Model DM responded most poorly to harvest, and had male age-distributions characteristic of the heaviest harvest. Two-year olds, although the modal age-class, were relatively less abundant than in similar harvests from the other 3 models. Cubs and adults aged 10-14 were relatively more numerous in Model DM harvests, because the most vulnerable sub-adult age-classes had been more severely depleted. In contrast, Model ADM, the most resilient to harvest, was characterized by a preponderance of sub-adults among males, and had relatively fewer animals from the less vulnerable age-classes. As with sustained yields, Model DDALL and DMADM were intermediate. Male age-structures from Model DDALL were slightly younger than from DMADM, probably because of the greater number of recruits at low densities produced by density-dependent natality rates.

Proportion males among the 4 models differed, but in all cases was lower with heavy harvests than with light harvests ($p < 0.001$, Table 18). As with male age-distributions, proportion males responded positively to the compensation afforded by density-dependent natality ($p < 0.005$, Table 18). Under intense harvest, proportion males was relatively higher in the 2 Models with density-dependent natality (DDALL and ADM). However, the inclusion of a direct link between adult male abundance and sub-adult male survival significantly reduced the proportion males at lower harvest levels ($p < 0.005$, Table 18). Lower harvests allowed restoration of the adult male component as populations

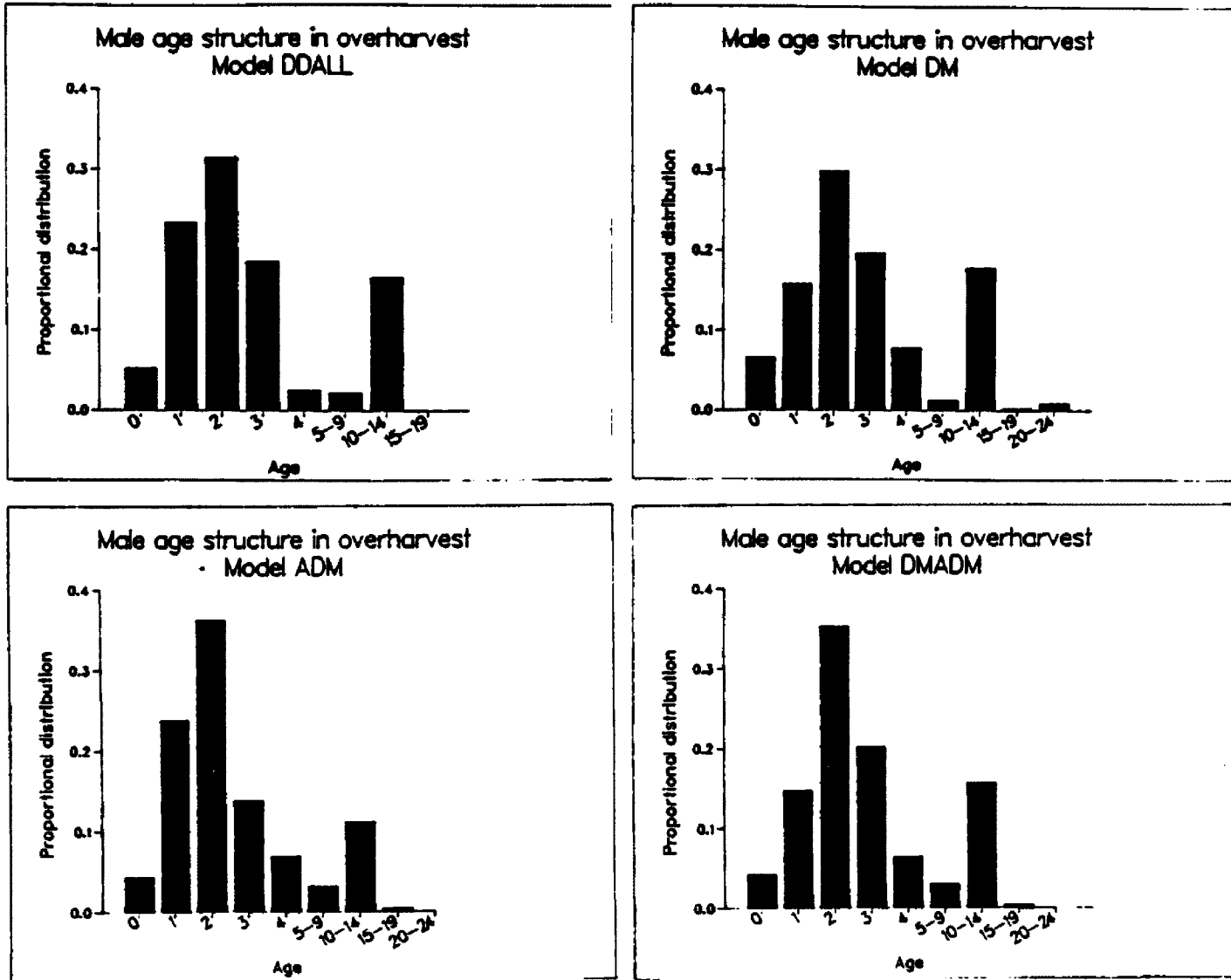


Fig. 52. Mean male age-distributions, showing the subtle differences between the 4 Specific Models. All distributions are harvest samples from overharvests beginning from 0.4K.

Table 18. Mean proportion males (values arcsined) in harvest age-structures for each of the 4 Specific Models. Each mean is from 10 replicate simulations at 0.7K, population with theoretical K=600. The low harvests were 24 and 27, the 2 lowest harvests at 0.7K for K=600. The high harvests were 48 and 51, the 2 highest harvests at 0.7K for K=600.

a. Mean proportion males (arcsined).

	Specific Model			
	DDALL	DM	ADM	DMADM
Low Harvest	56.65	56.14	54.36	54.65
High Harvest	51.50	50.13	51.39	49.59

b. ANOVA table

Source	df	MS	F	P
Harvest level	1	459.73	183.5	<0.001
Specific Models	3	13.00	5.2	<0.005
Density-dependent vs. -independent natality	1	14.37	5.7	<0.025
Adult male mortality function	1	24.45	9.8	<0.005
Interaction	3	8.36	3.3	<0.025
Error	72	2.50		
Total	79			

recovered toward equilibria. Among the 2 models with the direct link (ADM and DMADM), the renewed presence of adult males apparently depressed survival of sub-adult males, reducing their availability to the harvest. Harvest age-structures from these 2 models thus included relatively more females as populations recovered, accounting for the significant interaction between the 2 components of population regulation (Table 18).

Discrimination of Declining and Stable Populations

In the previous section, I characterized differences in age-structures of declining and stable grizzly bear populations. Here, I quantify those differences by (1) developing an index for discrimination between declining and stable populations, and (2) quantifying the sensitivity of the index. Because this is a management question, only the harvest data (i.e. data that are available to a manager) are used.

Discriminant Function Analysis.

I used discriminant function analysis (DFA) to separate age-structures from declining and stable populations. In generating discriminant functions, I used the least variable data: populations with $K=600$, in which all samples consisted of sums of frequencies from 3 consecutive years ("year-groups"). To increase sample size, data from all 4 Specific Models and from both cross-sections were pooled. Later, in testing the behavior of the discriminant functions, all data were subdivided into their original components. Discriminant functions were generated from data for each of the 3 year-groups. Of the 3, the equation generated from year-group 1 (years 2-4) was clearly the most powerful discriminator, and is the only equation discussed further. The equations from year-groups 2 (years 5-7) and 3 (years 8-10) are presented in Appendix 3, along with estimates of their sensitivity.

The 10 age-structure statistics described in Table 2 were

considered as discriminating variables. The discriminant function used 7 of the 10, listed in decreasing order of the magnitude of their standardized discriminant function coefficients (Table 19). These coefficients give the relative contribution of each variable to the discrimination.

The discriminant function was significant (Wilks' $\lambda = 0.724$, $\chi^2 = 242.56$, $df=7$, $p<0.0001$) but fairly weak. The canonical correlation was only 0.526, or about 27.6% of the total variation explained by the 2 groups. Lower scores were given to declining populations, higher scores to stable populations. Both groups appeared approximately normally distributed along the canonical axis, but their variance-covariance matrices were significantly different (Box's $M=187.4$, $df=281,533,004.5$, $p<0.0001$). The equation correctly predicted 222 of 309 year-group 1 samples from stable populations (71.8%), and 316 of 447 year-group 1 samples from declining populations (70.7%).

Interpretation of the Discriminant Function.

Variables reflecting the sex ratio in the harvest contributed more to discrimination than did variables that reflected proportions of young animals or average ages. Of the 7 standardized coefficients, proportions males among adults (MFAD) had the largest magnitude, proportion males among all ages (MFALL) had the 3rd largest. The next most important discriminating variables were the proportions of the harvest consisting of sub-adults. Sub-adults among males (MSUBAD) was 2nd in magnitude and the corresponding proportion for females (FSUBAD)

Table 19. Coefficients for the discriminant function discussed in the text. See Table 2 for formulae and definitions of each variable.

Variable	Standardized Coefficient	Unstandardized Coefficient
MFAD	4.70778	0.6916965
MSUBAD	3.02743	0.4895483
MFALL	-2.07158	-0.5412071
FSUBAD	-1.76279	-0.3430558
MMED	1.10874	2.6227130
MXBAR	-0.81701	-1.5784110
M58JUV	-0.65659	-0.0668214
Constant		-13.53516

was 4th. The 2 statistics of age among males, the median (MMED) and the mean (MXBAR), although included in the discriminant function, were relatively unimportant discriminators because the other variables took the role of indicating relative male age. The proportion of male prime-aged adults among prime-aged plus cubs (M58JUV) contributed little to the discriminant function.

The standardized coefficients (Table 19) are best interpreted in pairs: MFAD and MFALL, MMED and MXBAR, and MSUBAD and FSUBAD. In so doing, it is clear that the discriminant function identified what appear to be contradictions: the 2 members of each pair differed in algebraic sign. That 2 statistics measuring similar things contributed in opposing directions to the discriminant score is counter-intuitive. Note, however, that the positive coefficient was always larger in absolute magnitude than the negative coefficient. Thus, the variable with the positive coefficient tended to dominate when values for both variables were similar. Over some range of raw values, the 2 variables could contribute in opposite ways to the discriminant index; thus the interplay between the 2 also played a part in the final index.

Discriminant function scores increased with higher MFAD values. That is, higher proportion males among adults led to score values indicating stability, while lower proportion males among adults led to scores indicating decline. In seeming contradiction, the coefficient of MFALL was negative, indicating that lower proportions of males among all age-classes reflected stable populations. Most often, MFAD was not independent of MFALL, because adults were a sub-set of all animals. However, MFAD and MFALL could be independent to the degree that adults

were a small proportion of the total harvest. When most kills were of adults, MFAD and MFALL had to be similar, and the larger coefficient of MFAD dominated. But when the hunt contained few adults, MFAD and MFALL could differ from each other. In this situation, MFALL reflected primarily the sex ratio among **sub-adults** and **cubs** in the harvest. Age-structures with low MFAD and high MFALL values (indicating decline) contained mostly young males, along with a few old females, often cited as an indicator of over-harvest in ungulate populations (Fraser 1976, Reimers 1975). Age-structures with high MFAD and low MFALL (indicating stability) also had many more sub-adults than adults (to permit independence of the 2 variables), but a relatively larger proportion of the few adults present were males. The presence of old males in a harvest is often cited as evidence of a sustainable hunt (Troyer 1961). Thus the 2 sex-ratio variables, by virtue of their opposing coefficient signs, also contained information about the adult to sub-adult ratio among both sexes.

The relationship between MMED and MXBAR was analogous to that of MFAD and MFALL. The median male age was high in stable populations and low in declining populations. The mean male age, while a weaker discriminator, appeared to do just the opposite. In general, one expects means and medians to be highly correlated, but, in a distribution that is skewed to the right, they become less so as the distribution's variance increases. All grizzly bear harvest age-distributions examined in this thesis were skewed to the right. These highly skewed, highly variable distributions of males resulted in low medians relative to means, and low (declining) discriminant function scores. Declining

distributions reflected the predominance of both very young and older adult males in the harvest as the most vulnerable sub-adults were depleted. Conversely, male age-distributions from stable populations had medians close to their means, indicative of distributions with less variance and more nearly symmetrical shape. These stable distributions reflected the preponderance of the highly vulnerable sub-adult age classes.

The difference in sign between MSUBAD and FSUBAD was less complex; as noted earlier, male and female age-distributions acted independently. With overharvest, ages of males and of females moved in opposite directions. However, the positive sign of MSUBAD's coefficient requires some explanation. The effect is that declining populations had fewer sub-adults in male hunter-kill age-distributions, and stable populations more sub-adults. This seems to contradict the generally younger male age-distributions expected with overharvest. Consider, however, that as declining populations were depleted of sub-adult males, older males became vulnerable first. Only after the overharvest had proceeded long enough to deplete older males as well did male age-structures shift back towards the very young males, who then became vulnerable despite their legal protection because they were relatively so numerous. The harvest of females intensified only after males had declined; at this point, sub-adult females were harvested because they were more vulnerable than adult-females. Only with overharvest did females contribute substantially to the total harvest, and the greater vulnerability of sub-adults led to higher FSUBAD values, thus lower scores.

Noteworthy also in the discriminant function was the absence of either of the direct measures of average female age. Variables FMED and FXBAR, as well as F58JUV, failed to improve the discrimination, so were omitted. Their absence was consistent with the very weak correlation of female age with population size, seen earlier.

Power of the Discriminant Function

As presented in the Methods section, the power of the discriminant function was defined as its ability to correctly classify stable populations, given a probability α of misclassifying declining populations. Viewed another way, the power summarized in a single number the overall difference between age-structures of declining and stable populations.

The power of the discriminant function to classify stable populations in the absence of any other information was generally poor. The greatest power occurred for populations with $K=600$, where all data consisted of 3-year summed age-class frequencies (year-groups). Estimated power ranged from 37% from Model ADM to 58% for Model DMADM (Table 20). Power was considerably reduced if the same data were viewed as separate data sets from individual years (Table 21). Viewed this way, the most powerful discrimination was again with data from Model DMADM, (22%), the least from Model DDALL (13%).

Discrimination between decline and stability in smaller ($K=200$) populations was even less powerful. As with the larger populations, combining age frequencies into year-groups improved the power of the

Table 20. Power of the discriminant function for harvest samples from populations with K=600. Each sample consisted of a year-group made up of the summed age-class frequencies from 3 consecutive years. The expected Type I error was 0.10.

Specific Model	n	Critical Value	α	Power (%)
DDALL	560	1.08415	0.091	49.2
DM	522	0.95540	0.072	49.1
ADM	550	1.16946	0.080	37.3
DMADM	554	0.67942	0.101	58.3

Table 21. Power of the discriminant function for harvest samples from populations with K=600. Each sample consisted of a single year. The expected Type I error was 0.10.

Specific Model	n	Critical Value	α	Power (%)
DDALL	1835	3.83334	0.061	13.3
DM	1706	3.36093	0.066	16.2
ADM	1809	3.43374	0.064	16.0
DMADM	1817	2.94841	0.062	22.2

test. Populations with $K=200$ were discriminated with roughly the same power as those from $K=600$ populations in which individual years were treated as samples (Table 22). Small populations in which data had not been grouped by 3 consecutive years were the most difficult to correctly classify (Table 23). Note that in this case, even these low estimates of power are too high, because the Type I errors were consistently higher than the predicted α of 0.10.

The amount of separation between age-structures of declining and stable populations was generally similar among the 4 Specific Models. Discrimination tended to be most powerful with data sets from Model DMADM and least powerful with data sets from Model DDALL.

Age-structures from declining and stable populations were more distinct - and the discriminant function more powerfully detected the distinctions - if the populations being compared differed more from each other in harvest intensity and in the time they had been subjected to the differing harvest intensity. Sub-dividing the data sets by year-group, cross-section, and harvest pressure reflected improvements in discrimination accuracy.

Earlier, populations generated by Model DMADM were seen to be classified with a maximum of about 58% power. However, discrimination of Model DMADM populations was more powerful when data were sub-divided into single year-groups. Additionally, power increased with each year-group, because declining populations continued to decline while stable populations recovered toward equilibria (Table 24).

Harvest age-structures from declining and stable populations diverging from the lower ($0.4K$) cross-section were more distinct from

Table 22. Power of the discriminant function for harvest samples from populations with K=200. Each sample consisted of a year-group made up of the summed age-class frequencies from 3 consecutive years. The expected Type I error was 0.10.

Specific Model	n	Critical Value	α	Power (%)
DDALL	491	3.47562	0.060	15.4
DM	531	3.18747	0.094	22.8
ADM	534	2.71273	0.094	22.9
DMADM	534	2.93677	0.074	25.8

Table 23. Power of the discriminant function for harvest samples from populations with K=200. Each sample consisted of a single year. The expected Type I error was 0.10.

Specific Model	n	Critical Value	α	Power (%)
DDALL	1611	12.14496	0.111	17.4
DM	1747	11.35322	0.139	20.0
ADM	1763	11.44567	0.137	19.4
DMADM	1746	10.80458	0.128	23.0

Table 24. Power of the discriminant function as applied 1 year-group at a time. Data are from Model DMADM, theoretical K=600. The expected Type I error is 0.10.

Year-group	Years	n	α	Power (%)
1	2-4	193	0.116	58.3
2	5-7	193	0.107	62.5
3	8-10	1681)	0.083	63.9

1) Sample sizes in final year-groups are smaller because some declining populations have already gone extinct and are not included.

each other than were those at the upper (0.7K) cross-section (Table 25). The difference resulted from the more rapid divergence of the 2 trajectories at the lower cross-section. At 0.4K, declining populations were depleted quickly but stable populations grew for many years until they reached stable equilibria. At 0.7K, declining populations decreased slowly, while stable populations grew little because of their proximity to their eventual stable equilibria.

At both cross-sections, declining and stable harvest age-structures differed more from each other if only the extremes of harvest intensities were compared than if all harvests were included (Table 25). Discrimination was weak when examining only those populations whose harvest levels were in the probability band of the SYC. Discrimination power was greatest (about 86%) when comparing only populations at 0.4K that were subjected to either very high or very low harvest levels. The weakest discrimination (about 31%) was among 0.7K populations whose harvest levels were in the probability band of the SYC.

In addition to differentiating declining and stable systems initially at the same cross-section, the discriminant function also differentiated declining from stable populations that were subjected to the identical harvest level but from different cross-sections (Fig. 53). Power was generally greater when contrasting populations across cross-sections than across harvest levels (Table 26). The clearest discrimination found in any test (96%, with $\alpha = 0.10$) was between cross-section 0.4K and 0.7K populations in which all populations were subjected to a harvest level of 33 or 36 animals/year, $\alpha = 0.10$.

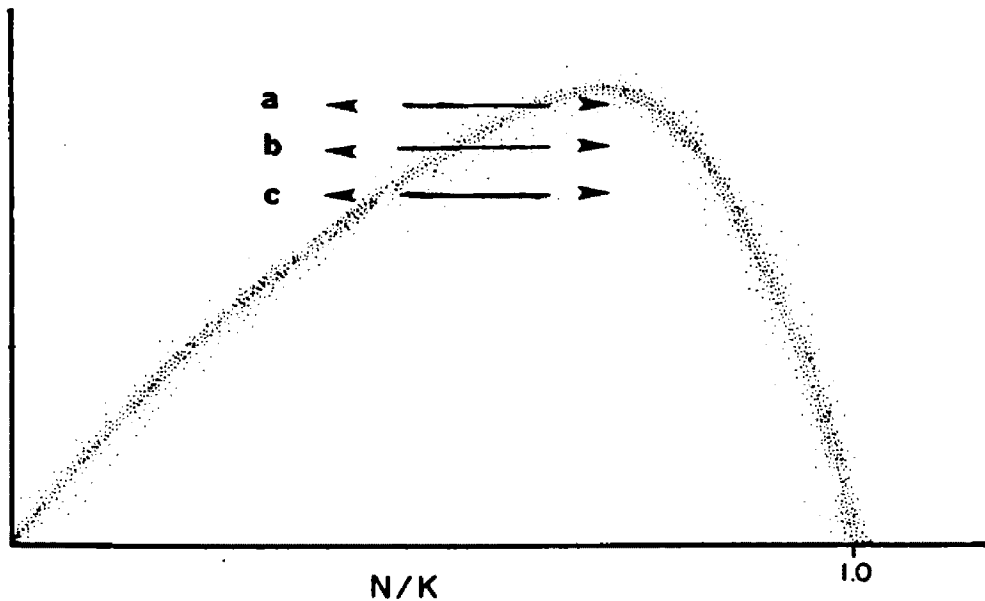


Fig. 53. A schematic diagram of a sustained yield curve, showing the comparisons made between age-structures of populations at different cross-sections subjected to the same harvest level. a. Populations above probability band at 0.4K but within it at 0.7K. b. Populations above probability band at 0.4K and below it at 0.7K. c. Populations within probability band at 0.4k and below it at 0.7K. Comparisons at point 'b' were the most sensitive.

Table 25. Power of the discriminant function, comparing 0.4K and 0.7K, and harvest intensities. Data are from Model DMADM, theoretical K=600. The expected Type I error is 0.10.

Cross-Section	Harvest level	n	α	Power (%)
0.4K	All	254	0.103	73.3
	$\leq 18, \geq 30$	182	0.084	86.3
	$> 18, < 30$	72	0.286	55.6
0.7K	All	300	0.111	50.6
	$\leq 33, \geq 45$	210	0.108	64.1
	$> 33, < 45$	90	0.118	30.8

Table 26. Power of the discriminant function to differentiate harvest samples from populations with identical harvests at cross-sections 0.4K and 0.7K. Data are from Model DMADM, theoretical K=600, and the expected Type I error is 0.10. Codes refer to Fig. 53.

Harvests	n		Code	Power
27-30	120	0.100	a	66.7
33-36	113	0.101	b	96.2
39-42	102	0.071	c	44.4

above the probability band at 0.4K and below it at 0.7K. Power was reduced when the harvested level occurred within the probability band at either cross-section.

Discrimination Using Single Variables

None of the 7 variables discriminated as powerfully when applied separately as did all 7 when considered together in the discriminant function. Using the same Model DMADM data that resulted in an estimated discrimination power of 58% when using the discriminant function, the maximum power obtained using a single statistic was about 42% with MFALL (Table 27). The other 6 statistics varied in their power from 39% to none at all.

The relative abilities of the 7 variables to separately differentiate decline from stability (i.e. their rank order of effectiveness) was not the same as their relative contributions to the discriminant functions as indicated by their standardized coefficients. The discrepancy results from the multivariate nature of the discriminant function. Because similar information about an age-structure is contained in more than 1 variable, the importance to the discriminant function of any 1 is only what new information it contributes in the presence of all the others. With each variable discriminating independently, the order of variables in Table 27 is a better reflection of their relative usefulness for discriminating Model DMADM populations.

Using the Discriminant Function as an Index to Decline

Table 27. Power of individual discriminating variables. Data are from Model DMADM, theoretical K=600; expected Type I error is 0.10.

Variable	Critical Value		α	Power (%)
	Transformed	Untransformed		
MFALL	47.60	0.545	0.068	41.7
MFAD	50.00	0.587	0.098	38.9
FSUBAD	47.22	0.538	0.092	15.3
MMED	2.62	2.615	0.092	14.4
M58JUV	16.27	0.079	0.157	10.2
MXBAR	3.58	3.581	0.095	4.2
MSUBAD	59.49	0.742	0.095	0.0

Age-structures from 3 consecutive years of data should be summed to create year-groups. The loss in temporal sensitivity to decline by lumping data is more than compensated by the reduced variability associated with larger sample sizes, and by the better representation of the 3-year cycles characteristic of grizzly bear reproductive biology. The 7 summary statistics are then computed, as shown in Table 2. Each is multiplied by its unstandardized coefficient, and the products are summed and the constant is added. The resulting index is the canonical score for that population.

The critical point to differentiate decline vs. stability depends on the population size, type of population regulation operating (i.e. Specific Model), years of harvest, and other factors described earlier. Knowing all these factors is impossible; if a biologist knew them, an age-structure index to decline would not be necessary. As a rough guide to insure that the probability of misidentifying a population actually in decline is 10% or less, I suggest a critical point of 0.85 for harvest sample sizes in the range 15-51/year (the modeled population with an unharvested equilibrium level of about 600) and 3.0 for harvest sample sizes in the range 5-17/year (modeled population with an unharvested equilibrium level of about 200). Clearly, theoretically optimal critical points vary continuously with sample size, but because simulations were conducted at only 2 equilibrium population sizes, these critical points are the only 2 I can quantify.

The power of this test is low. For the larger sample sizes, the

estimated power at $\alpha = 0.10$ is just over 50% (Table 28). For the smaller samples sizes, power is only about 22% (Table 29).

Confirmation Tests

To further test the procedure, I used it to predict group membership for 3 additional simulated data sets that were not used in developing the discriminant function.

1. Model DM populations with $K=600$, 3 cross-sections, 3 hunt levels. The data were created by the same procedure used to generate SYCs. For simplicity, populations were subjected to only 3 harvest levels: 24, 30 and 39. Unlike the SYC data, age-structure data were collected for 25 years (as opposed to only 10 in the SYC runs), and a 3rd cross-section, 0.95K - well to the right of N_{msy} , was used.

Reliability of discrimination was generally similar to the earlier tests for Model DM (Table 30). Type I errors tended to be higher than expected for populations at 0.95K. Many 0.95K populations that declined were mis-classified as stable while they were still relatively close to 0.95K.

This test, as well as all the preceeding calculations of discriminant function power, considered each year-group as an independent sample. However, some year-groups came from the same simulation run, while others were completely unrelated. An alternative approach was treating complete simulation runs as "samples", while continuing to score each year-group separately. This way, samples received as many scores as year-groups in the simulation. Often, some

Table 28. Best estimate of power of the discriminant function for harvest samples of 24-51 (K=600). Each sample is a year-group of 3 consecutive years. The critical value for each is 0.85.

Specific Model	α	Power (%)
DDALL	0.133	57.1
DM	0.085	50.9
ADM	0.108	49.0
DMADM	0.071	50.9
Unweighted mean	0.099	52.0

Table 29. Best estimate of power of the discriminant function for harvest samples of 5-17 (K=200). Each sample is a year-group of 3 consecutive years. The critical value for each is 2.00.

Specific Model	α	Power (%)
DDALL	0.071	24.7
DM	0.089	20.3
ADM	0.094	25.6
DMADM	0.083	19.0
Unweighted mean	0.084	22.4

Table 30. Power of the discriminant function for harvest samples from independently generated Model DM populations, K=600, using the critical point 0.85.

Cross-Section	n	α	Power (%)
0.4K and 0.7K	211	0.198	63.6
0.95K	99	0.410	70.0
All	300	0.257	65.6

Table 31. Power of the discriminant function where discrimination was made for a complete simulation run; declines are considered only those runs in which 2 consecutive year-groups were below the critical point. Data are from independently generated Model DM populations, theoretical K=600, using the critical point 0.85.

Cross-Section	n	α	Power (%)
0.4K and 0.7K	32	0.053	53.8
0.95K	12	0.000	85.7
All	44	0.042	65.0

scores indicated decline while others indicated stability. I classified the entire sample (i.e. an entire simulation run) as declining only if 2 consecutive year-groups received discriminant index score below the critical point. For this Model DM data, each sample consisted of up to 8 year-groups of 3 years each (year 1 was always ignored to produce $24/3 = 8$ groups, however some runs ended before year 25 because of population extinction). Viewed this way, entire populations were classified as declining if 2 consecutive year-groups' discriminant index' (out of the 8 possible) fell below the critical point, 0.85. This treatment sacrificed sample size (as well as temporal sensitivity) but retained power while decreasing the frequency of Type I errors (Table 31).

2. Unexploited Model DMADM populations subjected to initial harvesting. Although developed primarily to classify trajectories of populations initially in the unstable region of the SYC, the discriminant function's usefulness depends on its ability to classify trajectories elsewhere in population-harvest space. These Model DMADM simulations were run to test the power of the index on populations that had not previously been exposed to harvest. Data were the same as the unexploited populations described in the Description of Age-structures section. Harvest levels 40 and 50 were known to be greater than average MSY (from the previous quantifications of the SYC), and populations were labeled as declining when harvested at these levels. Harvest levels 10 and 20 were known to lead to stable equilibria.

The discriminant function performed with greater power for these initially unharvested populations than it did for cross-section

populations, but Type I errors occurred more frequently than expected (Table 32). As seen earlier, discrimination was clearer when comparing only the 2 most distinct harvest levels.

Viewing complete simulation runs as samples and classifying populations as declining only if they contained 2 consecutive year-groups whose scores fell below the critical point, power was improved and Type I errors were reduced (Table 33). Again, discrimination was more reliable when only the extreme harvest values were considered.

3. Rapidly growing harvested Model DDALL populations. As a final indication of the robustness of the discriminant function, it was tested against initially unexploited populations known to be increasing rapidly despite a sustainable harvest. I used Model DDALL and a harvest level of 24/year. Populations were allowed to reach unexploited equilibrium of about 600, then were run under a new carrying capacity of 1000 for 20 years. Because none of the simulations declined, Type I errors were not possible. Testing the discriminant function's power was equivalent to asking how often age-structures from growing populations appeared like those from declining populations.

Power was high (Table 34), indicating that harvest age-structures from growing populations most closely resembled those of stable populations, not declining populations. Viewing each simulation run as a sample and classifying only those that contained 2 consecutive "decline" year-groups as a declining population resulted in similar power.

Table 32. Power of the discriminant function for harvest samples from populations that were initially at K=600. Data were independently generated Model DMADM runs, and discrimination used the critical point 0.85.

Harvest Levels	n	α	Power (%)
10, 50	117	0.105	75.0
10,20,40,50	237	0.205	72.5

Table 33. Power of the discriminant function for harvest samples from populations that were initially at K=600, where discrimination was made for an entire simulation run. Data were independently generated Model DMADM populations, and discrimination used the critical point 0.85. Declines were considered only those runs with 2 consecutive year-groups below the critical point.

Harvest Levels	n	α	Power (%)
10, 50	20	0.100	90.0
10,20,40,50	40	0.100	70.0

Table 34. The power of the discriminant function as applied to Model DMADM populations growing from approximately 600 in response to a K of 1000, under a constant harvest of 24/year, and using 0.85 as the critical point.

Sample	n	Power
Year-groups	61	0.814
Entire simulation (2 consecutive <0.85 scores = "decline")	10	0.800

APPLICATION OF THE INDEX TO FIELD DATA

The discriminating index for declining and stable populations was applied to data from 4 separate areas, 3 from British Columbia and 1 from Montana.

British Columbia Data

Age structure data are collected on all grizzly bear kills in British Columbia. The data examined here consisted of check-station records from 3 widely disparate areas, 2 of which were considered to be stable or increasing, the other was thought to be overharvested (F. Tompa, British Columbia Fish and Wildlife Branch, pers. comm.). Each of the 3 data sets were blocks of 12 contiguous management units, 1 from the Northern Rockies, 1 from a coastal area, and 1 from a Southern Rockies area. The last area included the Flathead river drainage, adjacent to Montana and Glacier National Park. Data were from years 1976 through 1982, and included only known, legal kills.

The Northern Rockies area was believed to have lower density and lower productivity than the other 2. Additionally, the area was easily accessible by roads, and a substantial illegal and wounding kill was suspected (F. Tompa, pers. comm.). Productivity was thought to be high in the coastal block, with natality estimated at 0.76 cubs per reproductive female per year. Hunting pressure appeared to be below that which could be supported. The Southern Rockies block was thought to be stable or increasing slightly following the imposition of

stringent regulations. This area was believed to have been heavily harvested in the past, but during the 1976-1982 period had spring hunting seasons only, and regulations that protected all family groups (not just cubs), and that required a successful grizzly hunter to wait 5 years before applying for another permit.

These B.C. populations differed in several ways from the simulated populations that generated the discrimination index. The vital rates used in the simulations used "typical" Southern interior grizzly bear rates. These were probably appropriate for the Southern Rockies area, but were less so for the other 2. Natality rates in particular were probably greater than modeled in the coastal area, and lower than modeled in the Northern Rockies area. All areas featured spring hunting seasons; the coastal and Northern Rockies area also had fall seasons. Simulated populations were subjected only to fall harvests. Regulations for the Northern Rockies hunt allowed the taking of juveniles older than 1 year old; the model assumed protection of all juveniles while under their mother's care. Finally, a few bears in the data sets were aged at over 24 years; since the analytical procedures were designed to handle bears only to age 24, ages of these older bears were truncated at 24. These differences between simulated and real life-history rates should contribute to an added degree of caution when interpreting the analysis.

As expected from the extremely conservative nature of the discrimination test, most indices were below 0.85, the critical decision point for decline. In general, the Southern Rockies area appeared to be the least heavily hunted (Tables 35-37).

Table 35. Discriminant index scores for 3 populations in British Columbia, 1976-1982. Scores indicating stability would be greater than 0.85.

Area	Sample size	Index Score
Northern Rockies	393	-1.60823
Coastal	266	-2.52234
Southern Rockies	204	0.30919

Table 36. Discriminant index score for each population, by years 1976-1978, 1979-1981, and 1982-1983. One scores is greater than 0.85, indicating stability.

Area	Years	Index Score
Northern Rockies	1976-1978	-0.82585
	1979-1981	-1.70867
	1982-1983	-2.71358
Coastal	1976-1978	0.36079
	1979-1981	-2.03787
	1982-1983	-2.15462
Southern Rockies	1976-1978	-0.12947
	1979-1981	1.10188
	1982-1983	-0.70306

Data were also examined in 3 year-groupings, and by single years. The 8 years of data did not permit 3 year-grouping of 3 years each, so the final 2 years were grouped together. The Northern Rockies and coastal areas showed declining trends. The Southern Rockies area was scored as stable during years 1979-1981.

When examined year-by-year, the Southern Rockies area appeared more stable than when examined in year-groups. The first year's index was much lower than the others, consistent with the hypothesis that the population was recovering from overharvest. In the subsequent 7 years, 3 scores indicated stability and 2 others were near the critical point for stability.

The index values for the coastal area were unexpectedly low. One interpretation is that the vital rates used in the simulations were so different from those applicable to the coastal population that the index is meaningless. An alternative interpretation is that the coastal population had been harvested more heavily than was believed.

In all cases, the preponderance of values indicating decline must be interpreted with full knowledge of the low power of the test being applied. The discrimination index is designed to be conservative. That so many data sets were classified as declining supports the view that declining and stable age-structures are so similar that many stable populations must be wrongly classified to assure that few declining populations are wrongly classified.

Montana Data

Grizzly bear age-structure data have been collected in Montana since 1967. The data examined here are from 1970 through 1981. They were compiled by the Montana Department of Fish, Wildlife and Parks (Greer 1970 through 1982). Biologist Bob Klaver assisted in analyzing these data.

All data came from the area known as the "Northern Continental Divide Grizzly Bear Ecosystem" (USFWS 1981). Yearly sample sizes were smaller than for the British Columbia data. Additionally, hunting regulations were changed in 1975 when the grizzly was listed as Threatened under the U.S. Endangered Species Act. Greer (1970 through 1982) detailed the harvests and regulations.

Discriminant indices were surprisingly low (Table 38). The score when all 12 years were considered together was -3.17151 , considerably lower than the score from the ecologically similar Southern Rockies area in British Columbia. The score generated by data including only legal kills was lower (-4.41423) than that generated by data including only other types of recorded mortality, such as nuisance bears, accidents and known illegal kills (-1.75657).

The discriminant index did not respond exclusively to any single indicator, but rather to the complex interaction of all 7 variables examined. The index rose when the variables with positive coefficients were relatively greater than were the corresponding variables with negative coefficients (Fig. 55). Of interest was the decline in the index between the 2nd and 3rd time periods, despite increases in both percent males (MFAD) and average male age (MMED; Fig. 55).

These scores suggested a similar pattern of trend in harvest

Table 37. Discriminant index score for the Southern Rockies area for each year from 1976 through 1982.

Year	Index Score
1976	-7.64806
1977	0.47816#
1978	1.90944*
1979	0.08994
1980	14.76285*
1981	0.68983#
1982	-2.19233
1983	0.89005*

* - stable
- nearly stable

Table 38. Discriminant index scores for Montana grizzly bear harvests, years 1970-1972, 1973-1975, 1976-1978, and 1979-1981 (Greer 1971, 1982). Scores indicating stability would be greater than 0.85.

Year	Index Score
1970-1972	-3.22211
1973-1975	-1.91358
1976-1978	-3.80482
1979-1981	-3.50354

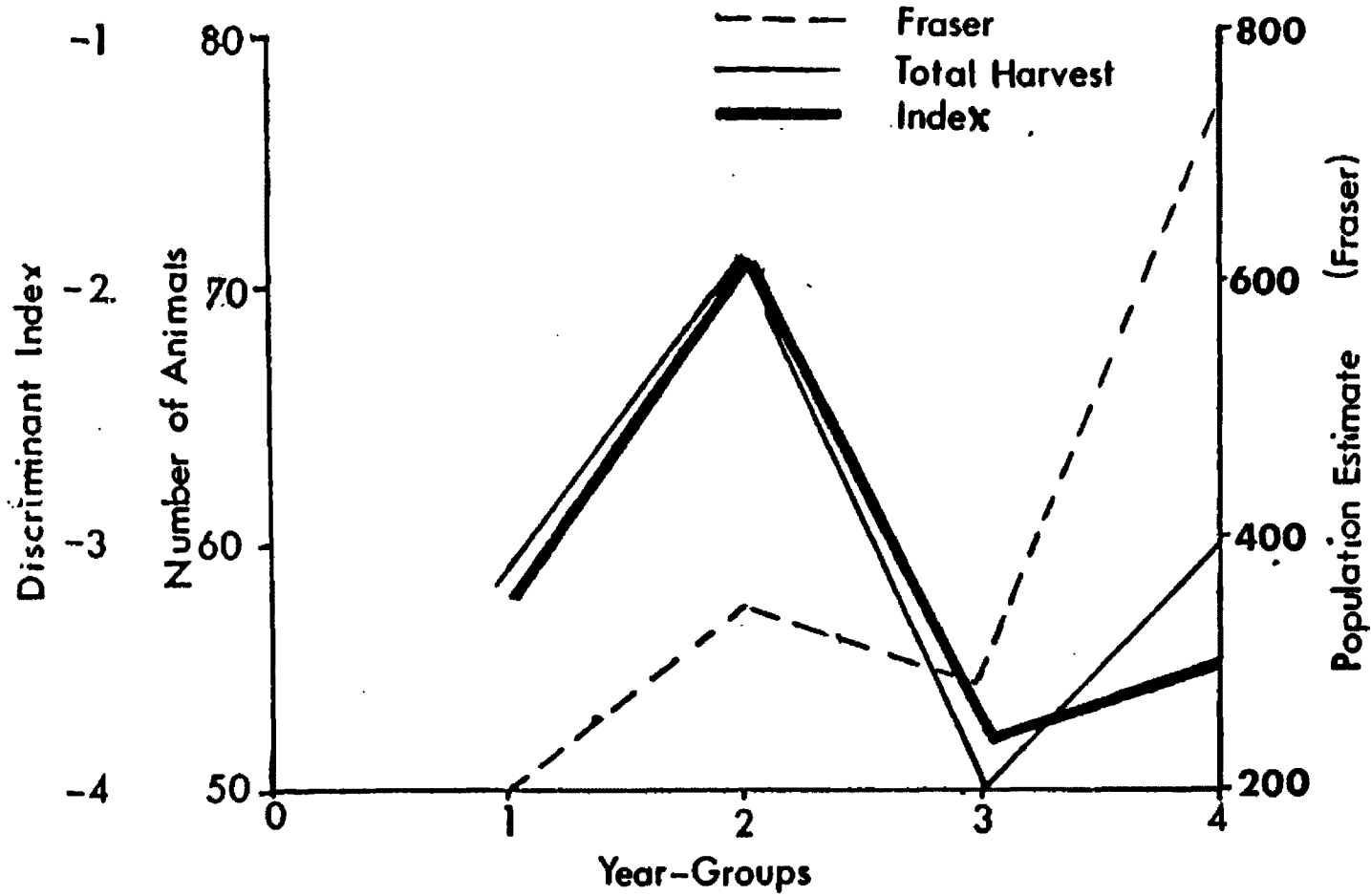
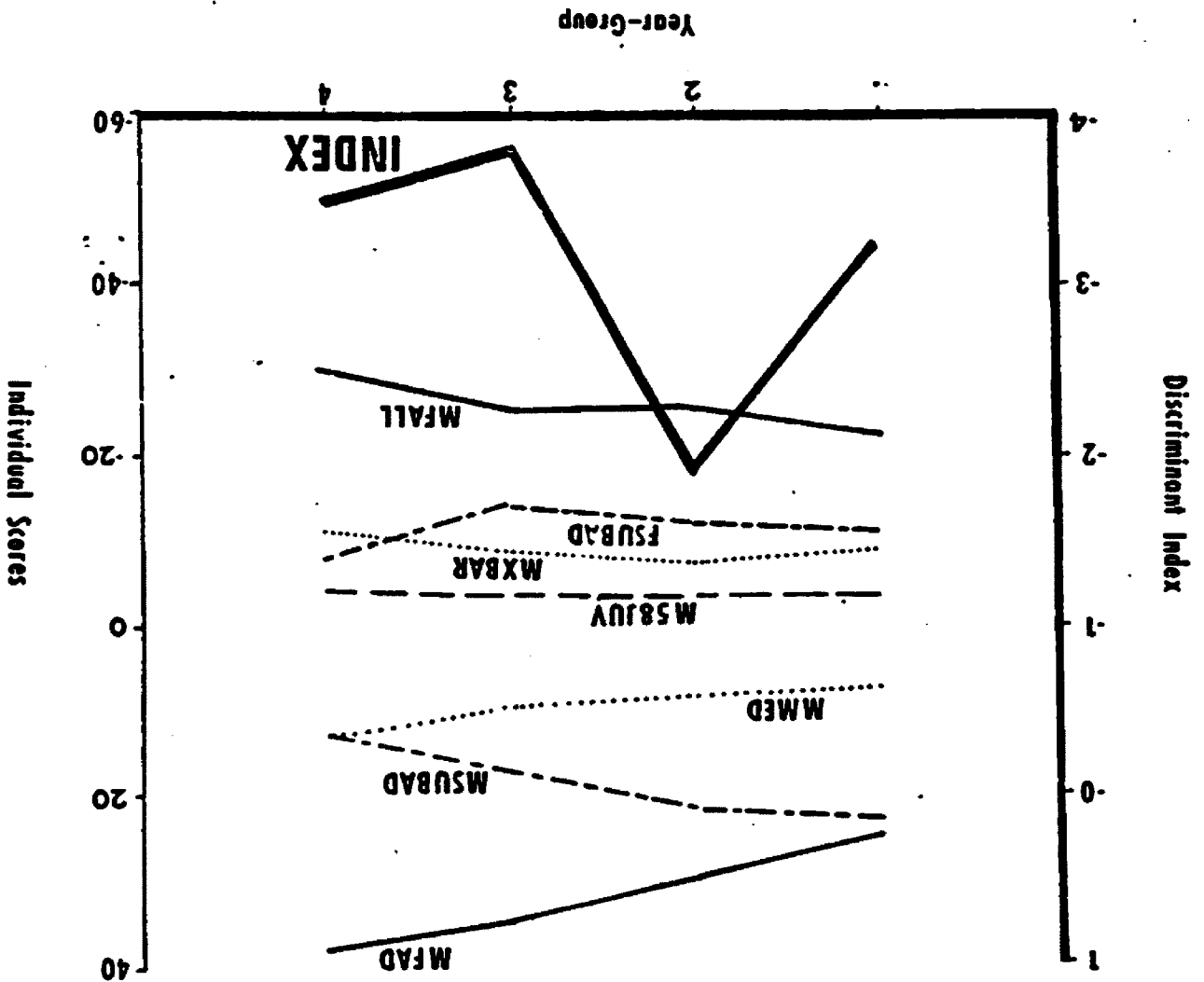


Fig. 54. The discriminant index as applied to Montana grizzly bear harvest data (Greer 1971-1982), compared with the analysis by Klaver (unpubl.) and the total known harvest each year. Klaver applied the technique suggested by Fraser et al. (1982) to calculate an estimated population during each time period. Year-groups: 1=1970-72, 2=1973-75, 3=1976-78, 4=1979-81. Note the 3 different scales along the vertical axis.

Fig. 55. The discriminant index as applied to the Montana grizzly bear harvest data, showing contributions made by the individual variables. Each of the 7 variables has been multiplied by its discriminant function coefficient; the index is the sum of the individual scores and the constant, -13.53516. Note the different scales of the individual scores and the resultant index. Variables are described in Table 2; year-groups are as in Fig. 54.



pressure (Fig. 54) as did analyses by Klaver (unpubl. data) using methods of Fraser et al. (1982). However, whereas the population estimates generated through Klaver's use of Fraser et al. (1982) suggest a general increase over the entire 12-year period, the discriminant index suggests a general decline. The discrepancy between these results and those of Klaver (unpubl. data) provides much food for thought, but little grounds for optimism that age-structure data can be interpreted unambiguously. The method of Fraser et al. (1982) assumes constant effort, while the simulation model that generated the discriminant index assumes constant harvest. We presently lack adequate data to determine which of these assumptions comes closest to reality.

DISCUSSION

The Simulation Model

The complex simulation model used in this thesis was developed because existing grizzly bear population models were inadequate to fully analyze harvest age-structures. By tracing individual animals through time, it avoided the biases inherent in Leslie-matrix based models when applied to animals that have extended parental care (Wu and Botkin 1980; M. Taylor, University of British Columbia, pers. comm.) Using this structure also elucidated some previously undocumented features of population dynamics of grizzly bears, and provided numerical verification of principles established by previous analytical models.

Age-structure was seen to be of paramount importance in the grizzly bear population dynamics. For example, when non-reproductives constituted greater than average proportions of total numbers, populations tended to decrease even when below K . When populations contained many reproductive females, they tended upward even when greater than K . Thus, the response of a population to its carrying capacity was mediated through its age-structure. Favorable age-structures buffered declines induced by poor environmental conditions, unfavorable age-structures moderated increases prompted by good environmental conditions.

Synchrony of breeding occurred as a consequence of the model parameters. Most females gave birth to their first litter at age 5; thereafter, they usually gave birth at approximately 3 year intervals.

Breeding synchrony was a major factor in the occurrence of strong and weak cohorts, seen throughout the simulations. Cohort strength persisted through time, creating cohort "waves" travelling toward the older age-classes. These cohort "waves" added variability to population structures and dynamics, and suggested that grizzly bear populations are most appropriately viewed in 3-year sets.

Variation in vital rates, as induced by variability in K, reduced average population levels (Table 6). This finding provided numerical verification of the bias inherent in deterministic population projection models (Boyce 1977). Lewontin and Cohen (1969) showed that, for populations without age-structure, variation in the environment reduced growth rates from that expected under deterministic environments. They demonstrated that, in an unlimited but varying environment, the realized growth rate r was less than the expected growth rate $\ln \lambda$ by approximately one-half the squared coefficient of variation of λ :

$$E(r) = (E[\ln l]) = \ln \lambda - \sigma^2 / 2\lambda^2$$

where:

λ = mean finite growth rate in the absence of variability

l = yearly finite growth rate (variable)

σ^2 = variance of l

and that the growth rate averaged over time was equal to the geometric

mean of 1, not the arithmetic mean.

Levins (1969) extended this work to populations with carrying capacity. He concluded that when K itself varied, the expected number in the population was a weighted harmonic mean of the individual values of K, with greater weight given to the more recent K values.

These 2 findings have similar implications. Since geometric means and harmonic means are both smaller than arithmetic means, variable environments produce smaller growth rates and/or lower expected populations than do deterministic environments.

Boyce (1977,1979) conducted simulations on age-structured populations and similarly concluded that variability in vital rates reduced expected population size. Further refinements along these lines were contributed by Tulijapurkar (1982) and Slade and Levenson (1982). The complexity of the present grizzly bear model prohibited analytical treatment, but the qualitative results of simulations with environmental stochasticity support the contention of Boyce (1977) that deterministic models overestimate population growth rates and resilience to harvests.

Furthermore, even in the absence of environmental variability, reduction in mean population size resulted from variation in vital rates caused by demographic stochasticity. The reductions in mean population size were minor for large populations, but grew in relative magnitude for populations below 100 animals (Fig 21). The extreme non-linearity in response was expected because demographic stochasticity varies in magnitude according to $1/\sqrt{N}$ (May 1974), where N is the expected population size.

The effect of environmental stochasticity on vital rates (and

thus on the reduction of realized population size) was greater than that exerted by demographic stochasticity. This too was expected. Vital rates were functions of N/K , so identical reductions in K , the denominator, had a greater effect on N/K than did reductions in N , the numerator.

Taken together, these findings constitute a powerful argument against using simple, deterministic models to gain insight into the behavior of small grizzly bear populations.

Sustainable Yield

Sustainable yields were complex functions of harvest rate, population age-structure, harvest age-structure, mechanism of population regulation, time frame, population size, and stochastic fluctuations in carrying capacity. Thus, sustained yield curves did not exist as such. Rather than sharply defined release points (Fig. 1), unstable regions contained probability bands (Fig. 25) within which the trajectory of a population could be predicted with a quantifiable probability, but never known with certainty.

Although only 2 cross-sections of the probability bands were explored - both being in the unstable portion - the probability band phenomenon doubtlessly characterized the entire range of population/harvest values. Implied by this stochastic view of sustained yield curves is that management must aim for harvests that have low probabilities of causing declines. The width of the probability band determines how far from the deterministic curve a sufficiently low probability lies. The existence of a probability band of sustainable

harvests effectively reduces the stable region of the population/harvest graph from that implied by a deterministic model (Fig 56). The stochastic curve implies that stable population levels are closer to K, and that stable harvests are further from MSY.

Sustained yield, as modeled in this thesis, assumes that the populations of interest have age-structures characteristic of populations previously subjected to harvesting. This is probably the case in most real world situations. Managers rarely have the opportunity to develop harvest regulations for populations that have never been exploited. Simulations of sustainable yield using unexploited age-structures would have generated very different results.

Modeling sustainable yields also shed light on common perceptions of how grizzly bear populations respond to harvests. Sustainable yields were influenced by the type of population regulation operating (Tables 12,13). Density-dependent birth rates offered greater compensation to harvest mortality than did increased sub-adult male survival resulting from the decline in the number of adult males. Biologists are not in complete agreement regarding the nature of population regulation in bears. McCullough (1981) stated that for the Yellowstone grizzly population of 1959-1970, "birth...declines as the number of adults increases...". thereby suggesting that natality was characterized by density-dependence. However, Bunnell and Tait (1981) "...consider that reproductive features are largely density-independent". Meanwhile, the exact role of adult males in regulating bear populations continues to be debated. One author (Stringham 1980) has written extensively on this subject, and

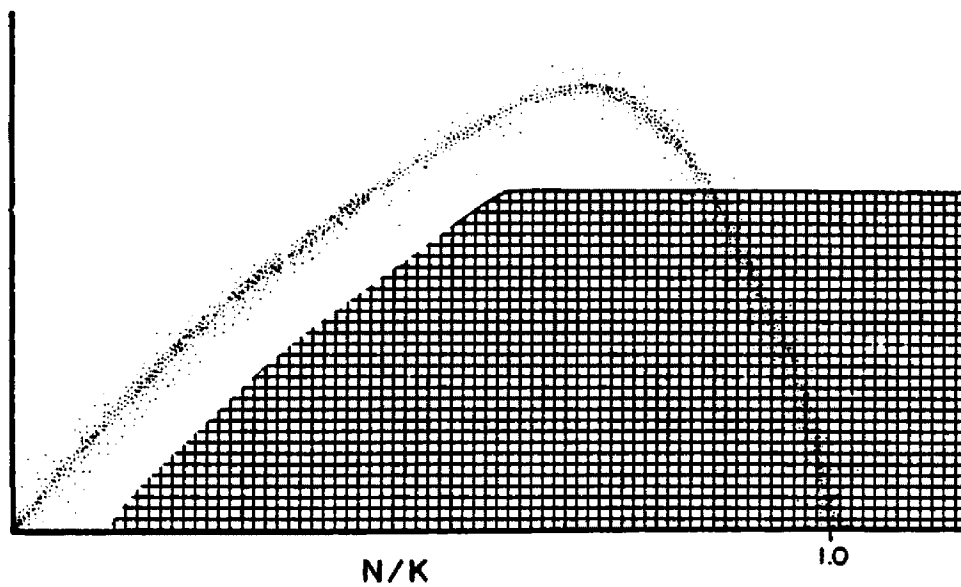


Fig. 56. A generalized sustained yield curve, showing the region of stability implied by the existence of the probability band. The area of stability, shown by cross-hatching, is the area below a reasonable probability that a population will decline. Contrast this area with that shown in Fig. 8.

exhaustively analyzed the Yellowstone data in attempting to specify mechanisms of adult male-mediated mortality. It has been proposed that if adult males inhibit population growth, hunting may act to release this regulation, thereby encouraging population growth (Kemp 1976, Bunnell and Tait 1981). The results of these simulations imply that, while adult males' influence is not trivial, density-dependent birth rates may make a larger contribution toward resilience to harvest (Tables 12,13). Therefore, our understanding of grizzly population response to harvest might be better served by research into the relationship between natality and density than into the exact way in which adult males impact other segments of the population. Population regulation mechanisms have been found to alter optimum harvest strategies in differential equation models (Clark and Tait 1982) and Leslie-matrix models (Samuel and Foin 1983).

As predicted by Boyce (1979) and shown analytically by Beddington and May (1977), variability in vital rates led to reductions in sustainable yields (Table 13). However, whereas Boyce (1979) was concerned primarily with reduction caused by climatic variability, these simulations demonstrated that reduction caused by demographic variability associated with small population size also occurs (Table 13). Small populations were unable to sustain the same proportional harvests as large populations. Thus, the common notion of a maximum sustainable rate of harvest (Bunnell and Tait 1980) as being a constant was inappropriate when applied to small populations.

Harvest age-structures

Harvests of grizzly bears are generally a small proportion of their standing population. Mean sustainable yields are small; yields that never result in decline are smaller yet. The small size of harvests has 2 implications for the resultant age-structures: (i) changes in age-structure caused by increased harvest are minor, and (ii) in any given sample, random variation plays a major role in determining the age-structure actually observed. Thus, in characterizing differences between age-structures from declining and stable populations, one is faced with very subtle differences that are often obscured by their inherent variability.

The outstanding characteristic of grizzly bear age-structures is inertia. Cohorts retain their integrity despite differential harvesting regimes (Fig. 34), and harvest changes that do translate into age-structure changes are subject to a pronounced time lag.

For a population initially at equilibrium, overharvesting causes characteristic changes in age-structure. These changes can be summarized as (i) continuously decreasing percentage males, especially among older animals, (ii) continuously decreasing male age, and (iii) slightly increasing female age (Tables 14,15, Figs. 33,35,38,39,40). With the exception of the third dynamic, these results largely support Gilbert et al. (1978). Their only conclusion explicitly contradicted by these simulations is that "the change in average age in the kill" (Gilbert et al. 1978, p. 261) is a useful indicator of population status. This statement could (perhaps erroneously) be interpreted as suggesting an average age without regard to sex. These simulations argue against analyzing sexes together. Male and female

age-distributions have distinct dynamics, and combining the 2 in the interests of increasing sample size simply obscures the dynamics of each.

Age-structures from populations with a prior history of overharvest also respond characteristically to overharvest, but changes are more subtle and variable. At the outset of this research, it was hoped that harvest age-structures might provide an early detection system for marginally over- or under-harvested populations near the unstable portion of the SYC. However, the similarity of even the most sensitive indices under the 2 opposite dynamics (Figs. 47,48), suggests that only extreme differences can likely be detected quickly.

In general, these results support the sentiments of Gilbert et al. (1978) that "Catastrophic changes in...age structure need little theory for interpretation. If only juvenile males are being killed, it does not take a model to tell managers that their bear population is in trouble". Unfortunately, interpreting "more subtle changes" is plagued with problems of sample size and variability.

One consolation is that, while harvest age-structures' response to decline was subtle and often overwhelmed by white noise, they responded qualitatively differently to a sharp and sudden population increase. This conclusion, seemingly at odds with Caughley (1974), can be reconciled by examining differences in assumptions between the present model and his.

Caughley (1974) performed an important service by clarifying some inherent limitations in interpreting age-ratios gathered from standing populations. He showed, for example, that age ratios were

unaffected when mortality rates were increased or decreased equally over all age-classes. More significantly, he showed that ratios of juveniles to adults were indistinguishable in declining and increasing populations. By reducing adult survival rates, his modeled population declined with $r=-0.2$; by increasing fecundity rates or juvenile survival, his modeled population increased with $r=0.2$. In both cases, age ratios behaved similarly. He thus concluded that increases and declines could cause identical changes in population age-structure.

While his paper caused a well needed re-evaluation of age ratio analyses by game biologists, it needn't have stopped age-structure analysis altogether. As shown here, under the assumption of constant harvest with unchanging relative vulnerabilities, harvest age-structures respond both to the standing population age-structure and to the availability of the most vulnerable age-classes. Population growth under stable harvest, as initiated by a rise in carrying capacity, provides a surplus of more vulnerable animals without diminishing the number of less vulnerable animals. Harvest age-structures during such an increase show no detectable changes despite the small increase in the relative proportion of young during the initial growth period (Fig. 50). But during population declines, harvest age-structures change predictably (if not always detectably) because, as vulnerable age-classes are depleted, the constant harvest demands that animals from less vulnerable age-classes be taken instead (Fig. 40). Caughley (1974) assumed that age ratios were calculated from unbiased samples of the standing population. Thus the apparent contradiction between the 2 conclusions is resolved. His caution against using age ratios applies

to an index such as cub:adult ratios from observations. It does not apply to harvest age-structure data as modeled here.

The Discriminant Index

The question most often asked by a manager when confronted with harvest age-structure data is: "is this population going up or down, or is it remaining stable?" The discriminant index developed in this thesis is an aid to answering that question. It was developed primarily for classifying populations existing near the unstable portion of the SYC; populations whose ultimate trajectory is either decline or return to stable equilibrium. It was seen to work about equally well for populations at other positions in population/harvest space.

However, there exist great difficulties in reliably detecting subtle differences with small samples. Like any other statistical test, the discriminant index performs best when asked to differentiate extremes. It performs poorly when the examined populations differ from each other only marginally. Also like other statistical tests, it performs better when supplied with large samples. However, unlike other problems addressed with statistical tests, sample size of harvest data is not independent of the test's outcome. In the real world, populations are not infinitely large, so achieving a large harvest sample may come only at the price of assuring population decline.

Unlike other approaches to analyzing age-structure data (e.g. Fraser 1976, Paloheimo and Fraser 1981), the discriminant index was generated by simulated, stochastic data, rather than an analytical, deterministic model. This approach enabled estimation of the power of

the test when applied to realistic data. Including an estimate of the index' power is among recommendations given by Eberhardt (1977).

The test is designed to be conservative. Using the suggested critical points of 0.85 (large samples) and 2.00 (small samples) results in probability of Type I of approximately 10%. A higher critical point would reduce Type I errors further, but at the cost of considerable power (Fig. 57). Accepting a 10% probability of mis-identifying a declining population is probably the best compromise of Type I and II errors. If 2 consecutive 3-year groups are considered and the population categorized as declining only if both indices are below the critical point, the probability of a Type I error can be reduced below 10%. (If harvest age-structures from both samples are completely independent, the Type I probability will be $0.10 \times 0.10 = 0.01$. However, harvest age-structures from consecutive year-groups are probably serially correlated. Under perfect serial correlation, the 2 age-structures will differ from each other only because of random noise, and the expected probability of Type I error will still be 0.10. A reasonable guess is that age-structure independence lies half-way between the extreme cases, resulting in an expected probability of Type I error of $(0.10 + 0.01)/2 = 0.055$). However, using the criterion of 2 consecutive declining indices further reduces the temporal sensitivity of the index. Because I recommend combining data from 3 consecutive years to form each age-structure, a decision based on 2 consecutive year-groups requires 6 years.

The discriminant index responds not to population size but to intensity of the harvest. Unfortunately, it is most sensitive at

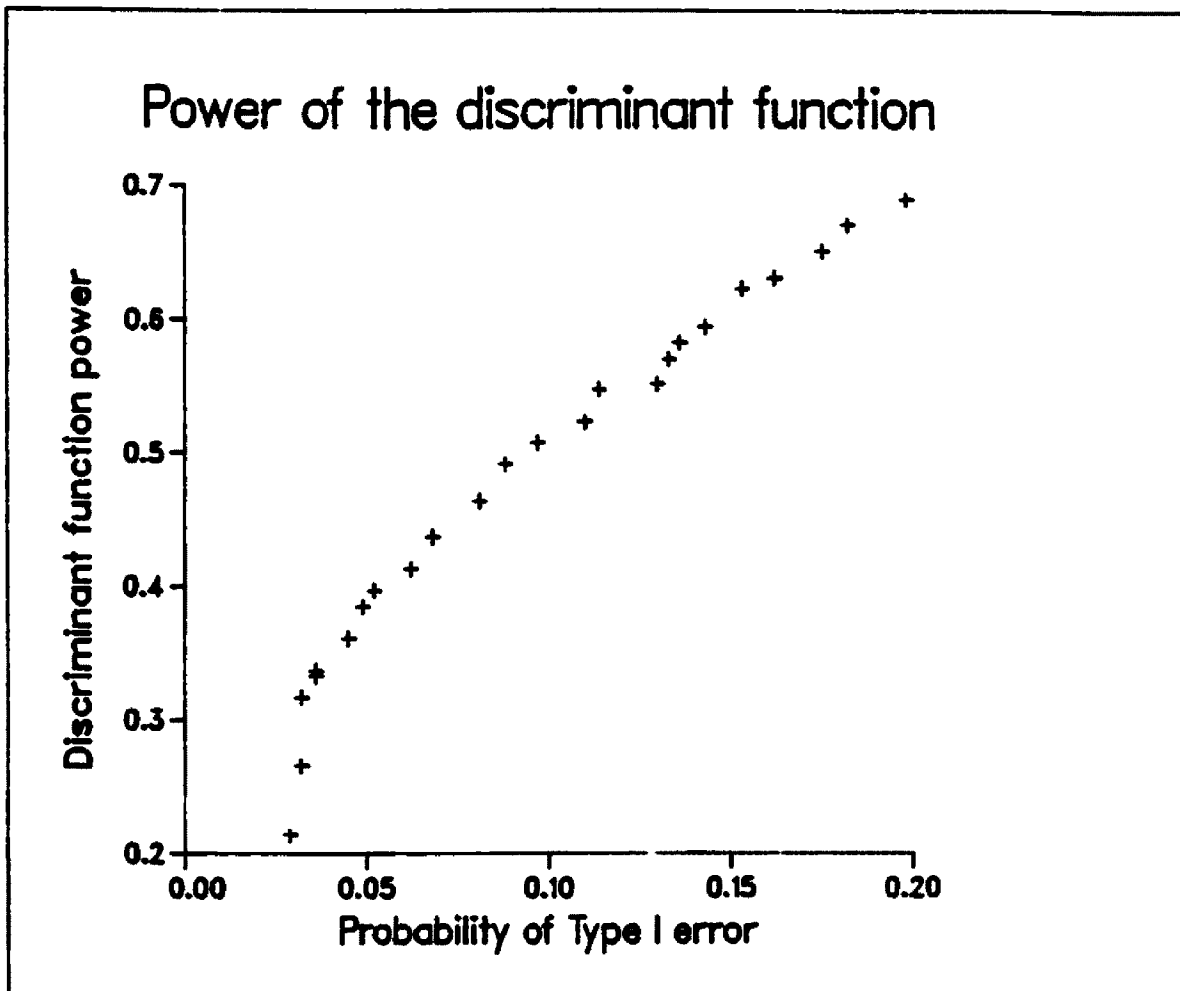


Fig. 57. The power of the discriminant index as a function of the probability of Type I errors. Type I errors are mis-classifying as a stable population one that is actually in decline.

harvest rates well above sustainable levels, and is least sensitive in the critical harvest-population region that divides sustainable harvest from overharvests (Fig. 58). Harvest levels around 5% can produce discriminant indices as high as 4 and as low as -2. Extremely low indices are guaranteed only at catastrophically high harvest rates.

Because the test's power is strongly related to sample size, questions of how to best increase the sample are pertinent. One alternative is to enlarge the unit of area studied, thereby increasing the number of animals assumed to operate as 1 population. However, doing so risks averaging together sub-populations with different dynamics and possibly overlooking local declines. Real world populations rarely behave homogeneously. Local patches of abundance and overharvest are probably the rule rather than the exception. In fact, a major weakness of this modeling effort is that it ignores heterogeneity below the level of the entire population. It is unclear how often assemblages of even as few as 200 grizzly bears can be considered a discrete population.

In some areas, it is possible to increase sample size by augmenting harvest data with that from bears live-captured for research. Can age-structure data from these captured bears be added to the analysis? The answer depends on whether or not relative vulnerabilities to capture and harvest can be assumed equal. If trapping occurs prior to the harvest and in the same general area, this question can be addressed by comparing the 2 age-structures. Because the 2 sample the same population (captured bears are assumed to have been released back into the population), similar relative vulnerabilities should yield

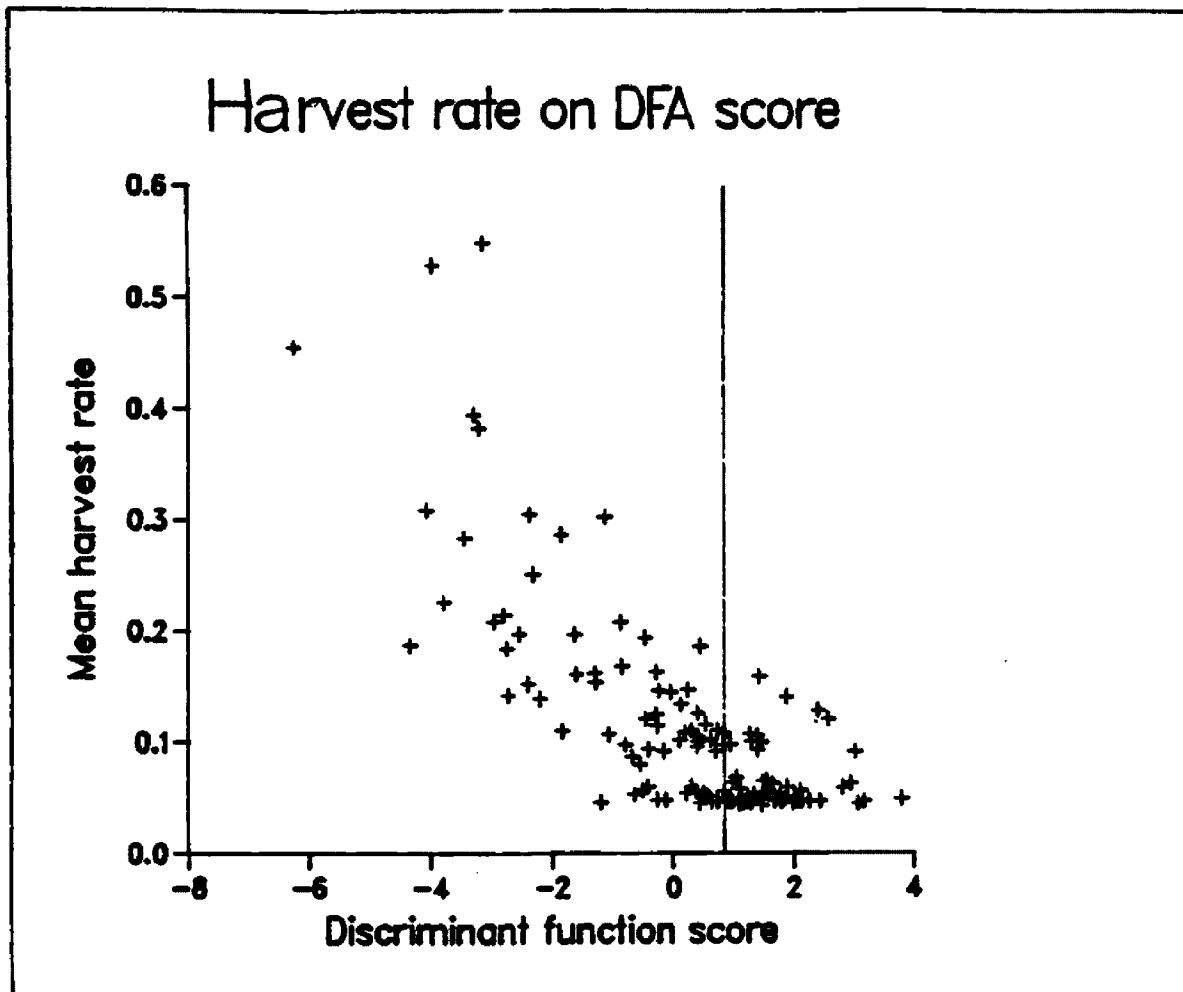


Fig. 58. Harvest rates associated with different values of the discriminant index. Harvest rates of 5% or below are associated with variable discriminant scores. Only at catastrophically high harvest rates is the discriminant index reliably low.

similar age-structures. However, tests of differences between distributions based on small samples are conservative. Real differences between age-structures might therefore be statistically insignificant, erroneously leading the investigator to conclude that combining data is justified.

In a few studies of black bears, sample sizes have been sufficient to compare age-structures from trapped and harvested bears. Raybourne (1976) compared harvested and trapped black bear age-structures from Virginia. He concluded that the trapped sample compared "...almost identically with harvest data for the same period". Statistical analysis of his data reveal that neither male age distributions nor male:female ratios are significantly different ($p > 0.10$). Recently, the Montana Department of Fish, Wildlife, and Parks was initiated trapping efforts in the Cabinet Mountains of northwestern Montana. There, black bear age-structures from trapping differed significantly from the age-structure of the harvested sample (G. Brown, Montana Department of Fish, Wildlife, and Parks, pers. comm.). Thus it appears that relative vulnerabilities to hunting and research trapping may or may not differ.

Assumptions and Research

The model upon which this analysis is based contains numerous assumptions, but the most critical appear to be those related to the nature of grizzly bear harvesting. Although there are presently little data to guide the modeling of grizzly bear harvests, such information can be collected by hunter surveys and statistical analyses of past harvests.

First, the model assumes a constant harvest. Implicit is that harvest effort increases continuously with overharvest, because the same number must be harvested from an ever decreasing population. A constant harvest model is clearly unrealistic beyond some lower boundary of population abundance; if only 20 bears remain, one can hardly expect 20 bears to be harvested. However, a constant effort model can similarly be valid only under restricted conditions. If effort is constant at all densities, populations are either always stable (if effort is below a critical level) or always declining to extinction (if effort is too high). The fact that some populations have exhibited stability under harvest while others have declined (and most have done some of each!) argues against constant effort as a reasonable model at all densities. Additionally, if effort is known to be constant, the size of the harvest is a direct index of population size, and sophisticated analyses are unnecessary. As suggested by Beddington and May (1977), the true situation is doubtlessly an intermediate one between constant harvest and constant effort. Although I would suggest that constant harvest is

the most appropriate model for the range of densities examined here, data on harvest effort can only improve such modeling efforts in the future. In particular, a reliable index of effort could help guide interpretation of the inconsistency between the long-term trend suggested by the analysis of Montana's 1970-1981 grizzly bear harvest offered here, and that presented by Klaver (unpubl. data).

Second, the model assumes each age-class has a relative vulnerability to harvest that is unaffected by population density. This constitutes a first approximation; we have no data to indicate otherwise. However, at least 2 scenarios in which this assumption is violated appear plausible. First, if hunters prefer a large animal, they will tend to select males over females. However, in a population that has been reduced by heavy harvest, mature females may be the largest bears remaining. Thus, at lower densities, female vulnerability may increase. Second, the model assigns very high vulnerabilities to sub-adult males primarily because they wander about more than other age-classes. The work of Kemp (1976) and Young and Ruff (1982) suggests that much of their wandering is in response to the presence of adult males. In a heavily harvested population with few adult males, sub-adult males may find it easier to establish a home range, thereby reducing their movements and, by extension, their vulnerability to harvest. Research into the relative vulnerabilities of age-classes and how these change under varying harvest regimes would add greatly to our knowledge of harvested grizzly bear dynamics.

MANAGEMENT SUMMARY

1. A stochastic, age-structured grizzly bear population projection model was developed, which traced individual animals through time. The model accurately portrayed such features of grizzly populations as litter size, breeding interval, age at first reproduction, survival rates, and longevity of individuals, as well as components impossible to simulate with traditional Leslie-matrix based models, such as synchrony of breeding and non-stationary age-structures.

2. When initiated at a small, arbitrary number, populations grew slowly towards equilibrium. However, declines occurred throughout the growth phase, i.e. even when resources were not limiting the population. The resulting increment curve included negative increments at all population densities. This view of population growth of a K-selected species implied that deterministic increment curves overestimate the potential of such populations to withstand non-selective harvests.

3. Portions of the sustained yield curve were quantified for populations that had unexploited equilibria of 200 and 600 animals. Sustainable yield at a given population level was not adequately portrayed by a single number; rather, sustainable yields occurred in broad probability bands.

4. Within the sustained yield probability band, the trajectory of a given population was influenced not only by its harvest rate, but by stochastic factors, including the age-structure of the standing population at the initiation of harvest, the age-structure of the animals killed during the harvest, and variability in the population's vital rates during the harvest, as affected by yearly variation in K .

5. Mean sustainable yields applied over 30 years were lower than those applied over 10 years. A constant harvest that did not induce detectable declines within 10 years often did so by year 30. Conversely, significant declines within 10 years never reversed themselves during the subsequent 20 years.

6. The mechanism of population regulation operating influenced sustainable yields. Populations with density-dependent natality withstood higher harvests than did populations with density-independent natality. Similarly, populations with sub-adult male survival a function of adult male abundance were more resilient to harvests than were populations with sub-adult male survival a function of total population size. The compensation to harvest mortality afforded by density-dependent natality was greater than that afforded by the adult-male mediated survivorship function for sub-adult males.

7. Sustainable yield, expressed as a proportion of the standing population, was inversely related to the magnitude of demographic

stochasticity. Because small populations were more influenced by demographic stochasticity than large populations, they had lower proportional sustained yields than larger populations. Thus, the concept of a constant proportion of the population as being harvestable was incorrect.

8. Stable harvests were characterized by a large proportion of vulnerable sub-adult males. Overharvests first showed increasing proportions of older males. Later, as older males were depleted, overharvests showed increasing proportions of juvenile males and sub-adult females.

9. Past demographics greatly influenced age-structures of harvested grizzly bear populations. Differences in age-structures of overharvested and safely harvested populations were minor. Changes that did occur were subject to a pronounced time-lag of up to 8 years.

10. The subtle changes in population age-structure that accompanied overharvest were categorized by 3 patterns: 1) harvest sex ratio shifted toward females, 2) males became younger, and 3) females became slightly older.

11. Harvest age-structures from populations that were allowed to increase (by increasing their carrying capacities) were more similar to stable harvests than to overharvests. Thus, age-structure indicators derived from a constant harvest with differential relative vulnerability

did not display the ambiguities of standing population age-ratios shown by Caughley (1974).

12. Patterns in age-structures were obfuscated by chance variability associated with small sample size, as well as the 3-year cycle of cohort abundance.

13. Differences in harvest age-structure of declining and stable populations were summarized and quantified by a 2-group discriminant function equation. The equation more accurately predicted population trajectory when only extremes in harvest regime were compared. It performed more efficiently when age-structure data from 3 consecutive years were pooled than when supplied with only a single years' data. It was more powerful with larger than smaller samples.

14. The power of the discriminant function was estimated by setting the probability of erroneously classifying a declining population as stable at 10%, and quantifying the percentage of stable populations correctly classified. Under circumstances typically confronting a manager, the power of the test was low: with large sample sizes, power was just over 50%; with small sample size, power was about 20%.

15. The subtlety of differences between age-structures of declining and stable populations is a result of the general inability of grizzly bear populations to withstand substantial harvest.

Age-structure changes occur because of harvesting, but grizzly bear harvests are necessarily small proportions of the standing population. Thus, while relatively small harvests can induce declines, they perturb age-structures only slightly. The symptoms of overharvest may therefore not be diagnosed until a population decline is well underway.

16. Grizzly bear harvesting must therefore be viewed conservatively. Harvesting a small population merely to gain information on population structure for purposes of analysis is unlikely to yield a net value. The only time such information is likely to be reliable is when the harvest itself has caused a major decline.

17. Decisions about harvesting small grizzly bear populations should be based on the best available information. However, it should be realized that even the best possible data contain inherent uncertainty; decisions must be made in the context of risk, rather than irrefutable scientific evidence.

APPENDIX A

Rate Functions Used in Simulation

Female Survival

Age	Rate at K	Minimum Rate	Maximum Rate	N/K @ 50%	N/K @ 95%
01	0.078	0.00	0.50	0.75	1.25
11	0.670	0.25	0.75	1.28	2.00
21	0.670	0.25	0.75	1.28	2.00
31	0.860	0.65	0.90	1.28	2.00
4	0.868	0.70	0.95	1.28	2.00
5	0.910	0.70	0.95	1.28	2.00
to					
12	0.910	0.70	0.95	1.28	2.00
13	0.860	0.65	0.90	1.28	2.00
to					
20	0.860	0.65	0.90	1.28	2.00
21	0.710	0.50	0.75	1.28	2.00
to					
24	0.710	0.50	0.75	1.28	2.00

1 Rates for juveniles not accompanied by mother.

Juvenile Survival

Age	Rate at K	Minimum Rate	Maximum Rate	N/K @ 50%	N/K @ 95%
0	0.936	0.700	0.950	1.40	2.00
to					
4	0.936	0.700	0.950	1.40	2.00

APPENDIX A (cont'd)

Rate Functions Used in Simulation

Male Survival

Age	Rate at K	Minimum Rate	Maximum Rate	N/K @ 50%	N/K @ 95%
01	.078	0.000	0.500	0.75	1.25
11	.600	0.100	0.750	1.22	2.00
21	.600	0.100	0.750	1.22	2.00
31	.762	0.300	0.900	1.22	2.00
4	.762	0.300	0.900	1.22	2.00
5	.892	0.700	0.950	1.22	2.00
to					
12	.892	0.700	0.950	1.22	2.00
13	.842	0.650	0.900	1.22	2.00
to					
20	.842	0.650	0.900	1.22	2.00
21	.692	0.500	0.750	1.22	2.00
to					
24	.692	0.500	0.750	1.22	2.00

1 Rates for juveniles not accompanied by mother.

APPENDIX A (cont'd.)

Rate Functions Used in Simulations

Breeding Probability of Lone Females

Age	Rate at K	Minimum Rate	Maximum Rate	N/K @ 50%	N/K @ 95%
0	0.000	0.000	0.000	-	-
to					
3	0.000	0.000	0.000	-	-
4	0.624	0.000	0.750	1.227	1.800
5	0.761	0.200	0.800	1.319	1.800
6	0.937	0.500	0.970	1.313	1.800
7	0.937	0.500	0.970	1.313	1.800
8	0.990	0.650	1.000	1.374	1.800
to					
24	0.990	0.650	1.000	1.374	1.800

Probability of Juveniles Leaving Mother

Age	Rate at K	Minimum Rate	Maximum Rate	N/K @ 50%	N/K @ 95%
0	0.000	0.000	0.000	-	-
1	0.135	0.000	0.270	1.000	2.000
2	0.700	0.670	0.730	1.000	2.000
3	0.900	0.900	0.900	-	-
4	0.900	0.900	0.900	-	-
5	1.000	1.000	1.000	-	-

APPENDIX A (Cont'd)

Rate Functions Used in Simulations

Relative Probability of Litter Size (1)

Age	Rate at K	Minimum Rate	Maximum Rate	N/K @ 50%	N/K @ 95%
5 to 24	0.180	0.180	0.180	-	-

Relative Probability of Litter Size (2)

Age	Rate at K	Minimum Rate	Maximum Rate	N/K @ 50%	N/K @ 95%
5 to 24	0.500	0.400	0.600	1.000	2.000

Relative Probability of Litter Size (3)

Age	Rate at K	Minimum Rate	Maximum Rate	N/K @ 50%	N/K @ 95%
5 to 24	0.240	0.000	0.480	1.000	2.000

APPENDIX B

Relative Vulnerabilities to Hunting

Age	Lone Males	Lone Females	Females w/young	Juvenile w/mother
0	7.00	2.00	-	0.05
1	7.00	2.00	-	0.20
2	7.00	2.00	-	0.20
3	7.00	2.00	-	0.20
4	7.00	2.00	-	0.20
5	1.00	0.80	0.20	-
to				
24	1.00	0.80	0.20	-

APPENDIX C

Coefficients for the discriminant function generated by data from year-group 2 (years 4-6). See table 2 for formulae and definitions of each variable.

Variable	Standardized Coefficient	Unstandardized Coefficient
MFAD	1.44725	0.1796125
MXBAR	-0.96162	-1.5989310
FSUBAD	-0.70831	-0.1387566
MMED	0.70546	2.3859020
MFALL	-0.42773	-0.0867705
MSUBAD	0.39645	0.0707136
FXBAR	-0.29075	-0.3862803
Constant		2.0157800

Power of the discriminant function for harvest samples from populations with K=600. Each sample consisted of a year-group made up of the summed age-class frequencies from 3 consecutive years. The expected Type I error was 0.10.

Specific Model	n	Critical Value	α	Power (%)
DDALL	560	1.79225	0.101	33.7
DM	522	1.98392	0.116	27.7
ADM	550	1.45592	0.108	32.3
DMADM	554	1.61980	0.091	35.6

APPENDIX C (continued)

Coefficients for the discriminant function generated by data from year-group 3 (years 8-10). See table 2 for formulae and definitions of each variable.

Variable	Standardized Coefficient	Unstandardized Coefficient
MFAD	0.79615	0.0872555
MXBAR	-0.72027	-1.0295560
MMED	0.54987	1.7081600
FSUBAD	-0.49168	-0.0924178
FXBAR	-0.21014	-0.2513383
M58JUV	0.17327	0.0233885
F58JUV	-0.11073	-0.0109361
FMED	0.10463	0.1294199
Constant		2.1305050

Power of the discriminant function for harvest samples from populations with K=600. Each sample consisted of a year-group made up of the summed age-class frequencies from 3 consecutive years. The expected Type I error was 0.10.

Specific Model	n	Critical Value	α	Power (%)
DDALL	560	2.10766	0.114	25.8
DM	522	2.43812	0.124	21.4
ADM	550	1.71332	0.108	27.7
DMADM	554	2.02480	0.112	27.3

REFERENCES

- Aune, K. and T. Stivers 1983. Rocky mountain front grizzly bear monitoring and investigation. Montana Fish and Game Res. Rep.
- Beddington, J.R. 1979. Harvesting and population dynamics. pp. 307-320 in Anderson, R.M., B.D. Turner, and L.R. Taylor, eds. Population Dynamics. The 20th Symposium of the British Ecological Society, London. Blackwell Scientific Publications, London. 434 pp.
- _____ and R.M. May 1977. Harvesting natural populations in a randomly fluctuating environment. Science. 463-465.
- Boyce M.S. 1977. Population growth with stochastic fluctuations in the life table. Theor. Pop. Biol. 12:366-373.
- _____. 1979. Population projections with fluctuating fertility and survivorship schedule. Proc. Summer Comp. Sim. Conf., Toronto 10: 385-388.
- Brauer, F. and D.A. Sanchez 1975. Constant rate population harvesting: equilibrium and stability. Theor. Pop. Biol. 8:12-30.
- Bunnell, F.L. and D.E.N. Tait 1980. Bears in models and reality - implications to management. pp. 15-23 in Martinka, C.J. and K.L. McArthur, eds., Bears - their biology and management. Bear Biol. Assoc. Conf. Ser. No. 3, Kalispell, Mt.
- _____. and _____ 1981. Populations dynamics of bears and management implications. pp. 75-98 in Fowler, C.W. and T.W. Smith, eds., Dynamics of large mammal populations. Wiley Press. 416pp.
- Caughley, G. 1974. Interpretation of age ratios. J. Wildl. Manage. 38:557-562.
- _____. 1977. Analysis of wildlife populations. Wiley Press. 234 pp.
- Clark, C.W. 1976. Mathematical Bioeconomics. Wiley Press. 1976.
- _____. and D.E.N. Tait 1982. Sex-selective harvesting of wildlife populations. Ecol. Modelling 14:251-260.
- Cole, L.C. 1951. Population cycles and random oscillations. J. Wildl. Manage. 15:233-252.
- Craighead, J.J. and F.C. Craighead, Jr. 1967. Management of bears in Yellowstone National Park. Environmental Research Institute and

Mont. Coop. Wildl. Res. Unit Report. 113 pp.

- _____, M.G. Hornocker, and F.C. Craighead, Jr. 1969 .
Reproductive biology of young female grizzly bears. J. Reprod.
Fert. Suppl. 6:447-475.
- _____, J.R. Varney, and _____. 1974. A population
analysis of the Yellowstone grizzly bears. Bull. 40, Mont. For.
and Cons. Sta., Univ. of Montana, Missoula, 20 pp.
- Eberhardt, L.L. 1977a. Applied systems ecology: models, data, and
statistical methods. pp. 43-55 in Innis, G.S., ed., New directions
in the analysis of ecological systems. Part I. Sim. Com. Proc.
Ser. 5(1).
- _____. 1977b. "Optimal" management policies for marine mammals.
Wildl. Soc. Bull. 5:163-169.
- _____. and Siniff, D.B. 1977. Population dynamics and marine
mammal management policies. J. Fish. Res. Board Can. 34:183-190.
- Fisher, R.A. 1958. The genetical theory of natural selection. Dover,
N.Y.
- Fowler, C.W. 1981. Density dependence as related to life history
strategy. Ecology 62(3): 602-610.
- _____, W.T. Bunderson, M.B. Cherry, R.J. Ryel, and B.B. Steele.
1980. Comparative population dynamics of large mammals; a search
for management criteria. Report no. MMC-77-20 to the U.S. Marine
Mammal Commission. National Technical Information Service NTIS
PB80-178627, Springfield, Va.
- Frankel, O.H. and M.E. Soule. 1981. Conservation and evolution.
Cambridge Univ. Press. 327 pp.
- Fraser, D. 1976 An estimate of hunting mortality based on the age and
sex structure of the harvest. pp. 237-273 in Hancock, J.A., and
W.E. Mercer, eds., Proc. of the 12th North Amer. Moose Conf. and
Workshop, St. John's, Newfoundland.
- _____, J.F. Gardner, G.B. Kolenosky, and S. Strathearn. 1982.
Estimation of harvest rate of black bears from age and sex data.
Wildl. Soc. Bull. 10(1): 53-57.
- Getz, W. 1983. Population dynamics: a per capita resource approach.
pp. 167-170 in Lamberson, R., ed., Mathematical models of renewable
resources, Vol. II., Humboldt State Univ. Math. Model. Group.
- Gilbert, J.R., W.S. Kordek, J. Collins, and R. Conley. 1978.
Interpreting sex and age data from legal kills of bears. pp.

253-262 in Hugie, R.D. ed., 4th Eastern black bear workshop. Greenville, ME. 409 pp.

Gill, J. 1953 Remarks on the analysis of kill-curves of female deer. 9th Northeast Section Wildlife Conf. 12 pp.

Glenn, L.P. 1973 Report on 1972 brown bear studies. Alaska Dept. Fish Game Proj. Prog. Rep. Fed Aid Wildl. Restor. Proj. W-17-4 and W-17-5. 16 pp.

_____. 1975. Report on 1974 brown bear studies. Alaska Dept. Fish Game Proj. Prog. Rep. Fed Aid Wildl. Restor. Proj. W-17-6 and W-17-7. 10 pp.

_____, J.W. Lentfer, J.B. Faro and L.H. Miller. 1976. Reproductive biology of female brown bears, Ursus arctos, McNeil River, Alaska. pp. 381-390 in Pelton, M.R., J.W. Lentfer, and G.E. Folk, eds., Bears - their biology and management. IUCN publ. New Ser. No. 40, Morges, Switzerland.

Goodman, D. 1981. Life history analysis of large mammals. pp. 415-436 in Fowler, C.W. and T.D. Smith, Dynamics of large mammal populations. Wiley Press. 477 pp.

Greer, K. 1971. Grizzly bear mortality and management programs in Montana during 1970. Job progress report W-120-R-2, Work plan IV, Job L-1.1, Mont. Dept. Fish Game.

Greer, K. 1972. Grizzly bear mortality and management programs in Montana during 1971. Job progress report W-120-R-3, Work plan IV, Job L-1.1, Mont. Dept. Fish Game.

Greer, K. 1973. Grizzly bear mortality and management programs in Montana during 1972. Job progress report W-120-R-4, Work plan IV, Job L-1.1, Mont. Dept. Fish Game.

Greer, K. 1974. Grizzly bear mortality and management programs in Montana during 1973. Job progress report W-120-R-5, Work plan IV, Job L-1.1, Mont. Dept. Fish Game.

Greer, K. 1975. Grizzly bear mortality and management programs in Montana during 1974. Job progress report W-120-R-6, Work plan IV, Job L-1.1, Mont. Dept. Fish Game.

Greer, K. 1976. Grizzly bear mortality and management programs in Montana during 1975. Job progress report W-120-R-7, Work plan IV, Job L-1.1, Mont. Dept. Fish Game.

Greer, K. 1977. Grizzly bear mortality and management programs in Montana during 1976. Job progress report W-120-R-8, Work plan IV, Job L-1.1, Mont. Dept. Fish Game.

- Greer, K. 1978. Grizzly bear mortality and management programs in Montana during 1977. Job progress report W-120-R-9, Work plan IV, Job L-1.1, Mont. Dept. Fish Game.
- Greer, K. 1979. Grizzly bear studies, statewide wildlife research. Job progress report W-120-R-10, Work plan V, Job L-1.1, job. no. 2, Mont. Dept. Fish Game.
- Greer, K. 1980. Grizzly bear studies, statewide wildlife research. Job progress report W-120-R-11, Work plan V, Job L-1.1, job. no. 2, Mont. Dept. Fish Game.
- Greer, K. 1981. Grizzly bear studies, statewide wildlife research. Job progress report W-120-R-12, Work plan V, Job L-1.1, job. no. 2, Mont. Dept. Fish Game.
- Greer, K. 1982. Grizzly bear studies, statewide wildlife research. Job progress report W-120-R-13, Work plan V, Job L-1.1, job. no. 2, Mont. Dept. Fish Game.
- Grier, J.W. 1979. Caution on using productivity or age ratios along for population inferences. Raptor Research 13(1):20-24
- Gross, J.E. 1969. Optimum yield in deer and elk populations. Trans. North Amer. Wildlife Conf. 34:372-386.
- _____. 1972. Criteria for big game planning: Performance measures vs. intuition. Tran. North Amer. Wildlife Conf. 37:246-259.
- Gulland, J.A. 1970. The effect of exploitation on numbers of marine mammals. pp. 450-467 in den Boer, P.J., and D.R. Gradwell, eds., Dynamics of Popciations. Center for Agric. Publ. and Doc., Wageninge, Netherlands.
- Harris, L.D. and I.H. Kochel 1981. A decision-making framework for population management. pp. 221-240 in Fowler, C.W. and T.D. Smith, eds., Dynamics of large mammal populations. Wiley Press 447 pp.
- Harris, R.B. 1984. Grizzly bear population trend monitoring - a resource for decision makers. U.S. Fish and Wildl. Serv. Tech. Note (in press).
- Hebert, D.M., D. _____ and B. Langin. 1983. An evaluation of census methods for grizzly bear. unpubl. internal draft, British Columbia Wildlife Branch, Victoria, B.C.
- Hensel, R.J., W.A. Troyer, and A.W. Erickson. 1969. Reproduction in the female brown bear. J. Wildl. Manage. 33:357-365.
- Holling, C.S. 1965. The functional response of predators to prey density and its role in mimicry and population regulation. Mem.

Ent. Soc. Can. 45:1-60.

- Jonkel C. 1982 5-year summary report. Border Grizzly Project. University of Montana, Missoula.
- Kemp, G.A. 1972. Black bear population dynamics at Cold Lake, Alberta, 1968-1970. pp. 26-31 in Herrero, S. ed., Bears - their biology and management. IUCN publ. New Ser. No. 23, Morges, Switzerland.
- _____. 1976. The dynamics and regulation of black bear, Ursus americanus, population in northern Alberta. pp. 191-197 in Pelton, M.R., J.W. Lentfer, and G.E. Folk, eds., Bears - their biology and management. IUCN publ. New Ser. No. 40, Morges, Switzerland.
- Knight, R.R., B.M. Blanchard, G. Brown, K.C. Greer, L.E. Oldernburg and L.J. Roop. 1983. Yellowstone Grizzly Bear Investigations - Report of the Interagency Study Team. U.S. Dep. Int. Nat. Park Serv. 52 pp.
- Leslie, P.H. 1945. The use of matrices in certain population mathematics. *Biometrika* 33:183-212.
- Lett, P.F., R.K. Mohn and D.F. Gray. 1981. Density-dependent processes and management strategy for the northwest Atlantic harp seal populations. pp. 135-158 in Fowler, C.W. and T.D. Smith, eds., Dynamics of large mammal population dynamics. Wiley Press 447 pp.
- Levins, R. 1969. The effect of random variations of different types on population growth. *Proc. Nat. Acad. Sci.* 62:1061-1965
- Lewontin, R.C. and D. Cohen 1969. On population growth in a randomly varying environment. *Proc. Nat. Acad. Sci.* 62: 1056:1060
- Martinka, C.J. 1974. Population characteristics of grizzly bears in Glacier National Park, Montana. *J. Mammal.* 55(1): 21-29.
- May, R.M. 1974. Stability and complexity in model ecosystems. Princeton University Press, Princeton, N.J.
- _____. 1977. Thesholds and breakpoints in ecoystems with a multiplicity of stable states. *Nature* 269: 471-477
- McClellan, B. 1983. Akamina-Kishinena grizzly bear study - annual report. British Columbia Fish Wildlife Branch, Cranbrook, B.C.
- McCullough, D. 1979. The George Reserve deer herd: Population ecology of a K-selected species. Univ. of Michigan Press, Ann Arbor, MI.
- _____. 1981 Population dynamics of the Yellowstone grizzly bear. pp. 173-196 in Fowler, C.J. and T.W. Smith, eds., Dynamics of large mammal populations. Wiley Press 417 pp.

- Metzgar, L.H. 1984. Stability in forage-ungulate-predator systems. Mathematical models of renewable resources, Vol. III, Proc. of 3rd Pac.Coast Resource Model. Conf., Davis, Cal. (in press)
- Mundy, K.R.D. and D.R. Flook. 1973 Background for managing grizzly bears in the national parks of Canada. Can. Wildl. Serv. Rep. Sereis No. 22. 35 pp.
- Nie ,N.H., C.H. Hull, J.G. Jenkins, K. Steinbrenner and D.H. Bent. 1975. SPSS - Statistical package for the social sciences, 2nd edition. McGraw-Hill Book Co. 673 pp.
- Noy-Meir, I. 1975. Stability of grazing systems: An application of predator-prey graphs. J. Ecol. 63:459-481.
- Overall, J.E. and C.J. Klett. 1972. Applied multivariate analysis. Mc-Graw Hill, N.Y.
- Paloheimo, J.E. and D. Fraser. 1981. Estimation of harvest rate and vulnerability from age and sex data. J. Wildl. Manage. 45:948-958.
- Pearson, A.M. 1975. The northern interior grizzly bear Ursus arctos L. Can. Wildl. Serv. Rep. Ser. No. 34, Ottawa.
- Peterman, R.M., C.W.Clark, and C.S. Holling. 1979. The dynamics of resilience: shifting stability domains in fish and insect systems. pp. 321-341 in Anderson, R.M., B.D. Turner, and L.R. Taylor, eds., Population dynamics. The 20th Symposium of the British Ecological Society, London, 1978. Blackwell Scientific Publ., London. 434 pp.
- Pianka, E.R. 1970. On r- and K-selection. Am. Nat. 104:592-597.
- Raybourne, J.W. 1976. A study of black bear populations in Virginia. pp. 71-81 in Trans. Northwest Sect. Wildl. Soc. (3). 1976.
- Reimers, E. 1975. Age and sex structure in a hunted population of reindeer in Norway. Proc. First Int. Reindeer and Caribou Symp. Biol. Pap., Univ. Alaska, Spec. Rep. 1: 181-188.
- Reynolds, H. 1976. North slope grizzly studies. Alaska Dept. Fish Game Fed. Aid Wildl. Rest. Rep. W-21-1, Vol. II, job 4.14R.
- Ricker, W.E. 1975. Computation and interpretation of biological statistics of fish populations. Bull. of Fish. Res. Board of Canada.
- Rogers, L.L. 1977. Social relationships, movements and population dynamics of black bears in northeastern Minnesota. Ph.D. Thesis. Univ. Minnesota, Minneapolis. 194 pp.
- Samuel, M.D. and T.C. Foin. 1983. Exploiting sea otter populations: a

- simulation analysis. *Ecol. Modelling* 20:297-309.
- Savidge, I.R. and J.S. Zeisenis. 1980. Sustained yield management. pp. 405-410 in Schemnitz, S.D., ed., *Wildlife Management Techniques Manual*, 4th edition. The Wildlife Society, Washington, D.C. 686 pp.
- Shaffer, M.L. 1978. Determining minimum viable population sizes: A case study of the grizzly bear (*Ursus arctos* L.). Ph.D. dissertation. Duke University, Durham, N.C. 142 pp.
- Silliman, R.P. and J.S. Gutsell. 1958. Exploitation of fish populations. *Trans. N. Am. Wildl. Conf.* 22:467-471.
- Slade, N.A. and H. Levenson. 1982. Estimating population growth rates from stochastic Leslie matrices. *Theor. Pop. Biol.* 22(3):299-308.
- Sokal, R.R. and J.F. Rohlf. 1981. *Biometry*, 2nd edition. W.H. Freeman and Co. 859 pp.
- Stirling, I., A.M. Pearson, and F.L. Bunnell. 1976. Population ecology of polar and grizzly bears in Canada. *Trans. N. Am. Wildl. Nat. Resource Conf.* 41:421-429.
- Stringham, S.F. 1980. Possible impacts of hunting on the grizzly/brown bear, a threatened species. pp. 337-349 in Martinka, C.J. and K.L. McArthur, eds., *Bears - their biology and management*. Bear Biol. Assoc. Ser. No. 4. 375 pp.
- _____. 1983. Roles of adult males in grizzly bear population biology. pp. 140-152 in Meslow, E.C., ed., *Bears - their biology and management*. *Int. Conf. Bear Res. and Manage.* 5. 336 pp.
- Tait, D.E.N. 1983. An analysis of harvest data. Ph.D. dissertation. University of British Columbia. 134 pp.
- Troyer, W.A. 1961. The brown bear harvest in relation to management on the Kodiak Islands. *Trans. N. Am. Wildl. Conf.* 26:460-469.
- _____. and R.J. Hensel. 1962. Cannibalism in brown bear. *Anim. Behav.* 10:231.
- Tulijapurkar, S.D. 1982. Population dynamics in variable environments. II. Correlated environments, sensitivity analysis and dynamics. *Theor. Pop. Biol.* 21:114-140.
- United States Fish and Wildlife Service. 1981. Grizzly Bear Recovery Plan. unpubl. report 194 pp.
- Wu, L.S-Y. and D.B. Botkin. 1980. Of elephants and men: A discrete, stochastic model for long-lived species with complex life histories. *Am. Nat.* 116(6):831-849.

- Young, B.F. and R.L. Ruff. 1982. Population dynamics and movements of black bears in east central Alberta. *J. Wildl. Manage.* 46(4):845-860.
- Zar, J.H. 1974. *Biostatistical analysis*. Prentice-Hall, Inc., Englewood Cliffs, N.J. 620 pp.